UCSF
UC San Francisco Electronic Theses and Dissertations

Title

A comparison between traditional two-dimensional cephalometry and a three-dimensional approach

Permalink

https://escholarship.org/uc/item/1tp649vs

Author

Adams, Gregory L.

Publication Date

2000

Peer reviewed|Thesis/dissertation

eScholarship.org Powered by the California Digital Library
University of California

A Comparison Between Traditional Two-Dimensional Cephalometry and a Three-Dimensional Approach

by

Gregory L. Adams, DDS

THESIS

Submitted in partial satisfaction of the requirements for the degree of

MASTER OF SCIENCE

in

Oral Biology

in the

GRADUATE DIVISION

of the

UNIVERSITY OF CALIFORNIA

San Francisco

Date

University Librarian

Acknowledgement

Dr. David Hatcher is a true visionary in the field of craniofacial imaging. His contributions to improving the diagnostic imaging tools we use in the field of orthodontics are unparalleled. He is a wonderful teacher and has raised my awareness and knowledge base of craniofacial imaging. I express my sincere gratitude for his advice and efforts in the completion of this project.

I extend my appreciation to Dr. Hassan Mostafavi for his expertise and support with the technical aspects of this project and to Craig Dial from Diagnostic Digital Imaging (DDI) for his assistance in the image acquisition of this project.

Dr. Stuart Gansky has made significant contributions throughout the development, design and analysis of this project. His statistical expertise, time, patience and effort have been invaluable. I am indebted to the other members of my thesis committee as well. Dr. Karin Vargervik and Dr. Arthur Miller guided the development of the project and the final form of this manuscript. These individuals have not only contributed to this project, but have contributed to my education and my development as a person over the past seven years. Thank you.

A special note of thanks goes to my co-residents who have provided friendship and helped to make the past three years more enjoyable. Finally, I express my sincere gratitude to my lovely fiancée, Eva, for her enduring love and support.

Abstract

The two-dimensional cephalogram is the standard used by orthodontists to assess skeletal, dental and soft-tissue relationships. This approach, however, is based on two-dimensional views utilized to analyze three-dimensional objects. The purpose of this project was to evaluate and compare a three-dimensional imaging system and traditional two-dimensional cephalometric methods with regard to accuracy in recording the anatomic truth. 13 landmarks were located by both methods on each of 9 dried human skulls and then compared to the gold standard of physical measurements. An intraclass correlation (0.995), variance (0.054 mm^2) and standard deviation (0.237 mm), averaged over 76 measurements, were derived from precision calipers in order to establish these physical measurements as a reliable gold standard to make comparisons of the two-dimensional and three-dimensional methods. The results of this study revealed a high amount of variability of mean difference from the gold standard inherent to the two-dimensional method (mean = 0.83 ± 6.94 mm) relative to the three-dimensional method (mean = -1.05 ± 0.54 mm). Paired t-tests found significant differences in 60 of 76 measurements comparing the conventional method to physical measures and in 64 of 76 measurements comparing the alternative three-dimensional system to physical measures. Additionally, a systematic bias of approximately – 1.0 mm (underestimation) was discovered in the three-dimensional method. Further refinement of the three-dimensional method should be able to eliminate this bias. However, bias of the two-dimensional cephalograms does not appear consistent across landmarks or easily correctable.

Table of Contents

List of Tables

List of Figures

Introduction

Among the routine procedures in any orthodontic office are obtaining, tracing, and analyzing cephalometric head films or cephalograms. To the layperson, the obvious question is "What information can be obtained from a lateral or frontal cephalometric headfilm?" According to Moyers et al.[1], cephalometrics is a radiographic technique for abstracting the human head into a measurable geometric scheme. Cephalometric radiography may be used: 1) for gross inspection, 2) to describe morphology and growth, 3) to diagnose anomalies, 4) to forecast growth, 5) to plan treatment, and 6) to evaluate treatment results. Gross inspection of the radiograph does not require identification, tracing, or measurement of the various dentoskeletal and soft tissue relationships, as it consists of a visual examination of the radiographic image only. All the other functions listed above, however, are principally concerned with the identification of specific landmarks and with the calculation of the various angular and linear variables that are described by means of these landmarks. All these procedures are potentially affected by several sources of error whose influence can vary to a great extent. Unfortunately, many of these sources of error are interrelated in such a way that a clear-cut distinction cannot easily be made.

Regardless of the way the head film is utilized, it is important to know how accurately measurements are being made and where the sources of error reside. Baumrind and Frantz[2] have described two general classes of error that occur in the estimation of cranial dimensions: "errors of projection" and "errors of identification".

Errors of projection result from the fact that the head film is a two-dimensional representation of a three-dimensional object. X-ray beams or threads are nonparallel and originate from a very small source leading to radiographs that are imperfect enlargements. The magnitude of the enlargement is related to the distances between the focus, the object, and the film.[3-7]

Head films are further affected by foreshortening linear distances between points lying in different planes and by radial displacement of all points and structures not lying on the central ray or principal axis. [2, 4-7] Additionally, projected angular measurements are incorrectly projected according to the laws of perspective.[8] Thus, an angle will appear more obtuse as it rotates away from an orthogonal (90 degree) angle to the source. Furthermore, landmarks and structures not situated in the midsagittal plane are usually bilateral, thus giving a dual image on the radiograph. These bilateral structures in the symmetric head do not superimpose in the lateral cephalogram because the fan of the x-ray beam expands as it passes through the head, causing a divergence between the images of all bilateral structures except those along the central beam. While recording the midpoints between these structures can to some extent compensate for the problem of locating bilateral structures subjected to distortion, this type of tracing is inadequate to describe a head that is truly asymmetrical.[9] In addition, in cases of mild asymmetry, it is difficult to differentiate between geometric imperfections and true subject asymmetry using a lateral cephalogram.[10]

Misalignment or tilting of the cephalometric components, the cephalostat or the film with respect to each other, as well as rotation of the patient's head in any plane of space, will introduce additional errors. Malposition of the patient in the cephalostat

produces an asymmetric projection of both linear and angular measurements on lateral cephalograms.[11] In the case of the frontal cephalogram, there is a chance that the apparent distance will be affected by a tilt of the head in the head holder, as this is more difficult to control in frontal than in lateral cephalograms.[12]

Errors of identification are the errors involved in the process of identifying specific landmarks on head films and are considered by many investigators to be the major source of error in cephalometrics.[2, 13-17] Many factors are involved in this uncertainty including: 1) the quality of the radiographic image, 2) the precision of landmark definition and the reproducibility of landmark location, 3) the operator, and 4) the registration procedure. Baumrind and Frantz state that "...errors in landmark identification are too great to be ignored; second, that the magnitude of error varies greatly from landmark to landmark; and, third, that the distribution of errors for most landmarks is not random but is, rather systematic, in the sense that each landmark has its own characteristic and usually noncircular envelope of error."[2] In a subsequent paper, Baumrind et al., consider the amount of error that may be tolerated in the clinical setting and state, "...our current measurement system, the angular head film measurement, is in most cases too inaccurate to differentiate all but the grossest changes".[11] The perception of this problem is not new and has been discussed in the literature as early as Hixon in 1956.[13]

USC LIBRARY

Three-dimensional imaging

The obvious advantages in producing images of the human skull using information derived from three-dimensions in space have been recognized for many years. Interest probably dates from the successful location of a metal object in the head by means of two orthogonal radiographs in 1897.[18] Lateral and frontal radiographs often are used separately in cephalometric analyses, but, with few exceptions, development of methods for integrating the two radiographic images to provide accurate three-dimensional models of the skull has not received the same attention as conventional two-dimensional cephalometry. This is surprising since the principles and applications of x-ray photogrammetry are well defined in other fields.[19-23] Recent development and refinement of three-dimensional reconstructions from computed tomography (CT) scan data[24-28] and the application of finite-element modeling to craniometric data recorded in three dimensions[29-31] have rekindled interest in the use of biplanar radiography, particularly in instances in which CT scanning is not justified.

History of Three-dimensional Imaging

From the very first introduction of the cephalostat, Broadbent and Bolton[32] stressed the importance of coordinating the lateral with the frontal films to arrive at an error-free definition of craniofacial form. For this purpose, they described the "Orientator", an acetate overlay to be placed over both standardized cephalograms after they were oriented jointly along their common Frankfort horizontal plane. One can imagine that in the exposure of a pair of cephalograms it is not the patient's head that is turned, but instead the cephalostat, itself. The lateral and frontal films would, in this case,

occupy positions 90° to each other, approximately 150 cm above the floor of the cephalostat. By keeping the films in register with respect to the head, one can draw the rays connecting the x-ray source to each landmark of either film as threads in space. The result is a pair of pyramidal sprays of radiographic threads or rays, intersecting at approximately 90° throughout the interior of the patient's head. Broadbent and Bolton[33] used the Orientator to correct for the enlargement inherent in the spread of the cephalostat x-ray beam. The pair of films can be flattened into one plane by unfolding them along the "corner" at which they approach each other, with each bundle of threads (x-ray paths) flattened to the side of the other film at the appropriate distance. The Orientator is the diagram of the flattened threads. When it is superimposed over the abutted pair of films, the points in each film that correspond to any particular locus in the other can be visualized.

The Broadbent method is conceptually sound. In practice, however, it is reported[34] to become difficult to apply and yields somewhat less reliable measurements than would be desired. Deficiencies inherent to this system have been pointed out.[34, 35]

First, the problem of landmark identification is consequential. The principle of combining data from two different projections implies the necessity of identifying the same landmark accurately and precisely on both images. In practice, the task of identifying the same point on both lateral and frontal head films with an acceptable degree of confidence is difficult, since the images of most of the anatomic structures in which we are interested differ in shape between the two projections.

Second, it is difficult to compensate for the differences in enlargement or projective displacement of structures located at different distances from the frontal and

lateral film surfaces. In this instance, we are concerned with physical and measurement problems. If the skull is partitioned conceptually into a series of planes parallel to the film plane, the enlargement factor for distances measured between points in any given plane will be the same, while the enlargement factors for all other planes will be different. If two planes are at different distances from the film surface, their enlargement factors will be different, regardless of the anatomy. Since the Broadbent system is in essence a spatial and temporal composite of two views, it follows that the enlargement factor for any given anatomic landmark will differ from the lateral projection to the frontal projection. Only by coincidence will the structure happen to be the same distance from both the lateral and the frontal film surfaces. This fact complicates the task of identifying landmarks on Broadbent film pairs, since only by coincidence will the image of any given anatomic structure have the same vertical (y) position on both films.

Various investigators have studied each of these problems since the Broadbent system was introduced in 1931. Savara[36] has conducted careful investigations on the problems of enlargement and reliability for a set of anatomic landmarks used in craniofacial measurements, although the results of these studies have not been applied clinically in orthodontics. In order to deal with the problem of differential enlargement, a number of other investigators have constructed specialized mechanical devices. These include the "compensator" of Wylie and Elasser[37] and the "modified compensator" of Vogel[38]. Vogel's method has been employed in at least one research study[39], but in general these solutions have been too tedious to become generally applicable, even in research settings.

The orthodontic community paid little attention to the frontal cephalogram when it was first introduced by Broadbent[32]. Since the clinical problems encountered by most orthodontists were of a symmetric nature, they were thought to be adequately recorded by the lateral view alone. The distortion or enlargement between left and right sides seems to have been ignored. In the past 20 years, however, the limitations of the lateral cephalogram have become more obvious as orthodontists begin to treat more severe, often asymmetric craniofacial anomalies. In this instance, the lateral cephalogram alone is of little clinical value in evaluating a patient with unilateral craniofacial microsomia.[40, 41]

In 1983, Grayson and colleagues[41, 42] produced standardized tracings of frontal and basilar films keyed to depth information as recorded from a standardized lateral cephalogram. This analysis attempts to visualize skeletal midlines at three selected depths of the craniofacial complex. When the midlines and associated anatomic structures are studied sequentially, the individual midlines are combined conceptually into a "warped midsagittal plane". Three acetate tracings are drawn for the lateral, frontal and basilar views and then superimposed revealing asymmetries found in each of the respective views. However, because no attempt is made to coordinate the information gained from one view to augment or locate points found in the complement views, this approach is essentially reduced to a two-dimensional technique using radiographs taken in three planes of space.

Other workers have pursued new sources of data that in various ways replace the lateral cephalogram by a different type of lateral information. Baumrind, Moffit, and

Curry[35, 43] discuss a theory to obtain true three-dimensional cephalograms from coplanar cephalometric stereo pairs in a 1983 paper. This method makes use of two cephalograms but rather than using orthogonal or biplanar views, they use coplanar lateral images which form what the authors call a "stereoscopic x-ray film pair". The apparatus requires that the subject be positioned in a head holder. A film is mounted in the usual position for a lateral cephalogram (the central ray passes through the porion-porion axis) and an exposure is made from a stationary x-ray source. Immediately after the exposure, the film is removed and a new film shifted into the same position by a cassette-changing device. The second film is then exposed from an alternate x-ray source located lateral to, but not at a 90° (orthogonal) angle to the first source. The x-ray tubes as well as the film position are fixed and the geometric relationships are known between the system components. With this information, Baumrind et al., contend it is mathematically possible to construct a three-dimensional map by identifying the same set of landmarks on each of the two images.

While this is essentially the same concept as the Broadbent model, Baumrind et al. believe that by using coplanar images as opposed to orthogonal, biplanar images, errors associated with landmark identification are reduced. The authors state, however, "there is no question that in cases where the point being measured can be reliably and unambiguously identified on both images, the solution for point location is mathematically strongest when the rays striking the point intersect at an angle close to 90 degrees".[35] While coplanar films may increase the precision in landmark identification of paired films, we should question whether this might decrease the accuracy to the anatomical truth. Additionally, this method also requires that the subject remain

motionless throughout the exposure process since the exposures do not occur simultaneously. This may prove to be a difficult task when employed with live patients, especially children. To date, there are no published data using Baumrind's proposed coplanar three-dimensional x-ray stereometry model.

During the mid-1980's, the finite element method was applied as a new approach to the analysis of cephalograms.[30, 31, 44-46] Finite element analysis is an engineering method that uses partial differential equations to interpolate loading values for intermediate points in irregular structures by dividing the structures into sets of regular geometric shapes (in the simplest case, into triangles).

The introduction of this new method does not, however, solve the problems related to prediction of growth changes. The following should be taken into consideration. The method requires accurate and precise measurement of the known landmarks in the system. As used by Moss et al.,[44] and Bookstein et al.,[47] the landmark location procedures are just as crude and error-prone as those of conventional cephalometric methods. Secondly, the utility of finite element analysis in assessing of growth and development processes has not been tested except to compare its findings with those of conventional methods. In other words, the idea that the method is useful is still an untested hypothesis.

In recent years, computed tomography (CT) and magnetic resonance imaging (MRI) have been used for evaluation of craniofacial anomalies, but because of the use of predefined windows, these views display only parts of the recorded information. Thus,

only structures within the scan plane are demonstrated optimally, whereas, for instance, it is difficult to assess the degree of maxillary hypoplasia on CT or MRI axial slices. Three-dimensional reconstructions of CT or MRI data may, however, reduce these problems because the image reconstruction involves all three dimensions.[26-28, 48] Unfortunately, these new methods are considered impractical for ordinary clinical use in orthodontics due to relatively high amounts of radiation exposure to the patient as well as considerable economic cost.

Mindful of the preceding considerations, we should strive to develop a system that better approximates the ideal imaging modality: a system that maximizes the desired information and minimizes the physiologic risk and economical cost to the patient. Hatcher[49] argues that the determination of anatomic truth requires the accurate portrayal of spatial orientation, size, shape, form, and the relationships of desired structures or features. For reasons, outlined herein, this determination may only be realized using three planes of space.

USF LIBRARY

Modern Imaging Techniques

Stereophotogrammetry is a technique developed by civil engineers to measure three-dimensional relationships of objects and terrains. This method has been applied in the construction of terrestrial maps using aerial photographs and imaging parameters such as angles, focal lengths, film-to-object distances, and marker-to-marker distances that are known. This theory has been referred to in Baumrind's articles[35, 43], but the methods have been limited to simple triangulation after associating landmarks on two or more

radiographs. The use of the "bundle adjustment method" is a technique developed by D. C. Brown in 1989[50] can further augment this theory. This technique self calibrates the system using large numbers of measurement points simultaneously to calculate the imaging device position as well as the desired three-dimensional point coordinates.

The addition of these techniques has resulted in recent technology developed by Acuscape™. In 1996 David Hatcher (radiology), Hassan Mostafavi (digital imaging), Charles Palm (photogrammetry) and Bill Harrell (cephalometrics) brought their expertise to bear on the problem of practical three-dimensional craniofacial imaging. They have since developed a methodology for identifying landmarks in calibrated and digitized x-ray and optical images. In a study by Quintero in 1998, the Sculptor™ program developed by this group was evaluated and deemed extremely accurate (within 0.221mm) in the measurement of distances on plastic cube and skull models.[51] In addition, the Sculptor™ program is purported to eliminate the need for a cephalostat head fixation mechanism. The self-calibration features previously described compensate for all magnification and rotation effects; a problem commonly found in other imaging systems.

Purpose, Specific Aims and Hypothesis

Purpose

The purpose of this study is to evaluate and compare a three-dimensional imaging system and traditional two-dimensional cephalometric methods with regard to accuracy in recording the anatomic truth.

Hypothesis

The identification of landmarks and linear measurements using three planes of space on dried human skulls derived from the Sculptor™ system will be closer in accuracy to the gold standard reference (physical measurements) than traditional two-dimensional cephalometry.

Specific Aims

Specific aim #1: To Develop a Gold Standard Reference

To calibrate and determine the accuracy and error uncertainty in three dimensions of the project test conditions and develop a reference system using precision calipers to physically measure distances in order to perform statistical comparisons of accuracy.

Specific aim #2: To Determine Two-Dimensional Accuracy

To statistically compare conventional two-dimensional cephalometric measurements to a gold standard reference developed in specific aim #1.

USF LIBRARY

Specific aim #3: To Compare Relative Accuracy of Measuring Modalities

To statistically compare computer generated linear distances utilizing the Sculptor™ three-dimensional cephalometric analysis method versus conventional two-dimensional cephalometric measurements and the gold standard.

LIBRARY

Materials and Methods

Subjects

Nine undocumented dried human skulls were obtained from the Anatomy Department at the University of California at San Francisco. Skulls of variable morphology were selected and included if all bony elements were intact. Radiopaque Beekley spots (Beekley Corporation, Prestige Lane, Bristol, CT 06010) were placed at thirteen specific skeletal landmarks to serve as a target for both physical and radiographic measurements. These metallic markers have an adhesive backing and were placed using defined criteria commonly used in two-dimensional cephalometrics and represented midsagittal and bilateral landmarks (Table 1). The skulls were then labeled and documented with photographs.

Physical Measurements

The distance between landmarks was determined by manual measurement using digital calipers with an achievable precision of 0.03 mm, according to the manufacturer. One measurement session consisted of 78 measures of each skull based on 13 landmarks (Table 1). In some cases, measurements were not physically possible due to the anatomy unique to each skull and the size of the calipers. These instances were noted and omitted.

USC LIBRARY

Table 1.

Definition of Skull Landmarks

1. Sella (S): the point representing the midpoint of the pituitary fossa (sella turcica)

2. Nasion (Na): the most anterior point of the frontonasal suture in the median plane

3. A Point (A): the deepest midline concavity on the maxilla between the anterior nasal spine and prosthion

4. B Point (B): the deepest midline concavity on the mandibular symphysis between pogonion and infradentale

5. Gnathion (Gn): the most anteroinferior point on the symphysis of the chin

6. Zygomaticotemporal suture - Right (Zyg R): the point of junction between the right zygomatic and right temporal bone

7. Zygomaticotemporal suture - Left (Zyg L): the point of junction between the left zygomatic and left temporal bone

8. Gonion - Right (Go R): the point of intersection between the right ramal plane and the right mandibular plane

9. Gonion - Left (Go L): the point of intersection between the left ramal plane and the left mandibular plane

10. Condylion - Right (Co R): the most central point of the right condylar head

11. Condylion - Left (Co L): the most central point of the left condylar head

12. Zygomaxillary suture - Right (Zyg R): the central point of the right zygomatic suture

13. Zygomaxillary suture - Left (Zyg L): the central point of the left zygomatic suture

LIST LIBRARY

To measure the error of the method, three skulls were selected for two additional measurement sessions giving a total of three measurement sessions. The mean distance, standard deviation, and mean variance associated with 76 measurements were calculated to determine intraoperator reliability. Intraclass correlations were calculated from the sums of squares of a 2-way ANOVA with replicate and subject effects. In two instances (S – Gn and S – B), it was not physically possible to obtain enough measurements for an intraclass correlation calculation.

Image Acquisition

A special proprietary calibration framework made up of previously surveyed radiopaque metal bearings (Acuscape Corporation, Quail Ridge Center, 1200 East Alosta Ave, Glendora, CA 91740) was secured on each skull for the imaging sessions. Each skull was then placed in the cephalostat and three images were acquired: standard lateral (90°), frontal (0°) and oblique (45°). All projections were established with the Frankfort Horizontal Plane approximately parallel to the floor. The standard lateral projections oriented the midsagittal plane parallel to the film. For frontal projections, the midsagittal plane was set perpendicular to the film. A single calibrated and trained technician (Craig Dial) performed all of the imaging. Care was taken to avoid changes in the orientation of the calibration framework.

USF LIBRARY

Conventional Cephalometric Measurements

Conventional cephalometric measurements were performed on the standard lateral cephalometric film (90°) and the frontal film (0°) with the same digital calipers used to obtain the physical measurements. The most appropriate radiographic projection for a given measurement was chosen in order to achieve the highest level of accuracy (Table 2).

Table 2.

Projection Utilization For Conventional Measurements

	S	Na	A	B	Gn	ZMX R	Zyg R	Co R	Go R	ZMX L	Zyg L	Co L
Go L	Frontal	Lateral	Lateral	Lateral	Lateral	Frontal	Frontal	Frontal	Frontal	Lateral	Lateral	Lateral
Co L	Frontal	Lateral	Lateral	Lateral	Lateral	Frontal	Frontal	Frontal	Frontal	Lateral	Lateral	
Zyg L	Frontal	Frontal	Frontal	Frontal	Lateral	Frontal	Frontal	Frontal	Frontal	Lateral		
ZMX L	Frontal	Frontal	Frontal	Lateral	Lateral	Frontal	Frontal	Frontal	Frontal			
Go R	Frontal	Lateral	Lateral	Lateral	Lateral	Lateral	Lateral	Lateral				
Co R	Frontal	Lateral	Lateral	Lateral	Lateral	Lateral	Lateral					
Zyg R	Frontal	Frontal	Frontal	Frontal	Lateral	Lateral						
ZMX R	Frontal	Frontal	Frontal	Lateral	Lateral			**Symmetric**				
Gn	Frontal	Lateral	Lateral	Lateral								
B	Lateral	Lateral	Lateral									
A	Lateral	Lateral										
Na	Lateral											

Because the radiopacity of the lead markers removes the subjectivity in landmark identification, only one observer was deemed necessary to perform all measurements. Four headfilms were selected and repeated measures performed to assess intraobserver error. The mean distance, standard deviation and error associated with each of the 78 measurements were calculated to determine intraoperator reliability. Additionally, a reproducibility margin (intraclass correlation) was calculated from the sums of squares in a 2-way ANOVA test.

Image Processing

Scanning of Images

The films were scanned using a flatbed scanner calibrated to determine precise pixels/mm in the horizontal (x) and vertical (y) directions. A transparency adapter was used and the scanner was set at a resolution of 150 dots per inch.

Calibration of Images and Setting the Reference Plane

This procedure spatially establishes all images into a three dimensional matrix. The ultimate goal is to have a true space (x, y, z) reference system assigned to the patient.

The calibration chain of events begins with imaging the calibration frame and patient in the same field of view from two or more points of view. The locations of the bearings in the framework are known and used to assign a reference system to the calibration frame. The unknowns include the patient and source reference systems. To compute the location of the source (7 degrees of freedom: x - width, y - height, z - depth, yaw, pitch, roll and focal length), the image sets are placed into a three dimensional matrix. The reference system from the calibration frame is then set to the patient.

Figure 1. Establishing a reference system

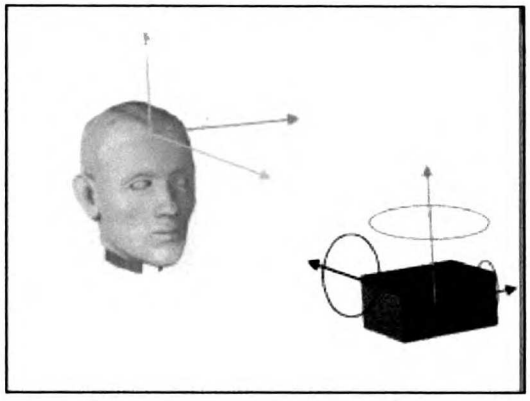

Figure 1 illustrates a reference system associated with the source and the calibration frame. At this point, the two systems are not linked. The source needs to be located with 7 degrees of freedom (7 DF; x, y, z, yaw, pitch, roll and focal length) relative to the calibration frame. This is done by taking a picture of the patient along with the calibration frame followed by calibrating the image. When the virtual calibration frame (known geometry of calibration markers) is fitted to the image of the calibration frame, there is a geometric transformation of the virtual frame that occurs. This geometric transformation is the key to mathematically locating the source with 7 DF.

Figure 2. Geometric transformation of framework to locate the source

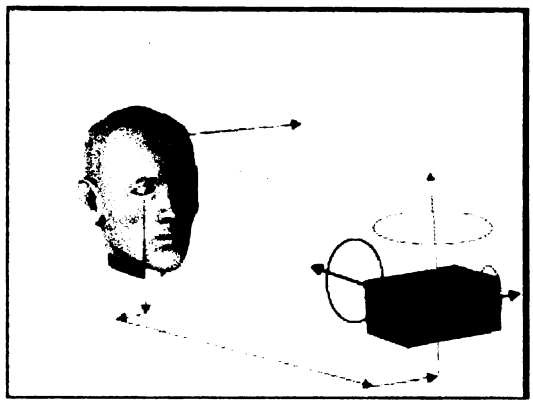

Figure 2 represents the geometric transformation that locates the source relative to the calibration frame with 7 DF and is repeated for all images. At the completion of this calibration process, all images have been placed into the same three-dimensional matrix (calibration frame reference).

The reference system can then be adjusted and set to the patient's anatomy as depicted by the rays emanating from the patient in Figure 3. This becomes the "patient specific reference".

Figure 3. Patient specific reference system

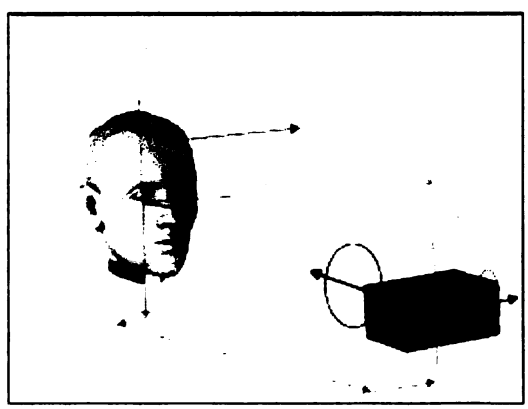

Figure 4. Schematic of imaging system

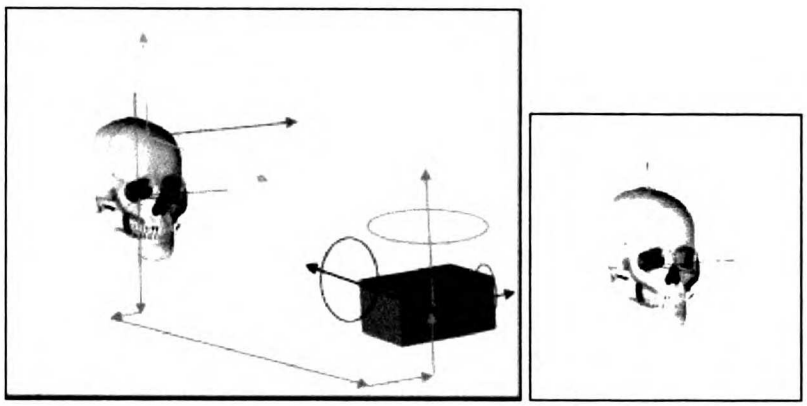

This patient specific reference system will apply to all anatomy contained in the three-dimensional space that is represented. Skulls served as the subjects in this project.

Figure 5. Schematic of x-ray angles

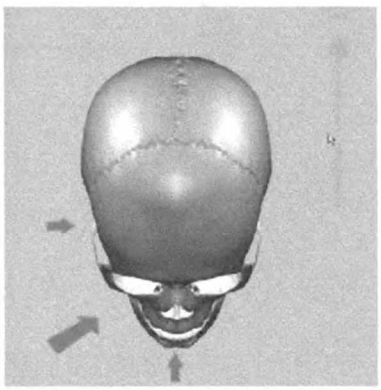

In Figure 5, the arrows represent the 3 cephalometric points of view and location of the three source positions (7 DF). The resultant images are merged into the same three-dimensional matrix and landmarks are located on the images from two or more different points of view. Triangulation math calculations can then be used to locate and record each landmark in space (x, y, z).

UCSF LIBRARY

Landmarking of Calibrated Images

Landmarking of the calibrated images consists of a triangulation process that uses known values to compute anatomic locations. These locations are described in x, y, and z values associated with the patient reference system.

Error Envelopes

When two right angle (90°) views are used to locate anatomic landmarks in three dimensions of space, the error envelope is as follows in Figure 6.

Figure 6. Orthogonal views

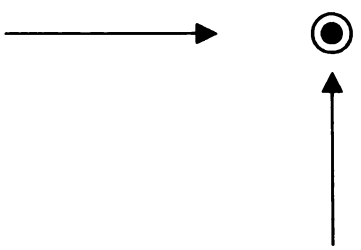

The black arrows represent the imaging point of view (ie., lateral and frontal ceph). The shaded dot represents the true anatomic landmark and the black circle represents the error envelope for triangulating this landmark location. The error envelope is circular and evenly distributed around the true answer.

Figure 7. Coplanar views

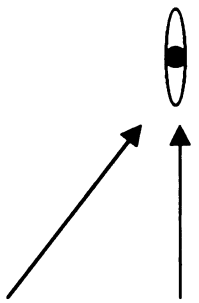

The imaging geometry shown in Figure 7 in contrast to orthogonal views reduces the error margin perpendicular to the beam angle and increases the error envelope in the direction parallel to the beam angle.

Figure 8. Three points of view:

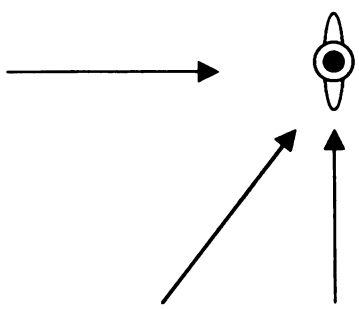

The geometry depicted in Figure 8 reduces the error envelope to the best (smallest) of all three points of view.

Distance Measurements

A Sculptor™ session computes the three-dimensional distance from the first point (x1, y1, z1) to the second point (x2, y2, z2) registered as identified landmarks within the program. The notation (x1, y1, z1) represents values on the three axes in three-dimensions of space. All measurements are then downloaded from Sculptor™ into a spreadsheet.

To measure the error of the method, three skulls were selected for two additional measurement sessions giving a total of three measurement sessions. The mean distance, standard deviation, and error associated with each of the 78 measurements were calculated to determine intraoperator reliability. From the data, a reproducibility margin (intraclass correlation) was calculated using 2-way ANOVA.

Statistical Evaluation

As previously mentioned, a 2-way ANOVA without replication was performed to evaluate the similarity of the three samples, separately, (physical, conventional, and Sculptor™) resulting in intraclass correlations for each of the measures. The following equation was used: $ICC = MS_{subject} - MS_{error}/MS_{subject} + (r+1)\ MS_{error}$, where $MS_{subject}$ is the mean square of the skulls from the ANOVA, MS_{error} is the mean square error from the ANOVA, and r is the number of replicates.

In order to test the original hypothesis, the data were analyzed by three additional statistical methods. First, the difference in sample means and standard error of the

difference in sample means were obtained for each measurement pair. These values were then used to compare physical measurements (gold standard) with Sculptor™ and conventional two-dimensional measurements, respectively. Based on intraclass correlations and variance, physical measurements were found to be highly accurate and allowed the use of paired t-tests to detect for significant differences between the Sculptor™ and conventional two-dimensional measurement systems. The Bonferroni correction method was not utilized in conjunction with the paired t-test in order to apply a more stringent statistical test to the respective systems since finding statistical significance means the system was different than physical measurements. Even without the Bonferroni correction, with 78 measures, one would expect almost four significant t-tests just by chance. The Bland-Altman method[52] was also applied, as it is an effective tool when two methods are compared but neither provides an unequivocally correct measurement. This method illustrates the magnitude of the difference with respect to the anatomic truth and distribution of points of the measurement variables. Simple Pearson correlations were not performed as this test can hide systematic discrepancies between measurements. Lastly, a scatter plot with smoothed lines was employed to illustrate the range and potential bias of the two methods.

LSU LIBRARY

Results

Physical Measurements as a Reference

A total of 1137 measurements were completed between markers on the nine dried skulls. Skull #6 was missing 3 lead markers (Co L, Co R, and B point) due to a shortage of supplies at the time of imaging. The missing lead markers resulted in the omission of these points in the subsequent statistical tests, thus only 45 measures of skull #6 were utilized. Additionally, the S - Gn and S - B distances were physically impossible to measure with the precision calipers due to the anatomy of the skulls and, consequently, were also omitted from the study as they did not have a gold standard comparison.

Repeated measures from the sums of squares in a two way ANOVA without replication indicate a high average intraclass correlation of 0.995 (Table 3). This test gives a mathematical value of the degree of similarity between measurements, which reflects the usefulness of this model to serve as a reference gold standard and by which the remaining experiments could be completed.[53] Values close to zero indicate poor reliability while those close to one indicate high reliability. To further establish the suitability of physical measurements as a reference, the variance (0.054 mm^2) and standard deviation (0.237 mm) were averaged across the 76 landmark distances.

Table 3.

Intraclass Correlation Values for Physical Measurements												
	S	Na	A	B	Gn	ZMX R	Zyg R	Co R	Go R	ZMX L	Zyg L	Co L
Go L	0.998	0.997	0.996	0.998	0.998	0.999	0.999	0.997	0.999	0.998	0.996	0.972
Co L	0.999	0.997	0.998	0.996	0.996	0.999	0.999	0.999	0.999	0.992	0.994	
Zyg L	0.997	0.999	0.994	0.999	0.999	0.999	0.999	0.999	0.999	0.996		
ZMX L	0.999	0.997	0.995	0.987	0.999	0.999	0.999	0.999	0.999			
Go R	0.994	0.998	0.997	0.999	0.998	0.999	0.999	0.987				
Co R	CNM*	0.992	0.992	0.998	0.999	0.996	0.994					
Zyg R	0.982	0.976	0.992	0.983	0.992	0.972						
ZMX R	0.998	0.999	0.997	0.995	0.997			Symmetric				
Gn	CNM*	0.999	0.995	0.999								
B	CNM*	0.998	0.984									
A	0.997	0.997										
Na	0.998											

CNM* = Could not measure

Mean Intraclass Correlation 0.995

Conventional Method

From the data, a mean reproducibility margin (intraclass correlation) of 0.983 was calculated from the sums of squares in a 2-way ANOVA test (Table 4). In two instances (Table 4 boldface), the intraclass correlation values are less than 0.900. For both of these measurements the range of measurement lengths between subjects is less than 0.30 mm, but the error is less than 0.025 mm. Correlation depends on the range of the true value in the sample. If this value is large, the correlation will be greater than if it is narrow.[52] In this instance, the range is extremely narrow between subjects leading to a deceptive intraclass correlation value.

USAF LIBRARY

Table 4.

Intraclass Correlation Values for Conventional Measurements												
	S	Na	A	B	Gn	ZMX R	Zyg R	Co R	Go R	ZMX L	Zyg L	Co L
Go L	0.999	0.999	0.999	0.999	0.999	0.999	0.999	0.999	0.999	0.999	0.999	0.994
Co L	0.999	0.999	0.999	0.999	0.998	0.999	0.999	0.999	0.999	0.999	0.998	
Zyg L	0.999	0.999	0.999	0.999	0.999	0.999	0.999	0.999	0.997	0.999		
ZMX L	0.999	0.999	0.999	0.999	0.999	0.999	0.998	0.999	0.999			
Go R	0.998	0.999	0.999	0.999	0.999	0.999	0.999	**0.451**				
Co R	0.999	0.999	0.999	0.999	0.996	0.999	0.999					
Zyg R	0.999	0.999	0.999	0.999	0.999	0.999						
ZMX R	0.994	0.999	0.999	0.999	0.999			Symmetric				
Gn	0.998	0.999	0.978	0.990								
B	0.999	0.997	**0.552**									
A	0.999	0.975										
Na	0.999											

Mean Intraclass Correlation 0.983

Table 5 (Appendix) presents the mean difference, standard deviation (SD), range and paired t-test P values for the 76 measurements observed with the conventional method versus the gold standard. The grand mean of the differences (mean of the mean differences) is 0.83 ± 6.94 mm. The standard deviation indicates a high amount of variation spanning almost 14 mm. In only 16 of the 76 (21%) measurements does the interval of the mean (mean ± SD) span zero, the value of the anatomic truth. Further, only 23 of the 76 (30%) are within 2 standard deviations of the anatomic truth.

The mean differences range from -12.13 mm (underestimation; Gn – Zyg R) to +13.61 mm (overestimation; Zyg R – Zyg L) of the true values. The actual differences range from –17.68 mm of the gold standard to +15.52 mm of the gold standard, respectively.

LSU LIBRARIES

Evaluation of the paired t-tests at $\alpha = .05$ reveals 70 of the 76 measures are significantly different from the physical measurements (gold standard). By chance, only three or four significant measurements were expected. Additionally, the six measures that do not indicate a significant difference have a coefficient of variation (SD/mean) of greater than 1, indicating that the standard deviation is greater than the mean and consequently, excessive variability is an issue for these measures.

Ranking the measurements according to mean difference and ranking based on variability did not reveal a pattern. Thus, particular landmarks do not seem to correspond with greater variability or mean error.

The Bland-Atman plots of the 76 measurement comparisons (Appendix Figures 9-84) reveal a low degree of precision resulting from the conventional, two-dimensional method as well as a low degree of accuracy regarding the anatomic truth. Individual plots vary greatly in both overestimation and underestimation and 95% confidence intervals rarely envelope the actual gold standard measurement. The measurement points are not in any sort of pattern within each plot nor between plots, signifying the absence of a relationship between mean length of the measurement and mean difference between two-dimensional and physical values.

Lastly, the scatter plot with smoothed lines (Figure 85) visually reinforces the high degree of variation and a low degree of precision and accuracy evident in the conventional cephalometric measuring system. **Overall**, the system appears to lack systematic bias. Each landmark pair, however, can either overestimate or underestimate the true value.

Figure 85. Scatter plot with smoothed lines

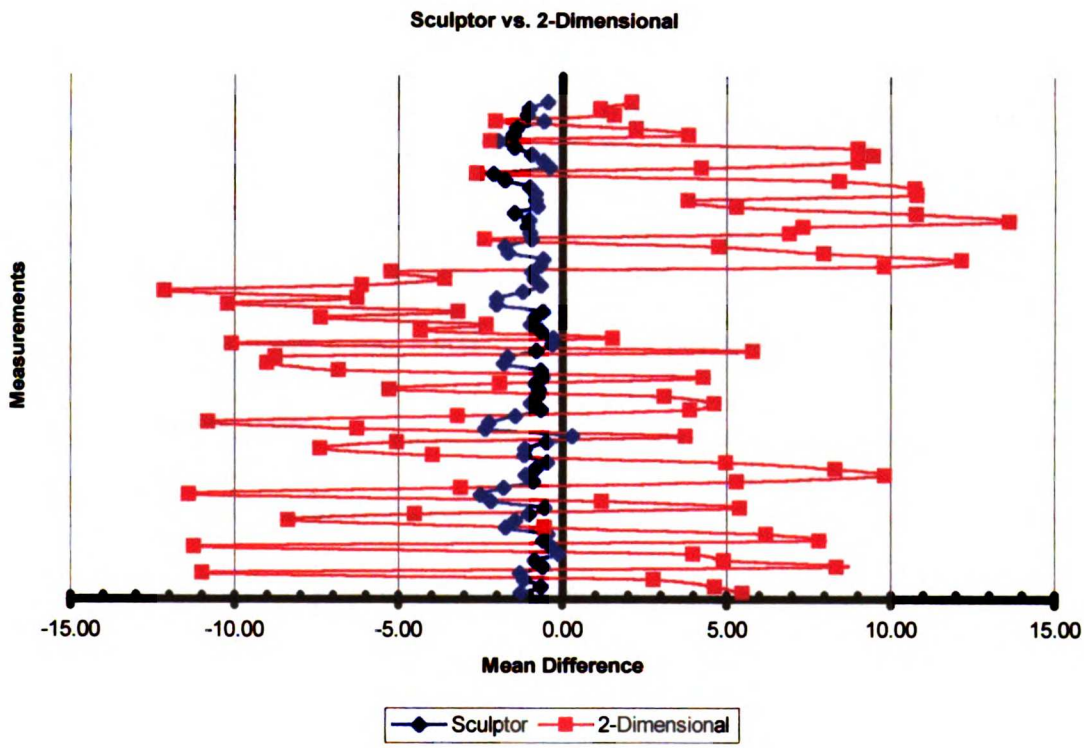

Sculptor™ Method

Analogous to the other measurement modalities a reproducibility margin for the Sculptor™ system (mean intraclass correlation) of 0.998 was calculated using 2-way ANOVA (Table 6).

UIST. LIBRARY

Table 6.

Intraclass Correlation Values for Sculptor™ Measurements

	S	Na	A	B	Gn	ZMX R	Zyg R	Co R	Go R	ZMX L	Zyg L	Co L
Go L	0.999	0.999	0.999	0.999	0.998	0.999	0.999	0.999	0.999	0.999	0.999	0.969
Co L	0.999	0.999	0.999	0.999	0.999	0.999	0.999	0.999	0.999	0.999	0.999	
Zyg L	0.999	0.998	0.999	0.996	0.999	0.999	0.999	0.999	0.999	0.997		
ZMX L	0.999	0.998	0.998	0.998	0.999	0.999	0.999	0.999	0.999			
Go R	0.999	0.999	0.999	0.999	0.995	0.999	0.999	0.999				
Co R	0.999	0.999	0.999	0.998	0.999	0.999	0.998					
Zyg R	0.995	0.996	0.999	0.999	0.999	0.979						
ZMX R	0.999	0.999	0.999	0.999	0.999			**Symmetric**				
Gn	0.998	0.999	0.999	0.999								
B	0.999	0.999	0.997									
A	0.999	0.997										
Na	0.999											

Mean Intraclass Correlation 0.998

Table 7 (Appendix) presents the mean difference, standard deviation, range, and P values for the 76 comparable measurements observed with the Sculptor™ method. The grand mean of the differences is –1.05 ± 0.54 mm. In only 12 of the 76 (16%) measurements are the anatomic truths within 1 standard deviation and in only 38 of the 76 (50%) measurements are the measurements within 2 standard deviations.

The mean differences of the Sculptor™ method range from –2.49 mm (Na – Co R) to +0.30 mm (A - ZMX L) and the actual mean differences range from –3.99 mm (A - Co R) of the gold standard to 2.96 mm (A - ZMX L).

Similar to the conventional method, the evaluation of the paired t-tests at $\alpha = .05$ presents 68 of the 78 measures as significantly different from the physical measurements. Further inspection reveals that the coefficients of variation for these measures are greater than 1, resulting in potentially excessive variation in these measures.

As with the two-dimensional estimates, ranking the measurements according to mean difference or variability did not reveal a pattern, corresponding with greater variability or mean error.

The Bland-Atman plots (Figures 9-84 Appendix) illustrate a high degree of precision resulting from the Sculptor™ method, yet there is a low degree of accuracy with an overall median of -0.94 mm and mean of –1.05 mm difference from the anatomic truth. The individual plots are useful in determining to what level the Sculptor™ program can be expected to underestimate the true anatomic measurement values. Similar to the conventional method, the Sculptor™ points are not in any sort of pattern within each plot nor between plots, signifying the absence of a relationship between mean length of measurement and mean difference between Sculptor™ and physical measurements.

A clear systematic bias of the Sculptor™ system is illustrated in the scatter plot with smoothed lines (Figure 85). Evaluation of the graph illustrates the propensity for this method to underestimate the anatomic truth by approximately 1.0 mm.

Comparison of Sculptor™ and the Conventional Method

Inspection of Tables 5 and 7 (Appendix) reveal that the grand mean values of the two measurement systems are approximately equal to ± 1.0 mm. However, the mean standard deviation of the conventional two-dimensional system is significantly greater (2-dimensional : 6.94 mm, Sculptor™ : 0.54 mm), illuminating a much higher variability of this method when compared to Sculptor™. Comparisons of the ranges also bring to light the much larger magnitude of potential error inherent in the conventional two-

USF LIBRARIES

dimensional cephalometric method. Both of these methods, however, are inaccurate and at least 50% of all measurements will result in erroneous values.

Evaluation with the Bland-Altman analysis (Figures 9-84) plots the two methods concurrently. The general lack of precision of the conventional method stands in stark contrast with Sculptor™, which tends to cluster tightly within approximately 0.5 mm. As mentioned earlier, there is no evidence of pattern between magnitude of measurement and the magnitude of error.

Finally, the scatter plot with smoothed lines (Figure 85) illustrates the overall relationship between the two methods and demonstrates nicely an apparent **overall** lack of bias in the traditional two-dimensional method and the noticeable bias of Sculptor™. This graph also illustrates the magnitude of the range of the means between the two methods with Sculptor™ demonstrating a relatively slight range of error in comparison with the two-dimensional method.

USF LIBRARY

Discussion

Cephalometric measurements are tedious to take and prone to error. They involve errors of projection, errors in identification, and errors of measurements.[2] The projection errors result because a cephalogram is a two-dimensional image of a three-dimensional object. The errors of identification involve the seemingly straightforward process of identifying landmarks. However, the main source of error in cephalometrics is landmark identification.[2, 14, 17]

One can define the reliability of a landmark as the extent to which a given anatomic structure yields the same result on repeated trials. In real world cephalometrics, the reliability of landmark identification seems to depend on the following factors: 1) quality of the x-ray film, 2) care in positioning the subject in the cephalostat, 3) care in using a constant plane-to-film distance, 4) anatomic knowledge of the orthodontist, 5) anatomic complexity of the region, 6) accuracy and precision of the orthodontist in identifying a landmark, and 7) accuracy and precision in recording a landmark.

It should be stated that the present study was not concerned with the separate problem of the reliability of landmark identification on different cephalograms on the same subject. Lead markers were used in this study to eliminate the ambiguity of landmark location and reduce the associated error in an effort to measure greatest achievable accuracy of the two systems. Hence, error estimations made in this study are idealized and may not be generalized to the *in vivo* situation.

Evaluation of the Conventional 2- Dimensional Measurement System

In this study, the mean differences range from -12.13 mm (underestimation; Gn – Zyg R) to +13.61 mm (overestimation; Zyg R – Zyg L). The inaccuracy and lack of precision found in this study demonstrate the limitations of two-dimensional cephalometrics.

The compounding errors inherent in two-dimensional cephalometry were evident in the standard deviation (6.84 mm) derived in this project. Many of the errors associated with two-dimensional cephalometrics explained in the introduction may have contributed to the resultant standard deviation. However, the errors of projection may have played the most significant role. For example, the significant overestimation of Zyg R – Zyg L (based on a frontal image) is likely due to magnification. In a symmetric skull, these landmarks should be approximately in the same plane of reference and at an orthogonal perspective in a frontal radiograph. The magnitude of enlargement or overestimation is related to the distances between the focus, the object, and the film.[3-7] The closer these points lay to the source and the greater the distance between these points (at a 90° plane), the greater the enlargement of the anatomic truth.

Three solutions to correct for magnification in conventional two-dimensional cephalometrics have been offered. First, it has been suggested that a magnification correction factor in addition to the use of long focus-object and short object-film distances may minimize these projection errors.[54] However, although relatively long focus-film distances are favorable, a focus-film distance of more than 280 cm does not significantly alter the magnitude of the projection error.[55, 56] Secondly, it has been suggested that the use of angular rather than linear measurements is a consistent way to

eliminate the impact of magnification, since angular measures remain constant regardless of the enlargement factor.[3] Unfortunately, angular measurements may be less sensitive to magnification, but are still inaccurate. Angular measurements may be affected by tilt and are sensitive to orientation and rotation of the test subject.[12] Lastly, the use of ratios may also be utilized for comparing radiographs of different magnification although the diagnostic interpretation of ratios for clinical applications in the individual cases is difficult and often unclear.

The gross underestimation of measurements such as Gn – Zyg R may be the result of projective displacement of landmarks in different planes of space. Many of the measurements used in this project lie in oblique planes of space. When these pairs of landmarks are not at a 90° angle to the source x-ray, projective displacement may occur in the form of foreshortening. Although the most optimal film was used for each measure, projective displacement of landmarks is unavoidable and uncorrectable using the conventional method.

LIBRARY

Evaluation of the Sculptor™ 3-Dimensional Measurement System

The evaluation of Sculptor™ in this project illuminated distinct advantages of this system as well as some current minor limitations. The grand mean and standard deviation of the differences for this three-dimensional measurement system was –1.05 ± 0.54 mm and the mean differences of the Sculptor™ method ranged from –2.49 mm (Na – Co R) to +0.30 mm (A - ZMX L). These values reveal that a high level of precision is attainable with this system. Sculptor™ also appears to be free of magnification error, but may have a systematic bias. This bias, however, is approximately –1.0 mm as illustrated

by Figure 85 and should be correctable either within the engineering of the software/calibration framework or with a simple mathematical correction factor.

The hypothesis of this study was directed at comparing the **overall** accuracy of conventional two-dimensional cephalometry and the Sculptor™ system. As evident by the series of Bland-Altman plots (Appendix Figures 9-84), the precision and accuracy for individual measurements were superior using the Sculptor™ system. The **overall** accuracy derived in this project, however, found Sculptor™ slightly less accurate (-1.05 mm vs. 0.83 mm) than conventional cephalometry.

The accuracy and precision of this system depends on two important computer-to-user interface processes: calibration and triangulation. Error in the Sculptor™ system is attributable to one or both of these processes. First, the problem of calibration of reference markers from the calibration frame to a common coordinate system requires computer-aided accurate marker identification of these control points on multiple images. Second, the problem of landmark registration requires computer-assisted accurate triangulation of landmark identification from multiple views.

Each imaging session consisted of three views and the resultant films were scanned and imported into the Sculptor™ software. Processing consisted of two parts: 1) calibration of the three images and 2) identification and triangulation of the landmarks using all three views. The three-dimensional spatial coordinates (x, y, z) were then automatically and mathematically registered in the system's database. At this point, determination of any three dimensional linear distances between any two previously identified landmarks is known.

USF LIBRARY

The precision, or measure of repeatability of the three-dimensional measurements was consistent with an intraclass correlation of 0.998, a value slightly exceeding the gold standard of physical measurements. The reader should keep in mind, however, that radiopaque lead markers were used in this project to aid in identifying all landmarks. The accuracy of the system in estimating individual measurements was significantly better than the two-dimensional method employed in the study, but was not perfect and demonstrated a mean bias of −1.05 mm.

The experiment with Sculptor™ may have had less than optimal accuracy for a number of possible reasons. The ease of calibration and triangulation are directly dependent on the stability of the calibration framework during the image acquisition process. The skulls utilized were dried human skulls of various sizes and the calibration framework was a recently developed model manufactured for patients. Because this framework was made for the living patient, the circumference of the framework, although adjustable, far exceeded the circumference of the skulls due to the lack of soft tissues. It was necessary, therefore, to modify the calibration framework to fit each of the subjects and may have lead to movement of the framework during the imaging session. Any movement of the framework during this process can alter the geometric relationship between the same points on various images. However, this type of error would have been expected to yield a random, non-directional bias.

Additionally, the survey of the calibration frame may have inaccuracies. There are two possible sources of error related to this. First, the physical measurements between the calibration points on the framework itself may be erroneous and, second, a new calibration framework not previously tested with the Sculptor™ software was

UNT. LIBRARY

utilized. There is a possibility of relaxation of the new calibration framework over time. This device was manufactured by bending a flat sheet of Lucite into a curve. Previous models utilized a curved piece of Lucite that did not require a bend. The engineers of the framework believe that this bent piece of Lucite may have relaxed over time rendering repeated surveys of the framework precise, but inaccurate. Unfortunately, this was not considered in the project design and a new survey immediately before or after the imaging session was not performed. Further, if this relaxation occurred following the imaging sessions, the original spatial relationships of the calibration framework cannot be recovered.

It is conceivable that the physical measurements were less accurate than the Sculptor™ system measurements or that there was a bias of overestimation in the physical measurements. The caliper survey of the skulls was not free of possible random or systematic errors, particularly since only one operator performed all physical measurements. Although three skulls were purposely measured on three different days, operator bias can occur when only one operator performs all measurements. Parallax error is always a potential when measuring a linear distance with a straightedge caliper.

Finally, the metallic markers were imbedded in a thin plastic coating and adhered to the dried skulls. The position of these markers may have changed over time and handling of the skulls during imaging and physical measurement sessions. The notion that all of the markers remained perfectly stable is unlikely and may have contributed to random errors.

Although each of these factors may seem insignificant when considered alone; when considered collectively, they can account for some of the variability in the study for

all three measurement modalities. The most likely explanation for bias in the Sculptor™ system would exist either in the physical survey of the calibration framework, distortion of the calibration framework, or the Sculptor™ software. Credence should also be given to the possibility of physical measurement bias given the slight amount (-1.05 mm) of mean difference found in the project.

Significance and Future Applications

Cephalometric radiography is likely to remain the most popular form of craniofacial imaging for some time, particularly for diagnostic use in patients for whom the more expensive methods and, in the case of CT scanning, greater exposure to radiation are not justified. The greatest handicap to progress in biplanar radiography is the acknowledged difficulty in identifying the same anatomic structures and reference points accurately on more than one film.[35, 43] Sculptor™ differs from earlier techniques in one important aspect. The location of reference points is under semiautomatic control by a computer that uses information from the landmark location on one radiograph to project an extrapolated imaginary estimation line ("epipolar line") onto the subsequent films. Thus, the computer itself assists in the location of reference points. The computer-aided approach (epipolar lines) to locate landmarks on multiple radiographs appears to be a great advantage, but the extent to which this function may increase the accuracy in landmark identification is unknown and should be studied.

Although this system has some current minor difficulties and unknown factors, with additional work, Sculptor™ promises to compete effectively against the three-dimensional CT scan, and so serve as one member of a family of complementary

methods for the study of craniofacial form. The inclusion of a third coplanar radiograph taken at a 45° angle offers improved flexibility for the location of reference points and provides more information, thus decreasing subsequent error. Three-dimensional coordinates of craniofacial reference points can be displayed as wire-frame models or analyzed in several ways that reduce the limitations imposed by conventional cephalometry in two dimensions. Three-dimensional coordinates and measurements derived from them also are free of the enlargement and projective error produced by radiography. In particular, the quantification of structural variation in three dimensions is likely to lead to more comprehensive insights into the nature of asymmetric conditions of the skull for which cephalometric analysis based solely on single-view radiographs is not entirely appropriate. Normative data for the three-dimensional cephalometric system may be collected easily, whereas such data are unlikely to ever exist for the more extensive visualizations of the CT scan. "Normal" children are not scanned, at least not with a view toward establishing normative data. Instead, they form a clinical residual category, having demonstrated negative findings in scans for the investigation of suspected diagnoses.

Considering the biologic cost (e.g. radiation) of a Sculptor™ series versus a CT scan, it is much more practical to anticipate a three-dimensional series to be repeated for longitudinal studies of growth, treatment outcomes, or relapse. Moreover, the economic cost of a cephalometric series is a negligible fraction of the cost of a CT scan and the young patient does not have to be sedated in the course of this procedure.

Mock surgery, originally introduced as a two-dimensional technique, gains in accuracy when accessed in a three-dimensional record. As information is gained from

both pre- and post-surgical records, the predictability of treatment outcomes is likely to improve, particularly in oblique planes of space. Similarly, new insight may be gained in growth prediction or growth modification. In all of these applications, three-dimensional cephalometric data may be recorded and manipulated by the use of equipment no more sophisticated than the now-ubiquitous personal computer.

For all of these reasons, our preliminary studies encourage us to expand and explore this system for obtaining craniofacial information in three-dimensions.

USF. LIBRARY

Conclusions

1) The conventional two-dimensional measurement system is both inaccurate and imprecise when compared to a gold standard of reference as determined by physical measurements on human skulls.

2) Measurements determined by the Sculptor™ three-dimensional cephalometric system is precise but inaccurate when compared to a gold standard of reference as determined by physical measurements. However, the inaccuracies are relatively minor and based on technical error or bias.

3) The linear distances generated by Sculptor™ are underestimated relative to the gold standard by approximately 1.0 mm.

4) The hypothesis that the Sculptor™ system would yield measurements of greater overall accuracy to the gold standard than the conventional two-dimensional cephalometric analysis must be rejected based on the findings of this project.

USF LIBRARY

References

1. Moyers RE, Bookstein FL, Hunter WS. Analysis of the craniofacial skeleton: Cephalometrics. *In* Moyers RE, ed. Handbook of Orthodontics. Chicago: Yearbook, 1988. pp. 247-309.
2. Baumrind S, Frantz RC. The reliability of head film measurements. 1. Landmark identification. Am. J. Orthod. 1971; 60(2):111-127.
3. Adams JW. Correction of error in cephalometric roentgenograms. Angle Orthod 1940; 10:3-13.
4. Brodie AG. Cephalometric roentgenology: History, technique and uses. J Oral Surg 1949; 7:185-98.
5. Hixon EH. Cephalometrics and longitudinal research. Am J Orthod 1960; 46:36-42.
6. Bjork A, Solow B. Measurements on radiographs. J Dent Res 1962; 41:672-83.
7. Salzmann JA. Limitations of roentgenographic cephalometrics. Am J Orthod 1964; 50:169-88.
8. Slagsvold O, Pedersen K. Gonial angle distortion in lateral head films: A methodologic study. Am J Orthod 1971; 71:554-64.
9. Grayson BH, McCarthy TG, Bookstein F. Analysis of craniofacial asymmetry by multiplane cephalometry. Am J Orthod 1984; 84:217-24.
10. Cook JT. Asymmetry of the craniofacial skeleton. Br J Orthod 1980; 7:33-8.
11. Baumrind S, Frantz RC. The reliability of head film measurements. 2. Conventional angular and linear measurements. Am J Orthod 1971; 60:505-17.

UNT. LIBRARY

12. Proffit WR. The search for truth: Diagnosis. *In* Proffit WR, White RP, eds. Surgical Orthodontic Treatment. St. Louis: Mosby Year Book, 1991. pp. 96-141.

13. Hixon EH. The norm concept and cephalometrics. Am J Orthod 1956; 42:898-919.

14. Savara BS, Tracey WE, Miller PA. Analysis of errors in cephalometric measurements of three-dimensional distances on the human mandible. Arch Oral Biol 1966; 11:209-17.

15. Richardson A. An investigation into the reproducibility of some points, planes and lines used in cephalometric analysis. Am J Orthod 1966; 52:637-51.

16. Gravely JF, Benzies PM. The clinical significance of tracing error in cephalometry. Br J Orthod 1974; 1:95-101.

17. Mitgaard J, Bjork A, Linder-Aronson S. Reproducibility of cephalometric landmarks and errors of measurement of cephalometric cranial distances. Angle Orthod 1974; 44:56-61.

18. Dennis J. A new system of measurement in x-ray work. Dent Cosmos 1897; 39:445-54.

19. Ghosh SK, Boulianne U. X-ray photogrammetry and floating lines in support of neurosurgery. Int Arch Photogram Remote Sensing 1984; 25:335-43.

20. McNeil GT. X-ray stereo photogrammetry. Photogram Eng 1966; 32:993-1004.

21. Singh RS. Radiographic measurements. Photogram Eng 1970; 36:1137-46.

22. Veress SA, Lippert FG, Takamoto T. An analytical approach to x-ray photogrammetry. Photogram Eng Remote Sensing 1977; 43:1503-10.

UofL LIBRARY

23. Adams LP. X-ray stereo photogrammetry locating the precise, three-dimensional position of image points. Med Biol Eng Comput 1981; 19:569-78.

24. Vannier MW, March JL. Craniofacial disorders. Diagn Imaging 1983(March):36-43.

25. Hemmy DC, David DJ, Herman GT. Three-dimensional reconstruction of craniofacial deformity using computed tomography. Neurosurg 1983; 13:534-41.

26. Maki K, Shibasaki Y, Fukuhara T. A new approach to mandibular growth employing x-ray CT. Dentistry in Japan 1989; 26:77-80.

27. Maki K, Okano T, Yamada S, Shibasaki Y. The application of three-dimensional quantitative computed tomography to the maxillofacial skeleton. J Dent Maxillofac Radiol 1997; 26:39-44.

28. Maki K, Miller AJ, Okano T, Shibasaki Y. Changes in cortical bone mineralization in the developing mandible: A three-dimensional quantitative computed tomography study. J Bone Miner Research 2000; 15:700-9.

29. Cheverud J, Lewis JL, Bachrach W, Lew WD. The measurement of form and variation in form: an application of three-dimensional quantitative morphology by finite-element methods. Am J Phys Anthropol 1983; 62(2):151-65.

30. Korioth TW, Romilly DP, Hannam AG. Three-dimensional finite element stress analysis of the dentate human mandible. Am J Phys Anthropol 1992; 88:69-96.

31. Korioth TW, Hannam AG. Mandibular forces during simulated tooth clenching. J Orofac Pain 1994; 8:178-89.

32. Broadbent BH. A new x-ray technique and its application to orthodontia. Angle Orthod 1931; 1:45.

UVSF LIBRARY

33. Broadbent BH, Bolton, Golden W. Bolton standards of dentofacial developmental growth. St. Louis: The CV Mosby Company, 1975.

34. Grayson B, Cutting C, Bookstein F, et al. The three-dimensional cephalogram: Theory, technique, and clinical application. Am J Orthod Dentofac Orthop 1988; 94:327-37.

35. Baumrind S, Moffitt FH, Curry S. Three-dimensional x-ray stereometry from paired coplanar images: a progress report. Am J of Orthod 1983; 84(4):292-312.

36. Savara BS. A method of measuring facial bone growth in three dimensions. Hum Biol 1965; 37:245-55.

37. Wylie WH, Elasser WA. Understated vertical projections of the head from lateral and posteroanterior roentgenograms. Am J Roentgenol 1948; 60:414.

38. Vogel CJ. Correction of frontal dimensions from head x-rays. Angle Orthod 1967; 37:1-8.

39. Mitani H, Brodie AG. Three plane analysis of tooth movement, growth, and angular changes with cervical traction. Angle Orthod 1970; 40(2):80-94.

40. Grayson BH, Boral S, Kolber A, McCarthy JG. Unilateral craniofacial microsomia: I. Mandibular analysis. Am J Orthod 1983; 84:225-230.

41. Grayson BH, McCarthy JG, Bookstein F. Analysis of craniofacial asymmetry by multiplane cephalometry. Am J Orthod 1983; 84(3):217-24.

42. Grayson BH, LaBatto F, McCarthy JG. The basilar multiplane cephalometric analysis. Part I. Landmark identification and tracing methodology. Part II. Method of analysis and its application to the study of craniofacial anomalies. Am J Orthod 1985; 88:503-516.

UofT LIBRARY

43. Baumrind S, Moffitt FH, Curry S. The geometry of three-dimensional measurement from paired coplanar x-ray images. Am J Orthod 1983; 84(4):313-22.

44. Moss ML, Shaklak R, Patel H. Finite element method modeling of craniofacial growth. Am J Orthod 1985; 87:453-72.

45. Inou F, Maki K. Biomechanical study of the human mandible on mechanical response of its shape and structure. *In* Computational Biomechanics, Hirawasa Y, Sledge C, Woo S, eds. Tokyo: Springer-Verlag, 1994. pp. 44-55.

46. Inou N, Iioka Y, Fujiwara H, Maki K. Functional adaptation of mandibular bone. *In* Hayashi K, Ishikawa H, eds. Biomechanics and Related Research. Tokyo: Springer-Verlag, 1996. pp. 23-42.

47. Bookstein F, Chernoff B, Elder R, Strauss R. Morphometrics in Evolutionary Biology. Special Publication No. 15 ed. Philadelphia: Academy of Natural Science, 1985.

48. Vannier MW, Marsh JL, Warren JO. Three dimensional CT reconstruction images for craniofacial surgical planning and evaluation. Radiology 1984; 150:179-85.

49. Hatcher DC. Maxillofacial Imaging. *In* McNeill C, ed. Science and Practice of Occlusion. Chicago: Quintessence Publishing, 1997. pp. 349-64.

50. Brown DC. Emerging trends in non-topographic photogrammetry. *In* Karera HM, ed. Non-topographic Photogrammetry. American Society for Photogrammetry and Remote Sensing, 1989.

UVJT. HDR

51. Quintero J-C. Validation of A Computer -Aided Approach to Three-dimensional Craniofacial Imaging. Oral Biology. San Francisco: University of California, San Francisco, 1998. pp. 81.

52. Bland JM, Altman DG. Statistical methods for assessing agreement between two methods of clinical measurement. Lancet 1986(February 8):307-10.

53. Landis JR, Koch GG. A review of statistical methods in the analysis of data arising from observer reliability studies (Part I). Statistica Neerlandica 1975; 29(3):101-23.

54. Franklin JB. Certain factors of aberration to be considered in clinical roentgenographic cephalometry. Am J Orthod 1952; 38:351-68.

55. Ahlqvist J, Eliasson S, Welander U. The effect of projection errors on angular measurements in cephalometry. Eur J Orthod 1988; 10(4):353-61.

56. Ahlqvist J, Eliasson S, Welander U. The effect of projection errors on cephalometric length measurements. Eur J of Orthod 1986; 8(3):141-8.

UofT. HDM

Table 6.

Conventional vs. Physical Measurements						
Measurement	Mean Difference (mm)	Standard Deviation (mm)	Minimum	Maximum	Range	P Value
S - Go L	5.50	2.58	0.16	8.77	8.61	0.0014*
S - Co L	4.66	0.93	3.55	5.84	2.29	0.0001*
S - Zyg L	2.78	2.06	-1.78	4.77	6.55	0.0037*
S - ZMX L	-10.97	2.83	-14.27	-6.32	7.95	0.0000*
S - Go R	8.36	1.65	6.05	10.92	4.87	0.0000*
S - Co R	4.93	0.96	4.02	5.93	1.91	0.0124*
S - Zyg R	4.00	2.60	1.17	10.07	8.90	0.0017*
S - ZMX R	-11.24	3.91	-16.84	-4.33	12.51	0.0000*
S - Gn	Could not Measure					
S - B	Could not Measure					
S - A	7.84	1.15	6.50	9.46	2.96	0.0000*
S - Na	6.22	0.84	5.51	7.41	1.90	0.0000*
Na - Go L	-0.54	1.81	-3.00	1.92	4.92	0.3994
Na - Co L	-8.36	2.23	-11.67	-5.32	6.35	0.0000*
Na - Zyg L	-4.49	1.93	-7.15	-1.32	5.83	0.0000*
Na - ZMX L	5.42	1.44	3.47	8.65	5.18	0.0001*
Na - Go R	1.20	1.60	-1.55	2.69	4.24	0.0544
Na - Co R	-11.38	2.19	-15.50	-7.94	7.56	0.0000*
Na - Zyg R	-3.09	3.10	-9.48	1.29	10.77	0.0173*
Na - ZMX R	5.32	1.82	1.32	6.97	5.65	0.0000*
Na - Gn	9.82	0.51	8.88	10.40	1.52	0.0000*
Na - B	8.32	0.32	7.73	8.74	1.01	0.0000*
Na - A	4.99	0.25	4.70	5.35	0.65	0.0000*
A - Go L	-3.96	1.47	-6.37	-2.05	4.32	0.0000*
A - Co L	-7.39	3.42	-13.20	-3.72	9.48	0.0005*
A - Zyg L	-5.04	2.49	-9.58	-1.46	8.12	0.0003*
A - ZMX L	3.76	1.70	0.83	6.41	5.58	0.0002*
A - Go R	-6.25	2.70	-11.73	-3.60	8.13	0.0001*
A - Co R	-10.80	1.79	-12.47	-7.58	4.89	0.0000*
A - Zyg R	-3.20	3.60	-8.88	2.11	10.99	0.0282*
A - ZMX R	3.89	1.86	1.14	6.95	5.81	0.0002*
A - Gn	4.63	0.62	3.51	5.49	1.98	0.0000*
A - B	3.11	0.55	1.94	3.69	1.75	0.0000*
B - Go L	-5.28	2.60	-8.21	-1.22	6.99	0.0007*
B - Co L	-1.90	2.50	-3.98	3.84	7.82	0.0695
B - Zyg L	4.31	4.78	-5.45	10.22	15.67	0.0543
B - ZMX L	-6.83	2.76	-10.79	-2.24	8.55	0.0006*
B - Go R	-9.01	2.74	-12.34	-4.35	7.99	0.0000*
B - Co R	-8.75	2.83	-13.22	-3.45	9.77	0.0001*
B - Zyg R	5.81	5.04	-6.00	10.29	16.29	0.0138*
B - ZMX R	-10.09	2.44	-13.89	-6.21	7.68	0.0000*

Table 6 continued

Conventional vs. Physical Measurements						
Measurement	**Mean Difference (mm)**	**Standard Deviation (mm)**	**Minimum**	**Maximum**	**Range**	**P Value**
B - Gn	1.54	0.36	0.93	2.02	1.09	0.0000*
Gn - Go L	-4.32	2.51	-7.60	-0.53	7.07	0.0010*
Gn - Co L	-2.31	3.04	-7.38	1.15	8.53	0.0689
Gn - Zyg L	-7.36	2.55	-11.79	-4.69	7.10	0.0000*
Gn - ZMX L	-3.17	2.46	-6.67	0.59	7.26	0.0048*
Gn - Go R	-10.19	3.56	-15.52	-4.81	10.71	0.0000*
Gn - Co R	-6.25	2.90	-11.17	-1.21	9.96	0.0005*
Gn - Zyg R	-12.13	2.65	-17.68	-8.58	9.10	0.0000*
Gn - ZMX R	-6.12	2.68	-11.23	-2.02	9.21	0.0001*
ZMX R - Go L	-3.59	6.37	-10.71	7.29	18.00	0.1292
ZMX R - Co L	-5.23	3.01	-10.07	-1.10	8.97	0.0017*
ZMX R - Zyg L	9.80	1.40	7.90	11.70	3.80	0.0000*
ZMX R - ZMX L	12.15	1.16	9.38	13.60	4.22	0.0000*
ZMX R - Go R	7.97	1.02	6.83	9.89	3.06	0.0000*
ZMX R - Co R	4.78	1.70	1.88	7.21	5.33	0.0001*
ZMX R - Zyg R	-2.38	1.93	-6.32	0.41	6.73	0.0062*
Zyg R - Go L	6.93	3.48	1.84	13.32	11.48	0.0003*
Zyg R - Co L	7.35	2.43	4.40	12.08	7.68	0.0001*
Zyg R - Zyg L	13.61	2.10	8.33	15.52	7.19	0.0000*
Zyg R - ZMX L	10.79	1.22	9.18	12.57	3.39	0.0000*
Zyg R - Go R	5.32	0.91	4.24	6.73	2.49	0.0000*
Zyg R - Co R	3.83	0.44	3.05	4.65	1.60	0.0000*
Co R - Go L	10.81	1.29	9.32	12.86	3.54	0.0000*
Co R - Co L	10.75	0.91	9.27	12.35	3.08	0.0000*
Co R - Zyg L	8.44	0.95	7.09	9.91	2.82	0.0000*
Co R - ZMX L	-2.60	2.17	-5.26	1.54	6.80	0.0118*
Co R - Go R	4.24	1.49	2.57	5.90	3.33	0.0003*
Go R - Go L	9.01	0.97	7.57	10.14	2.57	0.0000*
Go R - Co L	9.48	5.22	-2.66	14.42	17.08	0.0013*
Go R - Zyg L	9.01	2.36	4.45	12.30	7.85	0.0000*
Go R - ZMX L	-2.19	3.66	-6.39	5.68	12.07	0.1059
ZMX L - Go L	3.85	0.82	2.26	4.82	2.56	0.0000*
ZMX L - Co L	2.26	1.27	0.56	3.98	3.42	0.0015*
ZMX L - Zyg L	-2.04	1.46	-4.24	0.07	4.31	0.0030*
Zyg L - Go L	1.60	1.28	-0.73	3.40	4.13	0.0054*
Zyg L - Co L	1.17	0.66	0.18	2.08	1.90	0.0015*
Co L - Go L	2.11	1.19	-0.46	3.26	3.72	0.0016*

Grand Mean	0.81
Standard Deviation of Mean	6.94
Mean Standard Deviation	2.11

UNT HDRL

Table 7.

Sculptor ™ vs. Physical Measurements						
Measurement	Mean Difference (mm)	Standard Deviation (mm)	Minimum	Maximum	Range	P Value
S - Go L	-1.27	0.34	-1.72	-0.91	0.81	0.0000*
S - Co L	-0.65	0.73	-1.84	0.30	2.14	0.0807
S - Zyg L	-1.19	0.66	-2.75	-0.51	2.24	0.0007*
S - ZMX L	-1.30	0.57	-2.09	-0.39	1.70	0.0001*
S - Go R	-0.59	0.88	-1.33	1.47	2.80	0.0763
S - Co R	-0.85	0.08	-0.91	0.76	0.15	0.0029*
S - Zyg R	-0.11	0.42	-0.52	0.80	1.32	0.4757
S - ZMX R	-0.33	0.32	-0.82	0.28	1.10	0.0145
S - Gn	Could not Measure					
S - B	Could not Measure					
S - A	-0.57	1.41	-2.17	1.53	3.70	0.2886
S - Na	-0.44	0.74	-1.05	0.97	2.02	0.2005
Na - Go L	-1.72	0.41	-2.27	-1.07	1.20	0.0000*
Na - Co L	-1.43	0.53	-2.54	-0.90	1.64	0.0001*
Na - Zyg L	-1.03	0.26	-1.49	-0.78	0.71	0.0000*
Na - ZMX L	-0.53	0.26	-0.95	-0.13	0.82	0.0003*
Na - Go R	-2.17	0.80	-3.36	0.55	2.81	0.0000*
Na - Co R	-2.49	0.49	-3.26	-1.81	1.45	0.0000*
Na - Zyg R	-1.78	0.48	-2.73	-1.02	1.71	0.0000*
Na - ZMX R	-0.89	0.43	-1.89	-0.48	1.41	0.0002*
Na - Gn	-1.12	0.35	-1.40	-0.30	1.10	0.0000*
Na - B	-0.81	0.22	-1.08	-0.45	0.63	0.0000*
Na - A	-0.45	0.28	-0.82	-0.06	0.76	0.0024*
A - Go L	-1.16	0.87	-2.58	0.14	2.72	0.0039*
A - Co L	-1.15	0.62	-2.00	-0.15	1.85	0.0012*
A - Zyg L	-0.47	0.62	-1.27	0.75	2.02	0.0537
A - ZMX L	0.30	1.20	-1.16	2.96	4.12	0.4732
A - Go R	-2.35	0.80	-3.51	-1.22	2.29	0.0000*
A - Co R	-2.24	0.92	-3.99	-1.09	2.90	0.0002*
A - Zyg R	-1.43	0.45	-2.36	-0.89	1.47	0.0000*
A - ZMX R	-0.66	0.33	-1.17	-0.01	1.16	0.0003*
A - Gn	-0.97	0.40	-1.75	-0.43	1.32	0.0001*
A - B	-0.75	0.32	-1.22	-0.33	0.89	0.0003*
B - Go L	-0.72	0.37	-1.21	-0.10	1.11	0.0008*
B - Co L	-0.82	0.29	-1.21	-0.52	0.69	0.0003*
B - Zyg L	-0.59	0.32	-1.06	-0.19	0.87	0.0027*
B - ZMX L	-0.66	0.31	-1.13	-0.35	0.78	0.0013*
B - Go R	-1.78	0.57	-2.65	-0.99	1.66	0.0000*
B - Co R	-1.66	0.61	-2.47	-0.54	1.93	0.0001*
B - Zyg R	-0.79	0.65	-1.49	0.33	1.82	0.0113*
B - ZMX R	-0.31	0.44	-0.91	0.26	1.17	0.0897

Table 7 continued.

Sculptor™ vs. Physical Measurements						
Measurement	**Mean Difference (mm)**	**Standard Deviation (mm)**	**Minimum**	**Maximum**	**Range**	**P Value**
B - Gn	-0.28	0.32	-0.76	0.14	0.90	0.0438*
Gn - Go L	-0.65	0.35	-1.16	0.09	1.25	0.0006*
Gn - Co L	-0.97	0.31	-1.53	-0.51	1.02	0.0001*
Gn - Zyg L	-0.85	0.48	-1.69	-0.11	1.58	0.0007*
Gn - ZMX L	-0.60	0.86	-2.07	1.17	3.24	0.0717
Gn - Go R	-2.01	0.36	-2.71	-1.57	1.14	0.0000*
Gn - Co R	-2.01	0.32	-2.50	-1.60	0.90	0.0000*
Gn - Zyg R	-1.20	0.34	-1.56	-0.79	0.77	0.0000*
Gn - ZMX R	-0.65	0.42	-1.17	-0.03	1.14	0.0018*
ZMX R - Go L	-0.84	0.23	-1.21	-0.55	0.66	0.0000*
ZMX R - Co L	-0.92	0.26	-1.33	-0.55	0.78	0.0000*
ZMX R - Zyg L	-0.67	0.23	-0.97	-0.35	0.62	0.0000*
ZMX R - ZMX L	-0.57	0.57	-1.06	0.83	1.89	0.0164*
ZMX R - Go R	-1.65	0.55	-2.70	-0.84	1.86	0.0000*
ZMX R - Co R	-1.74	0.76	-2.88	-0.71	2.17	0.0003*
ZMX R - Zyg R	-0.93	0.36	-1.45	-0.41	1.04	0.0001*
Zyg R - Go L	-0.98	0.36	-1.40	-0.34	1.06	0.0000*
Zyg R - Co L	-1.06	0.33	-1.58	-0.69	0.89	0.0000*
Zyg R - Zyg L	-1.01	0.32	-1.61	-0.51	1.10	0.0000*
Zyg R - ZMX L	-1.45	0.55	-2.51	-0.63	1.88	0.0000*
Zyg R - Go R	-0.76	0.46	-1.34	0.28	1.62	0.0012*
Zyg R - Co R	-0.81	0.54	-1.74	-0.18	1.56	0.0038*
Co R - Go L	-0.81	0.49	-1.53	-0.20	1.33	0.0023*
Co R - Co L	-0.99	0.57	-2.30	-0.40	1.90	0.0016*
Co R - Zyg L	-1.75	0.37	-2.47	-1.33	1.14	0.0000*
Co R - ZMX L	-2.09	0.61	-2.86	-1.24	1.62	0.0000*
Co R - Go R	-0.38	0.33	-0.87	0.06	0.93	0.0224*
Go R - Go L	-0.57	0.47	-1.37	0.14	1.51	0.0067*
Go R - Co L	-0.93	0.47	-1.95	-0.40	1.55	0.0090*
Go R - Zyg L	-1.45	0.56	-2.56	-0.80	1.76	0.0001*
Go R - ZMX L	-1.94	0.52	-3.05	-1.44	1.61	0.0000*
ZMX L - Go L	-1.50	0.65	-2.49	-0.72	1.77	0.0001*
ZMX L - Co L	-1.39	0.38	-2.20	-0.99	1.21	0.0000*
ZMX L - Zyg L	-0.55	0.35	-1.36	-0.22	1.14	0.0015*
Zyg L - Go L	-1.07	0.63	-2.04	-0.31	1.73	0.0009*
Zyg L - Co L	-1.01	0.38	-1.54	-0.36	1.18	0.0001*
Co L - Go L	-0.43	0.33	-0.95	0.08	1.03	0.0074*

Grand Mean	-1.05
Standard Deviation of Mean	0.57
Mean Standard Deviation	0.49

Figure 9.

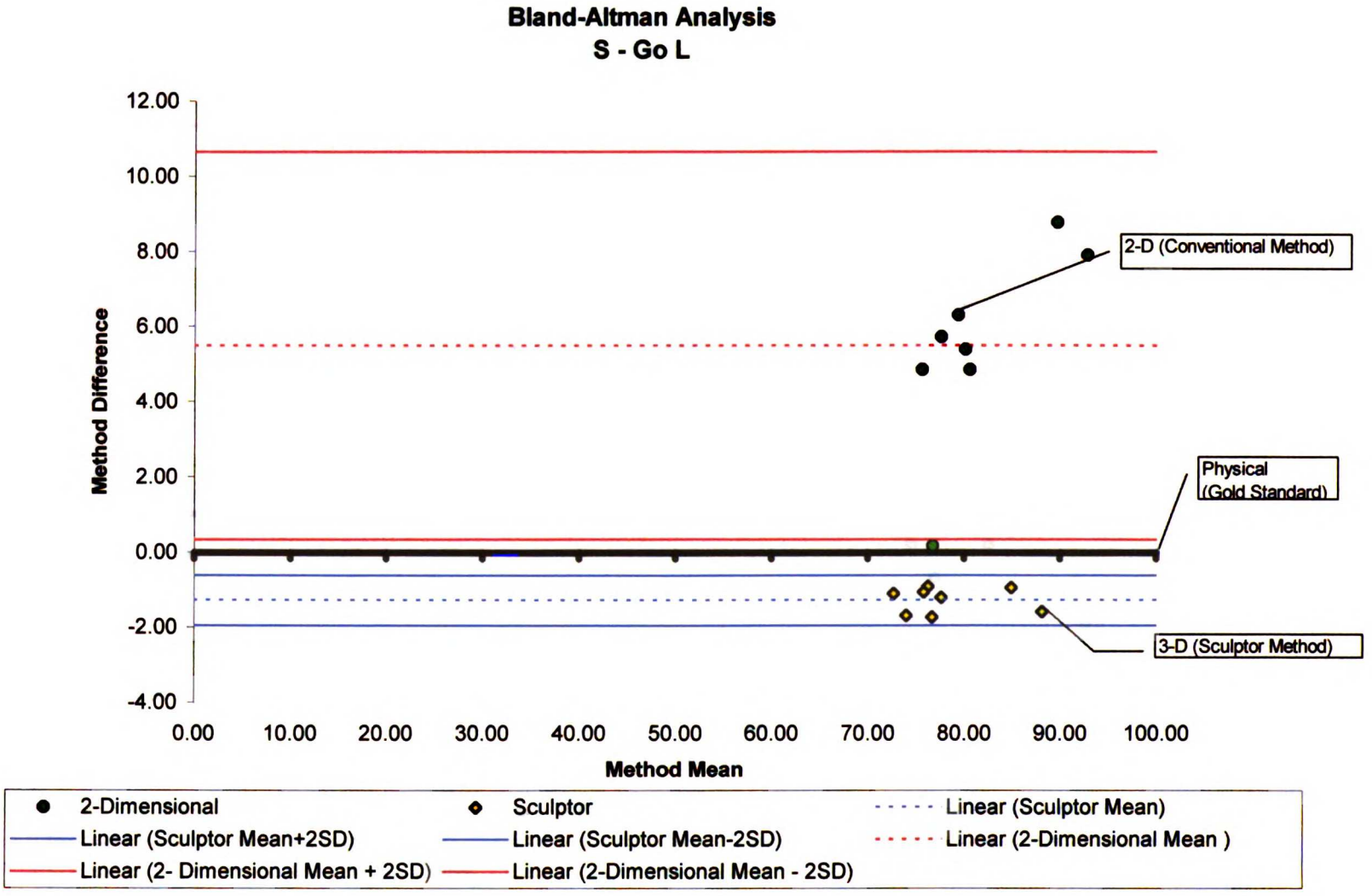
Bland-Altman Analysis
S - Go L
Method Difference
12.00
10.00
8.00
6.00
4.00
2.00
0.00
-2.00
-4.00
0.00
10.00
20.00
30.00
40.00
50.00
60.00
70.00
80.00
90.00
100.00
Method Mean
2-D (Conventional Method)
Physical (Gold Standard)
3-D (Sculptor Method)
2-Dimensional
Sculptor
Linear (Sculptor Mean)
Linear (Sculptor Mean+2SD)
Linear (Sculptor Mean-2SD)
Linear (2-Dimensional Mean)
Linear (2- Dimensional Mean + 2SD)
Linear (2-Dimensional Mean - 2SD)

Figure 10.

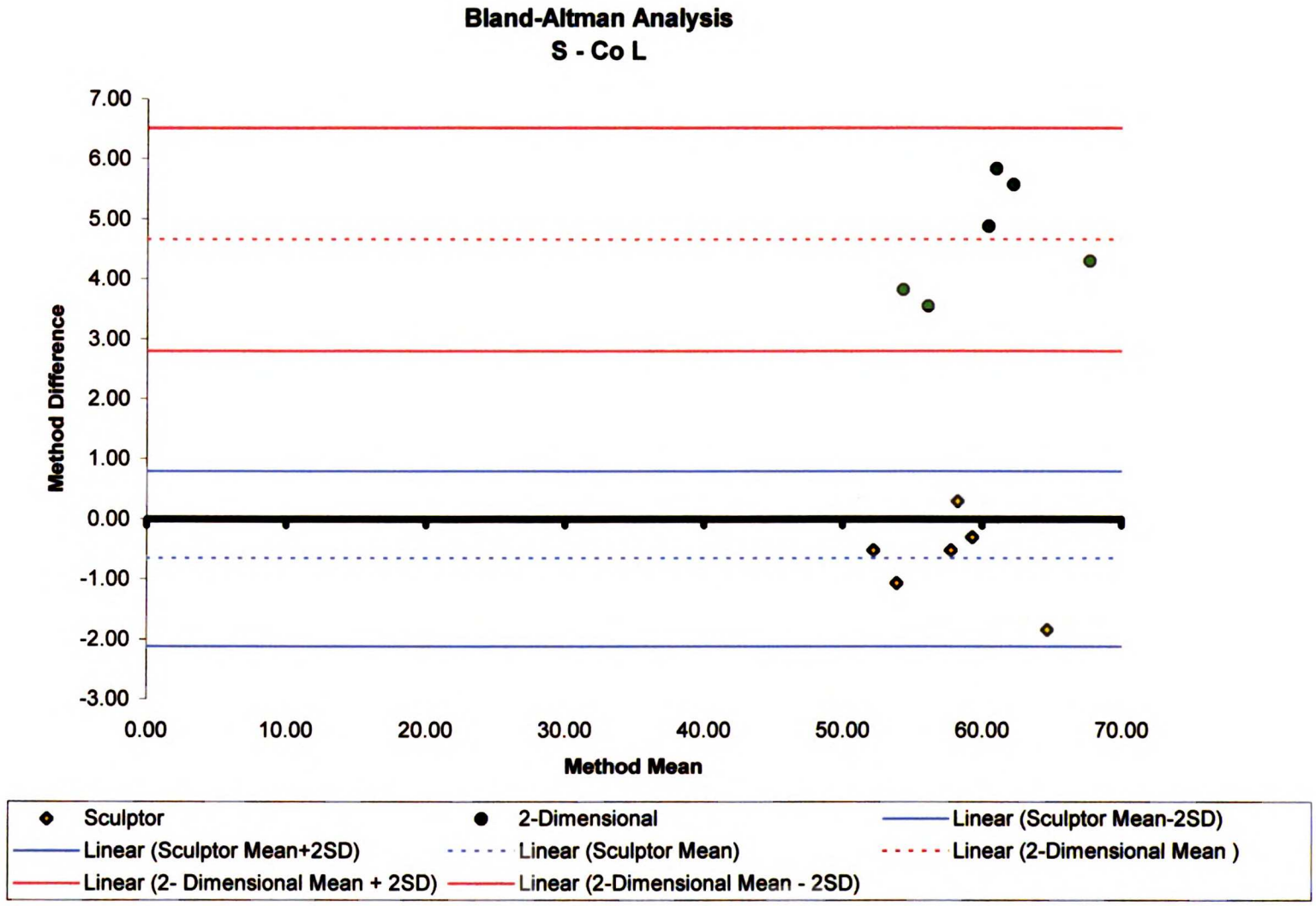
Bland-Altman Analysis
S - Co L
Method Difference
7.00
6.00
5.00
4.00
3.00
2.00
1.00
0.00
-1.00
-2.00
-3.00
0.00
10.00
20.00
30.00
40.00
50.00
60.00
70.00
Method Mean
Sculptor
2-Dimensional
Linear (Sculptor Mean-2SD)
Linear (Sculptor Mean+2SD)
Linear (Sculptor Mean)
Linear (2-Dimensional Mean)
Linear (2- Dimensional Mean + 2SD)
Linear (2-Dimensional Mean - 2SD)

Figure 11.

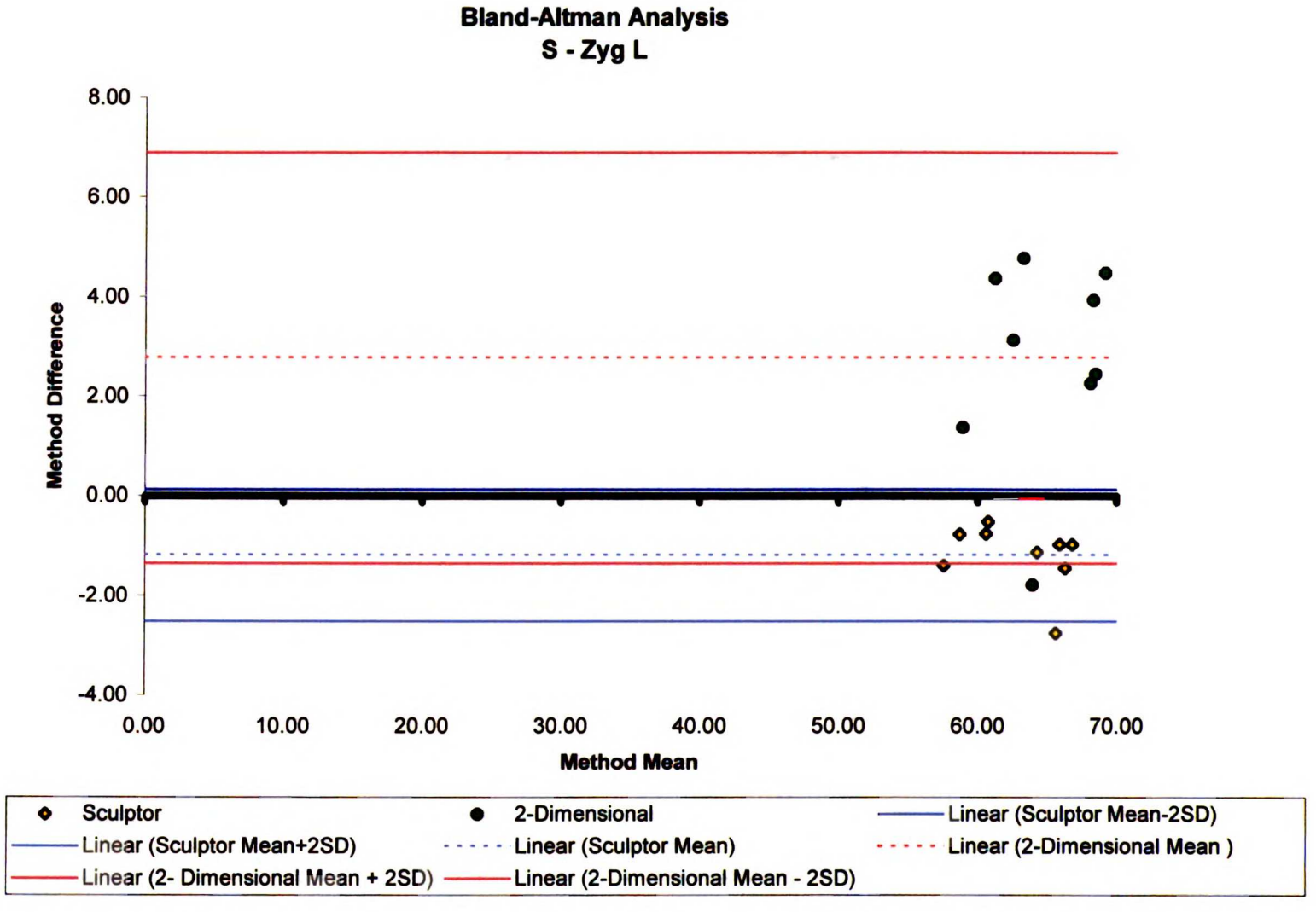
Bland-Altman Analysis
S - Zyg L
8.00
6.00
4.00
2.00
0.00
-2.00
-4.00
Method Difference
0.00
10.00
20.00
30.00
40.00
50.00
60.00
70.00
Method Mean
Sculptor
2-Dimensional
Linear (Sculptor Mean-2SD)
Linear (Sculptor Mean+2SD)
Linear (Sculptor Mean)
Linear (2-Dimensional Mean)
Linear (2- Dimensional Mean + 2SD)
Linear (2-Dimensional Mean - 2SD)

Figure 12.

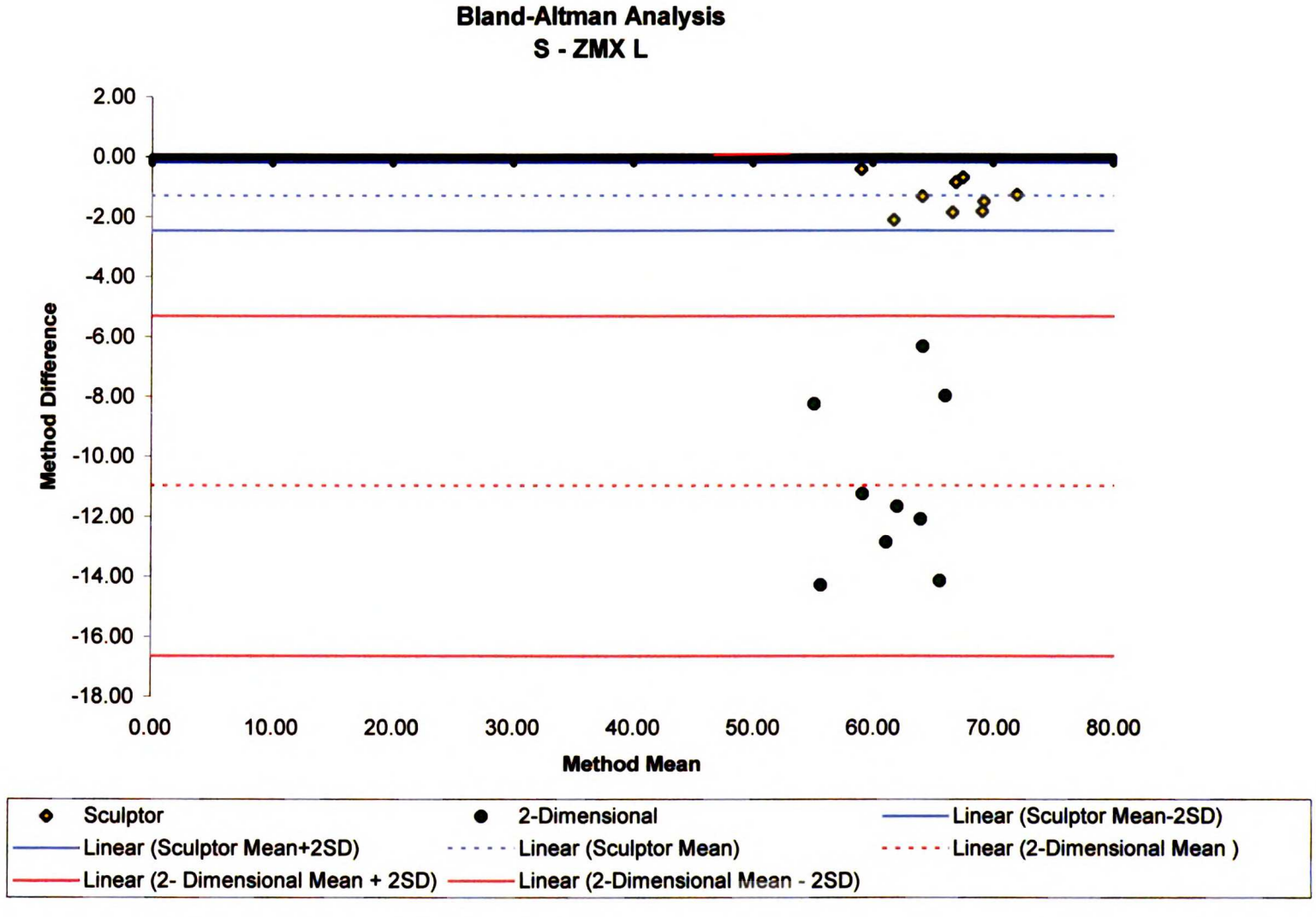
Bland-Altman Analysis
S - ZMX L
Method Difference
2.00
0.00
-2.00
-4.00
-6.00
-8.00
-10.00
-12.00
-14.00
-16.00
-18.00
0.00
10.00
20.00
30.00
40.00
50.00
60.00
70.00
80.00
Method Mean
Sculptor
2-Dimensional
Linear (Sculptor Mean-2SD)
Linear (Sculptor Mean+2SD)
Linear (Sculptor Mean)
Linear (2-Dimensional Mean)
Linear (2- Dimensional Mean + 2SD)
Linear (2-Dimensional Mean - 2SD)

Figure 13.

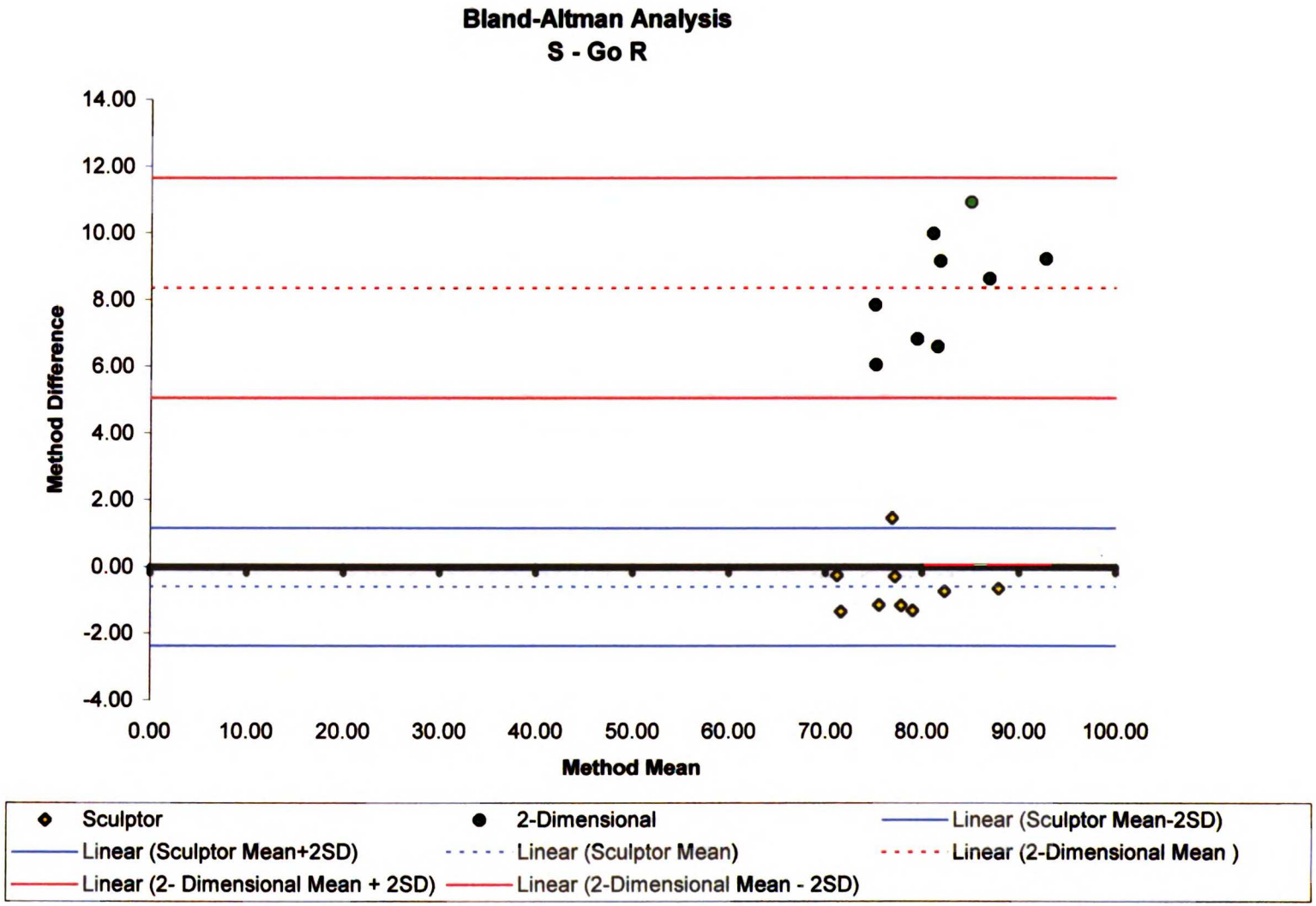
Bland-Altman Analysis
S - Go R
Method Difference
14.00
12.00
10.00
8.00
6.00
4.00
2.00
0.00
-2.00
-4.00
0.00
10.00
20.00
30.00
40.00
50.00
60.00
70.00
80.00
90.00
100.00
Method Mean
Sculptor
2-Dimensional
Linear (Sculptor Mean-2SD)
Linear (Sculptor Mean+2SD)
Linear (Sculptor Mean)
Linear (2-Dimensional Mean)
Linear (2- Dimensional Mean + 2SD)
Linear (2-Dimensional Mean - 2SD)

Figure 14.

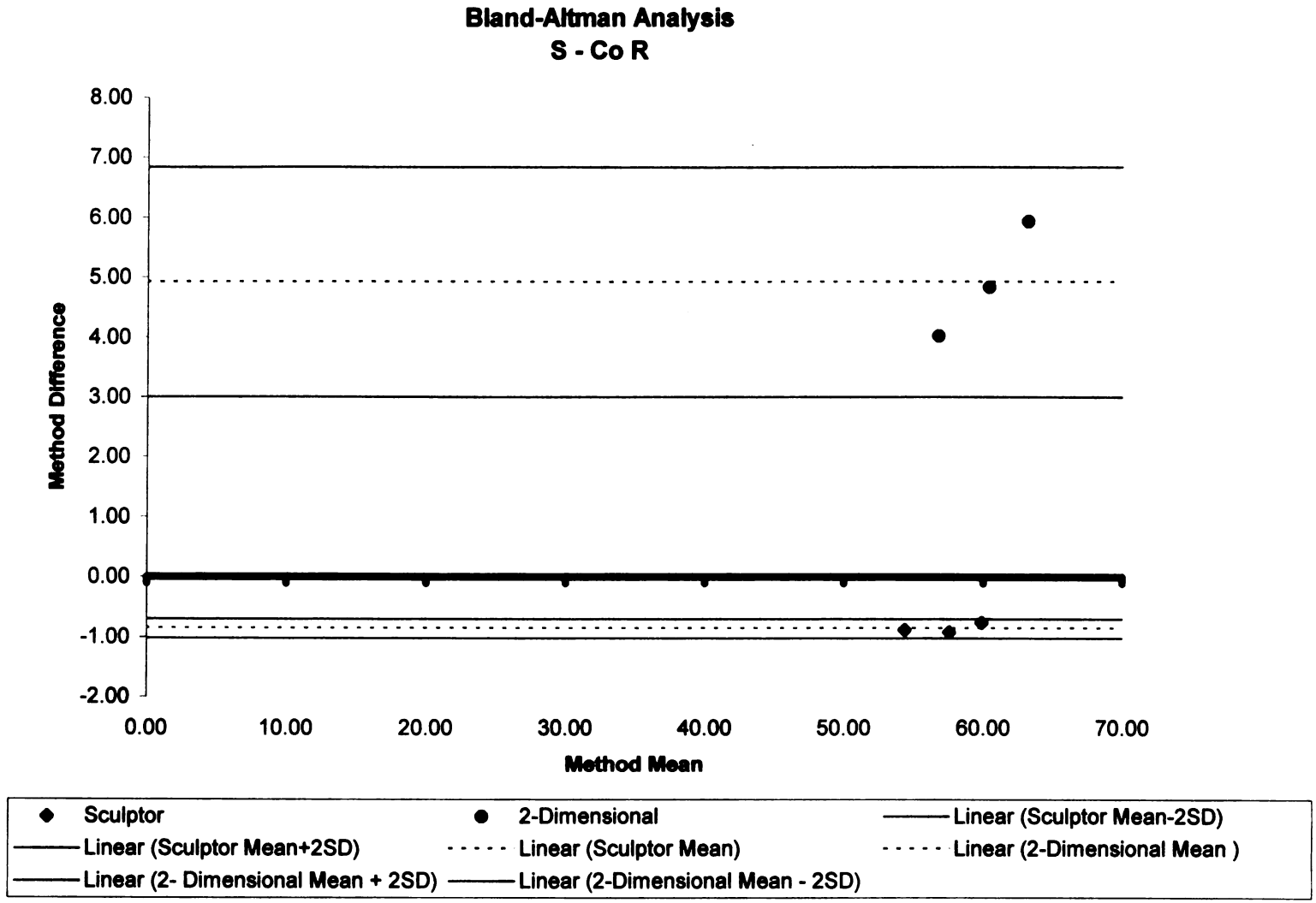
Bland-Altman Analysis
S - Co R
Method Difference
8.00
7.00
6.00
5.00
4.00
3.00
2.00
1.00
0.00
-1.00
-2.00
0.00
10.00
20.00
30.00
40.00
50.00
60.00
70.00
Method Mean
Sculptor
2-Dimensional
Linear (Sculptor Mean-2SD)
Linear (Sculptor Mean+2SD)
Linear (Sculptor Mean)
Linear (2-Dimensional Mean)
Linear (2- Dimensional Mean + 2SD)
Linear (2-Dimensional Mean - 2SD)

Figure 15.

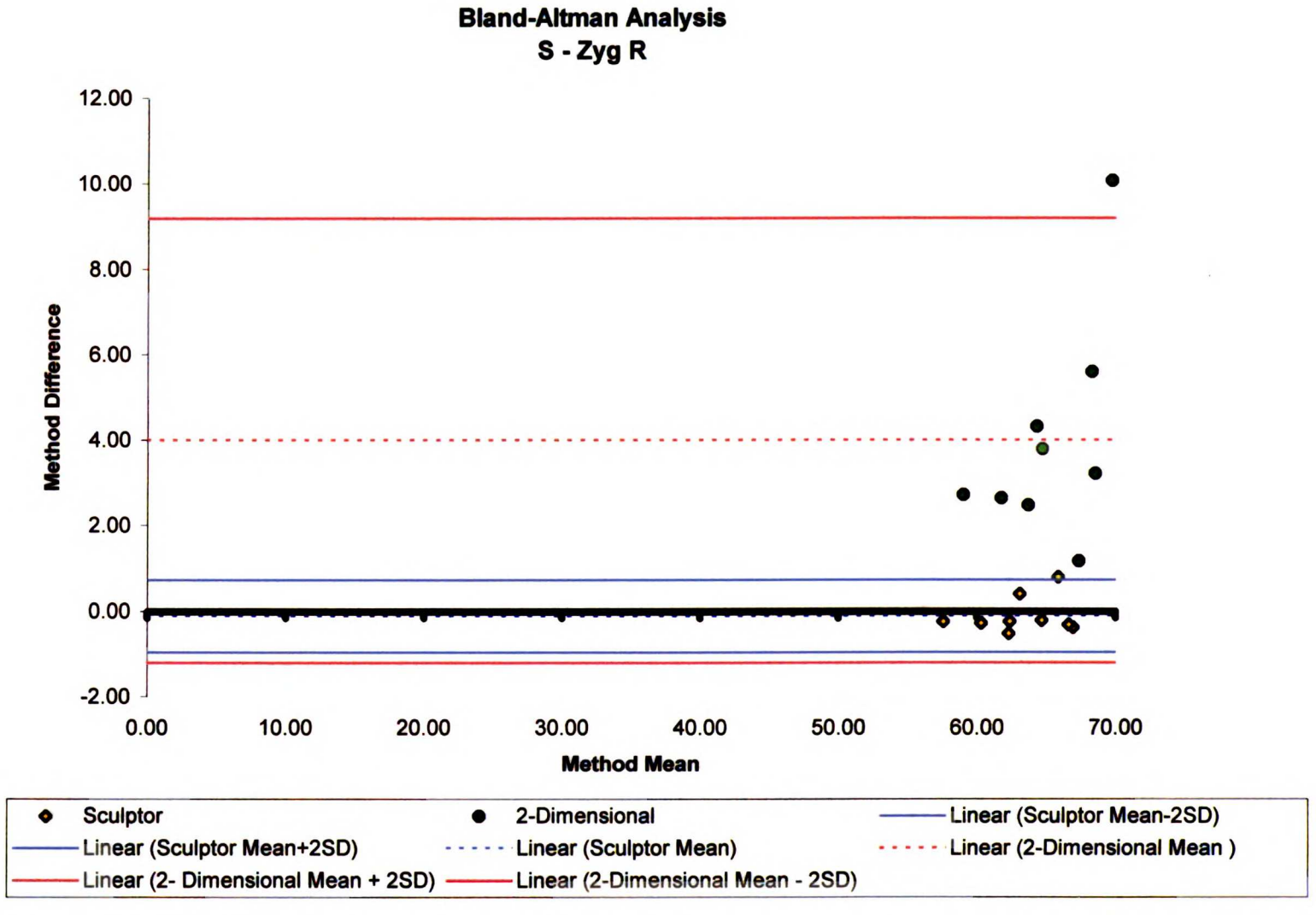
Bland-Altman Analysis
S - Zyg R
12.00
10.00
8.00
6.00
4.00
2.00
0.00
-2.00
Method Difference
0.00
10.00
20.00
30.00
40.00
50.00
60.00
70.00
Method Mean
Sculptor
2-Dimensional
Linear (Sculptor Mean-2SD)
Linear (Sculptor Mean+2SD)
Linear (Sculptor Mean)
Linear (2-Dimensional Mean)
Linear (2- Dimensional Mean + 2SD)
Linear (2-Dimensional Mean - 2SD)

Figure 16.

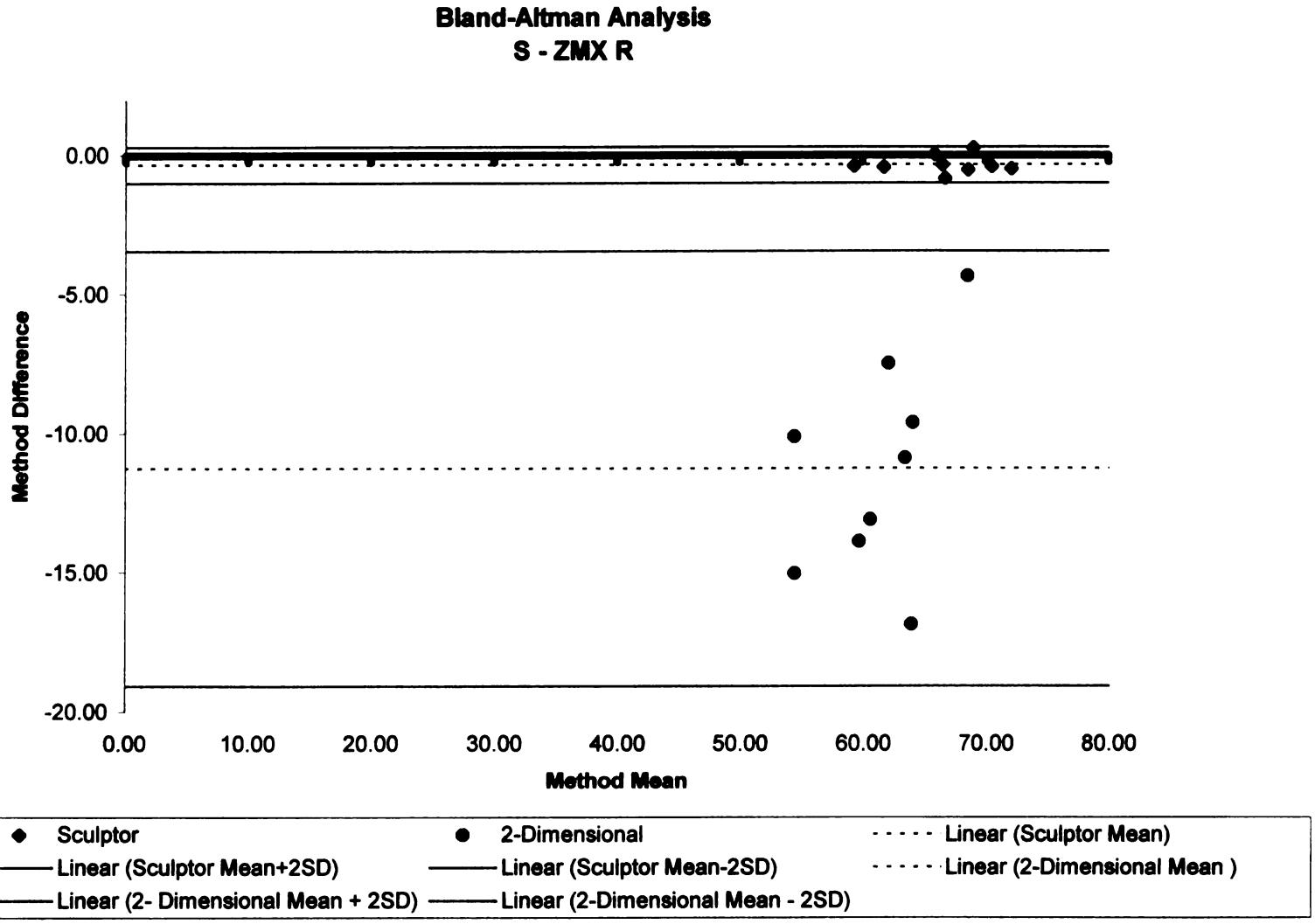
Bland-Altman Analysis
S - ZMX R
0.00
-5.00
-10.00
-15.00
-20.00
Method Difference
0.00
10.00
20.00
30.00
40.00
50.00
60.00
70.00
80.00
Method Mean
Sculptor
2-Dimensional
Linear (Sculptor Mean)
Linear (Sculptor Mean+2SD)
Linear (Sculptor Mean-2SD)
Linear (2-Dimensional Mean)
Linear (2- Dimensional Mean + 2SD)
Linear (2-Dimensional Mean - 2SD)

Figure 17.

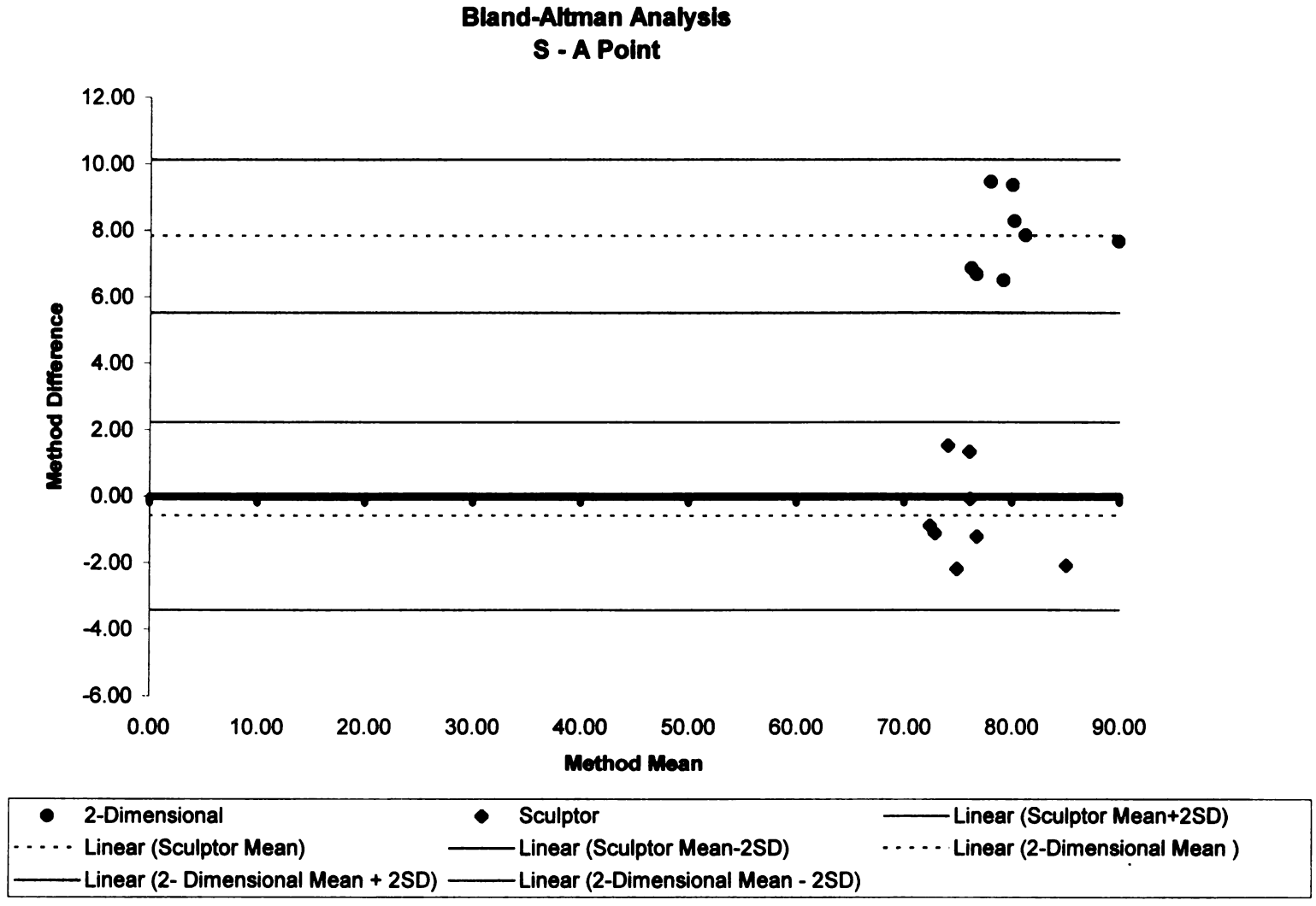
Bland-Altman Analysis
S - A Point
Method Difference
12.00
10.00
8.00
6.00
4.00
2.00
0.00
-2.00
-4.00
-6.00
0.00
10.00
20.00
30.00
40.00
50.00
60.00
70.00
80.00
90.00
Method Mean
2-Dimensional
Sculptor
Linear (Sculptor Mean+2SD)
Linear (Sculptor Mean)
Linear (Sculptor Mean-2SD)
Linear (2-Dimensional Mean)
Linear (2- Dimensional Mean + 2SD)
Linear (2-Dimensional Mean - 2SD)

Figure 18.

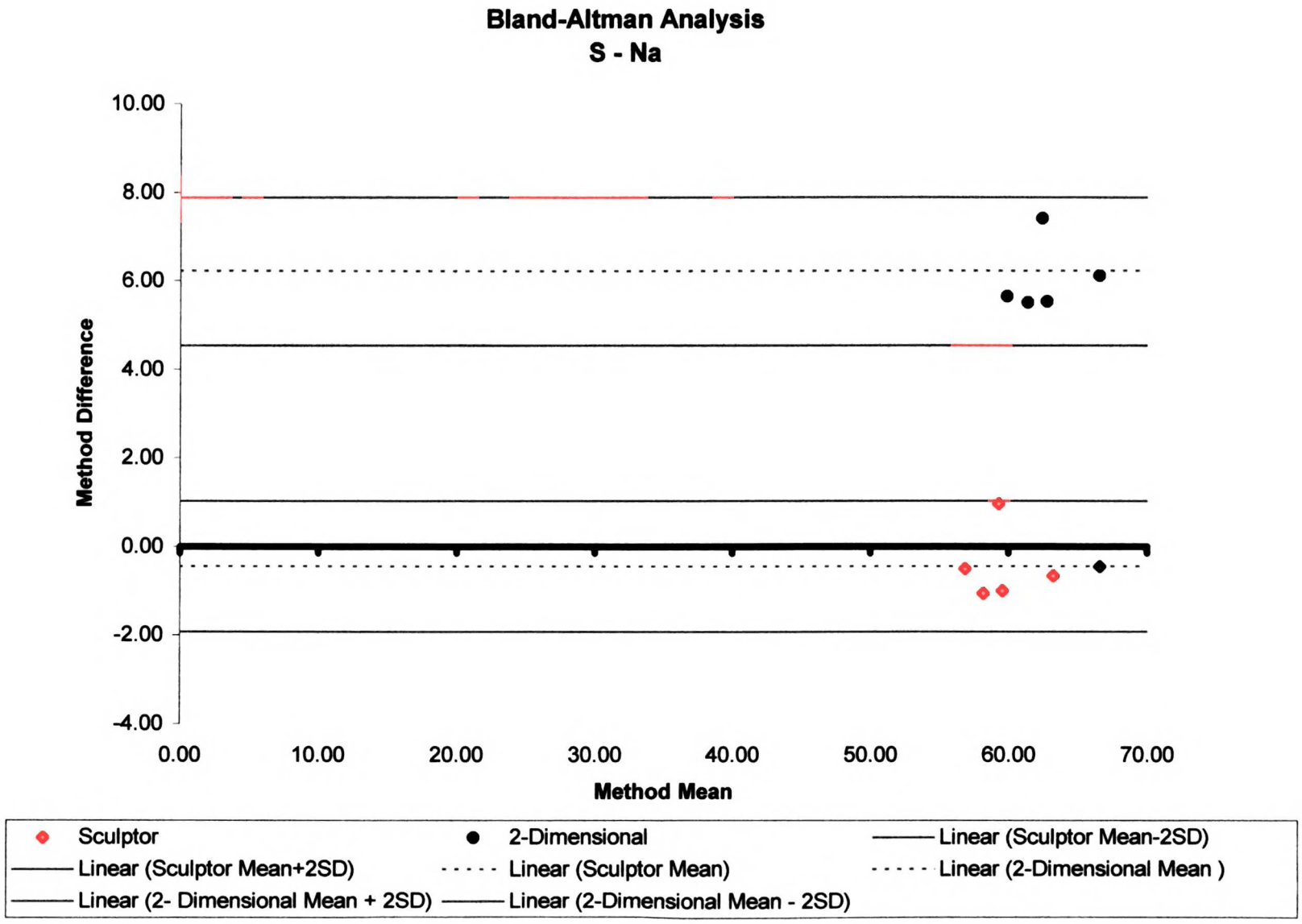
Bland-Altman Analysis
S - Na
Method Difference
10.00
8.00
6.00
4.00
2.00
0.00
-2.00
-4.00
0.00
10.00
20.00
30.00
40.00
50.00
60.00
70.00
Method Mean
Sculptor
2-Dimensional
Linear (Sculptor Mean-2SD)
Linear (Sculptor Mean+2SD)
Linear (Sculptor Mean)
Linear (2-Dimensional Mean)
Linear (2- Dimensional Mean + 2SD)
Linear (2-Dimensional Mean - 2SD)

Figure 19.

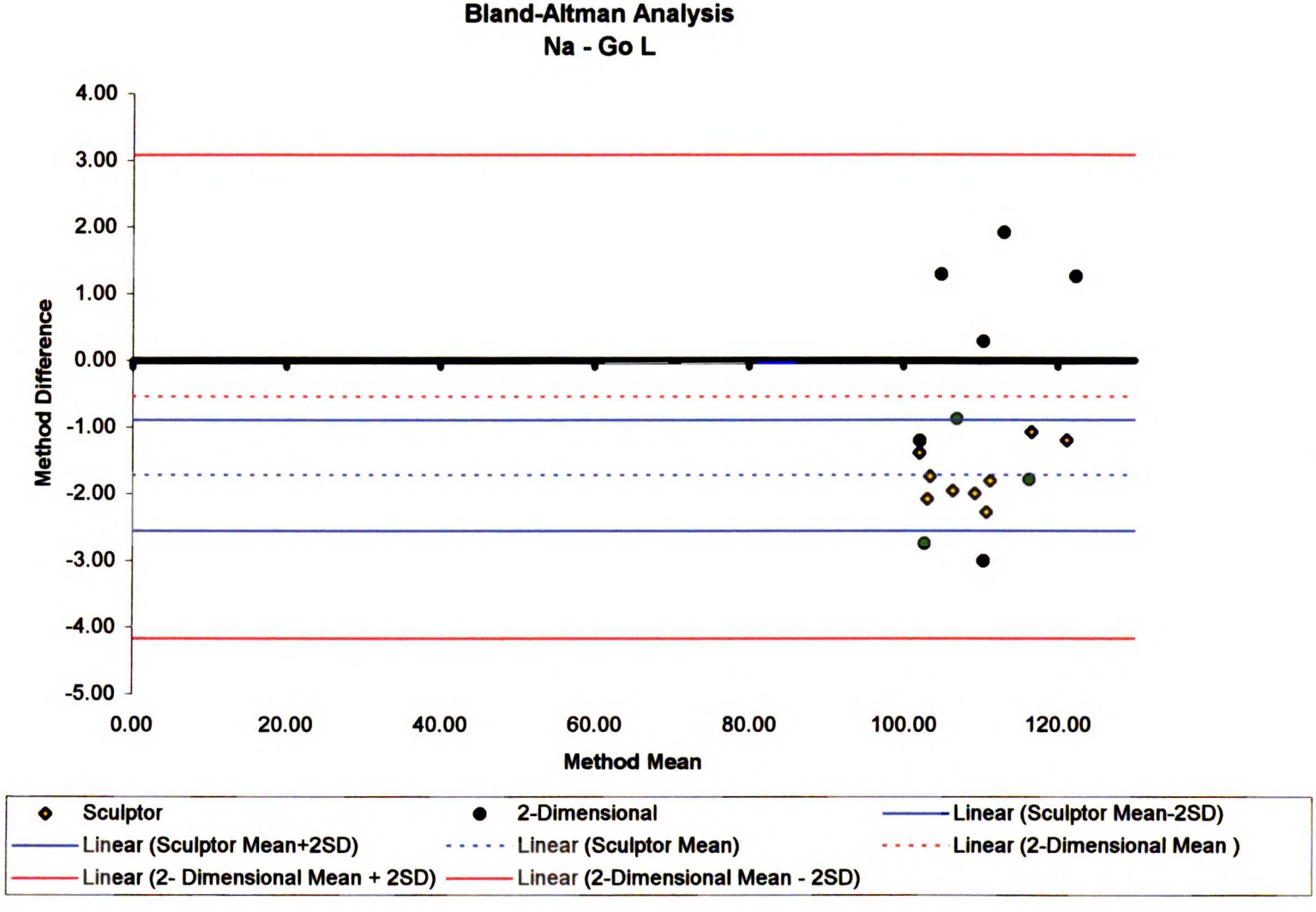
Bland-Altman Analysis
Na - Go L
Method Difference
4.00
3.00
2.00
1.00
0.00
-1.00
-2.00
-3.00
-4.00
-5.00
0.00
20.00
40.00
60.00
80.00
100.00
120.00
Method Mean
Sculptor
2-Dimensional
Linear (Sculptor Mean-2SD)
Linear (Sculptor Mean+2SD)
Linear (Sculptor Mean)
Linear (2-Dimensional Mean)
Linear (2- Dimensional Mean + 2SD)
Linear (2-Dimensional Mean - 2SD)

Figure 20.

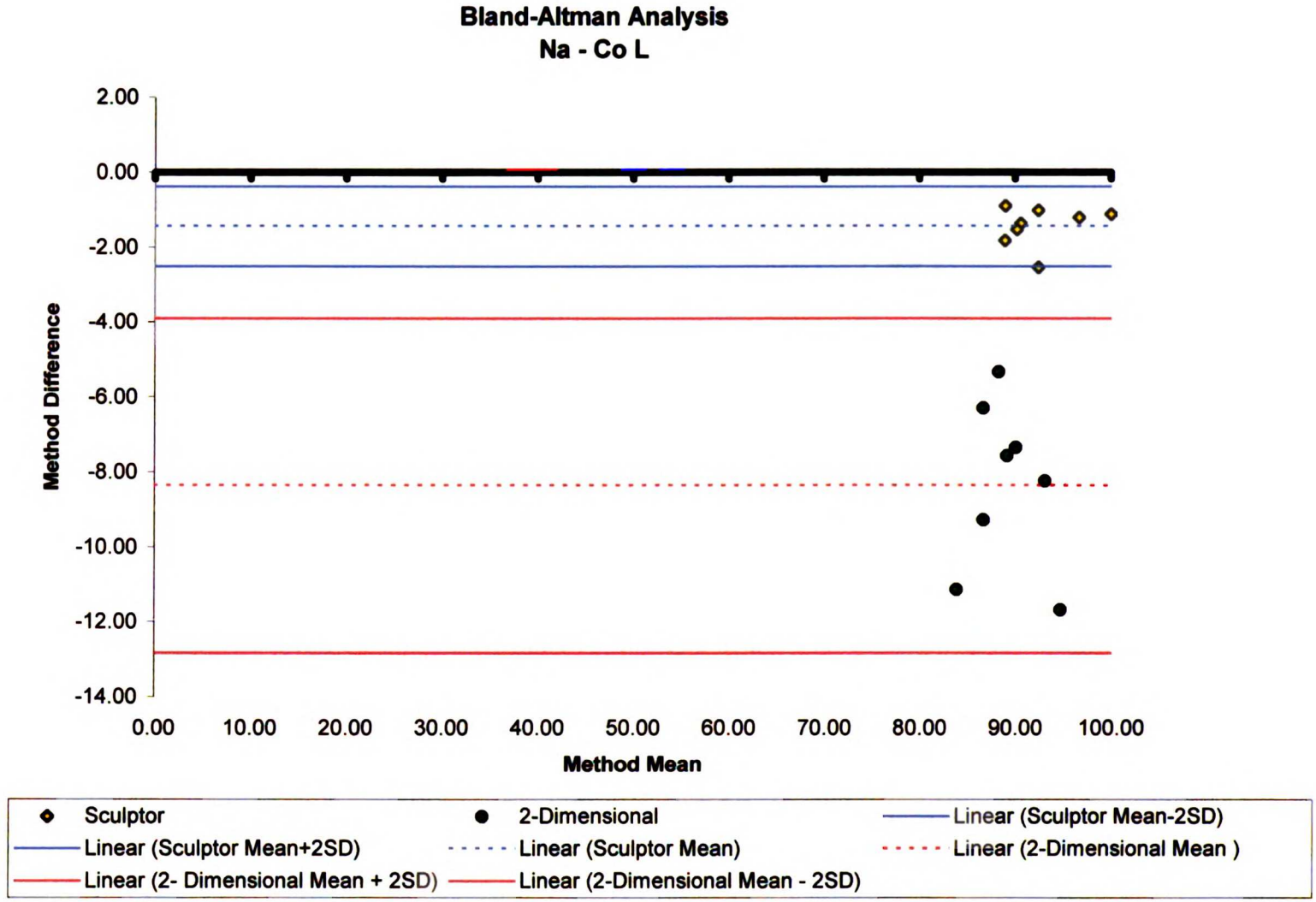
Bland-Altman Analysis
Na - Co L
Method Difference
2.00
0.00
-2.00
-4.00
-6.00
-8.00
-10.00
-12.00
-14.00
0.00
10.00
20.00
30.00
40.00
50.00
60.00
70.00
80.00
90.00
100.00
Method Mean
Sculptor
2-Dimensional
Linear (Sculptor Mean-2SD)
Linear (Sculptor Mean+2SD)
Linear (Sculptor Mean)
Linear (2-Dimensional Mean)
Linear (2- Dimensional Mean + 2SD)
Linear (2-Dimensional Mean - 2SD)

Figure 21.

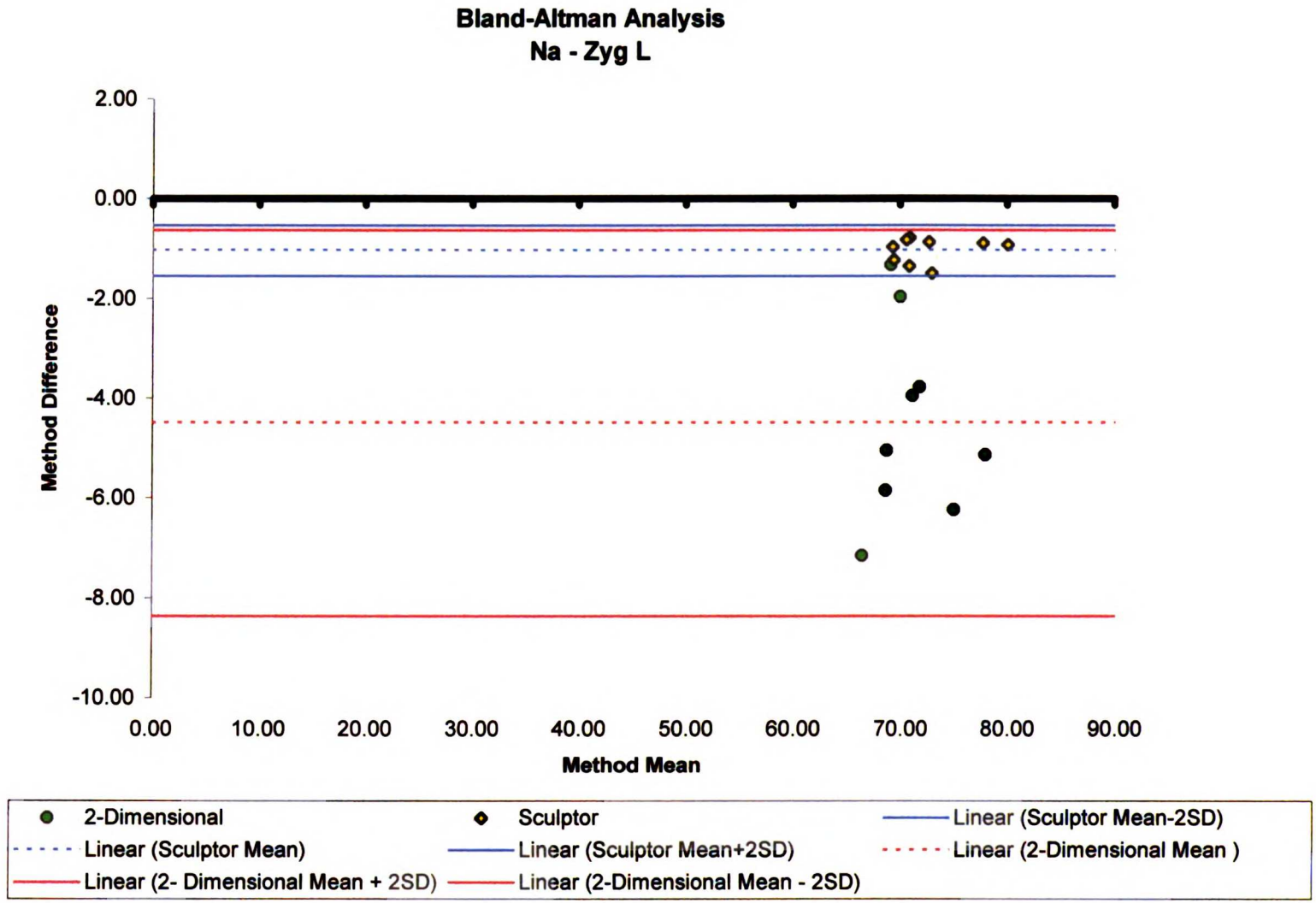
Bland-Altman Analysis
Na - Zyg L
Method Difference
2.00
0.00
-2.00
-4.00
-6.00
-8.00
-10.00
0.00
10.00
20.00
30.00
40.00
50.00
60.00
70.00
80.00
90.00
Method Mean
2-Dimensional
Sculptor
Linear (Sculptor Mean-2SD)
Linear (Sculptor Mean)
Linear (Sculptor Mean+2SD)
Linear (2-Dimensional Mean)
Linear (2- Dimensional Mean + 2SD)
Linear (2-Dimensional Mean - 2SD)

Figure 22.

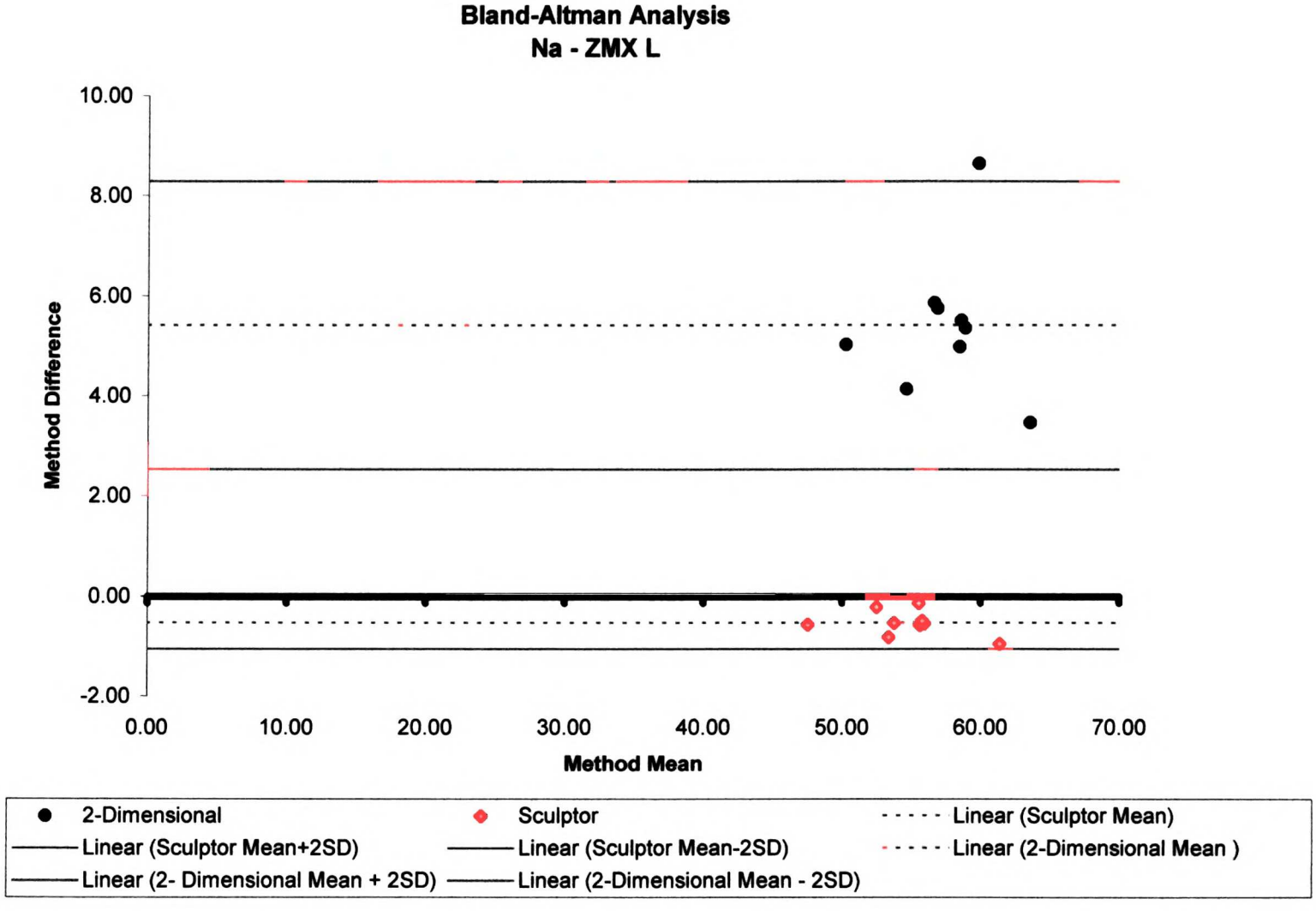
Bland-Altman Analysis
Na - ZMX L
Method Difference
10.00
8.00
6.00
4.00
2.00
0.00
-2.00
0.00
10.00
20.00
30.00
40.00
50.00
60.00
70.00
Method Mean
2-Dimensional
Sculptor
Linear (Sculptor Mean)
Linear (Sculptor Mean+2SD)
Linear (Sculptor Mean-2SD)
Linear (2-Dimensional Mean)
Linear (2- Dimensional Mean + 2SD)
Linear (2-Dimensional Mean - 2SD)

Figure 23.

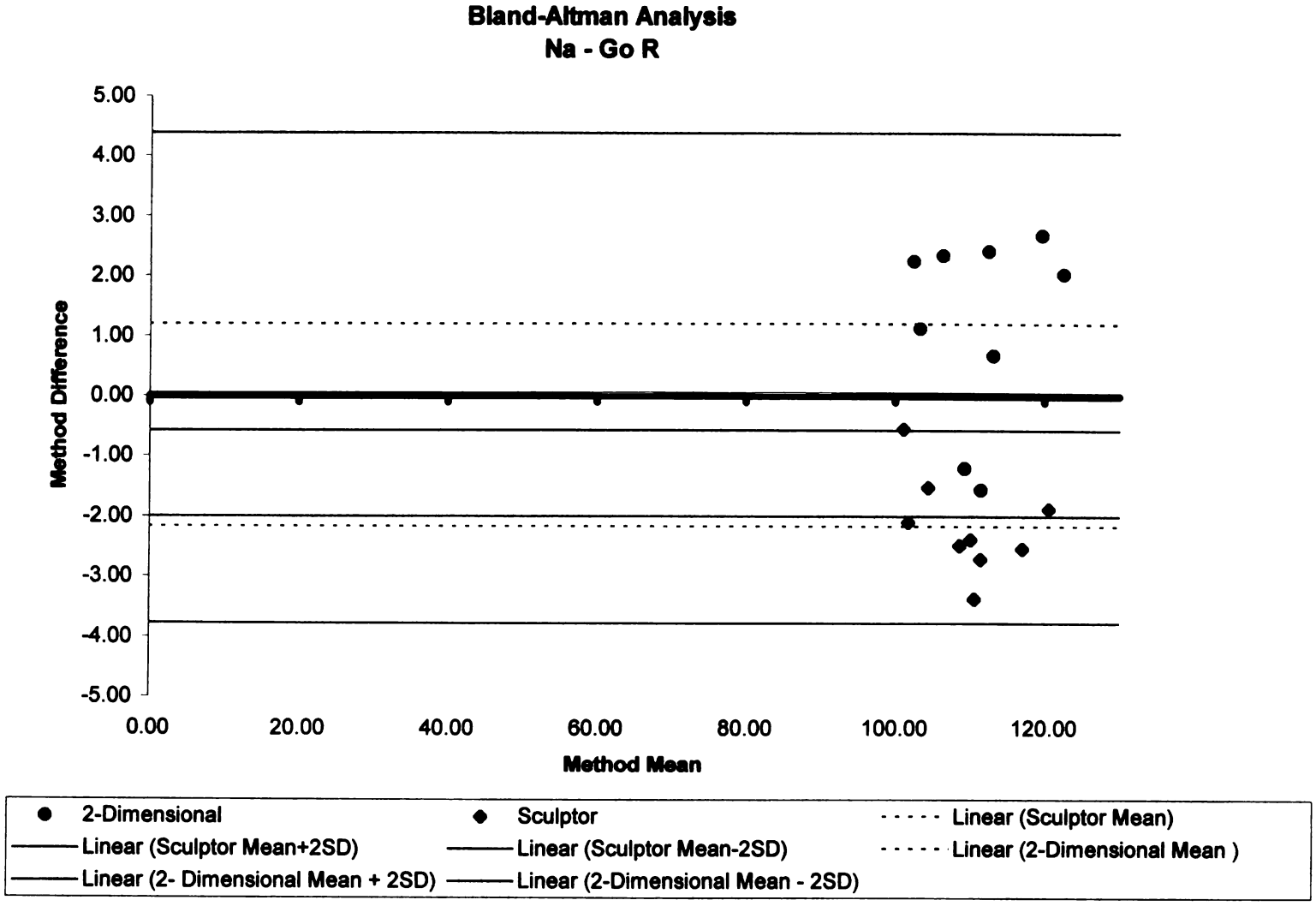
Bland-Altman Analysis
Na - Go R
Method Difference
5.00
4.00
3.00
2.00
1.00
0.00
-1.00
-2.00
-3.00
-4.00
-5.00
0.00
20.00
40.00
60.00
80.00
100.00
120.00
Method Mean
2-Dimensional
Sculptor
Linear (Sculptor Mean)
Linear (Sculptor Mean+2SD)
Linear (Sculptor Mean-2SD)
Linear (2-Dimensional Mean)
Linear (2- Dimensional Mean + 2SD)
Linear (2-Dimensional Mean - 2SD)

Figure 24.

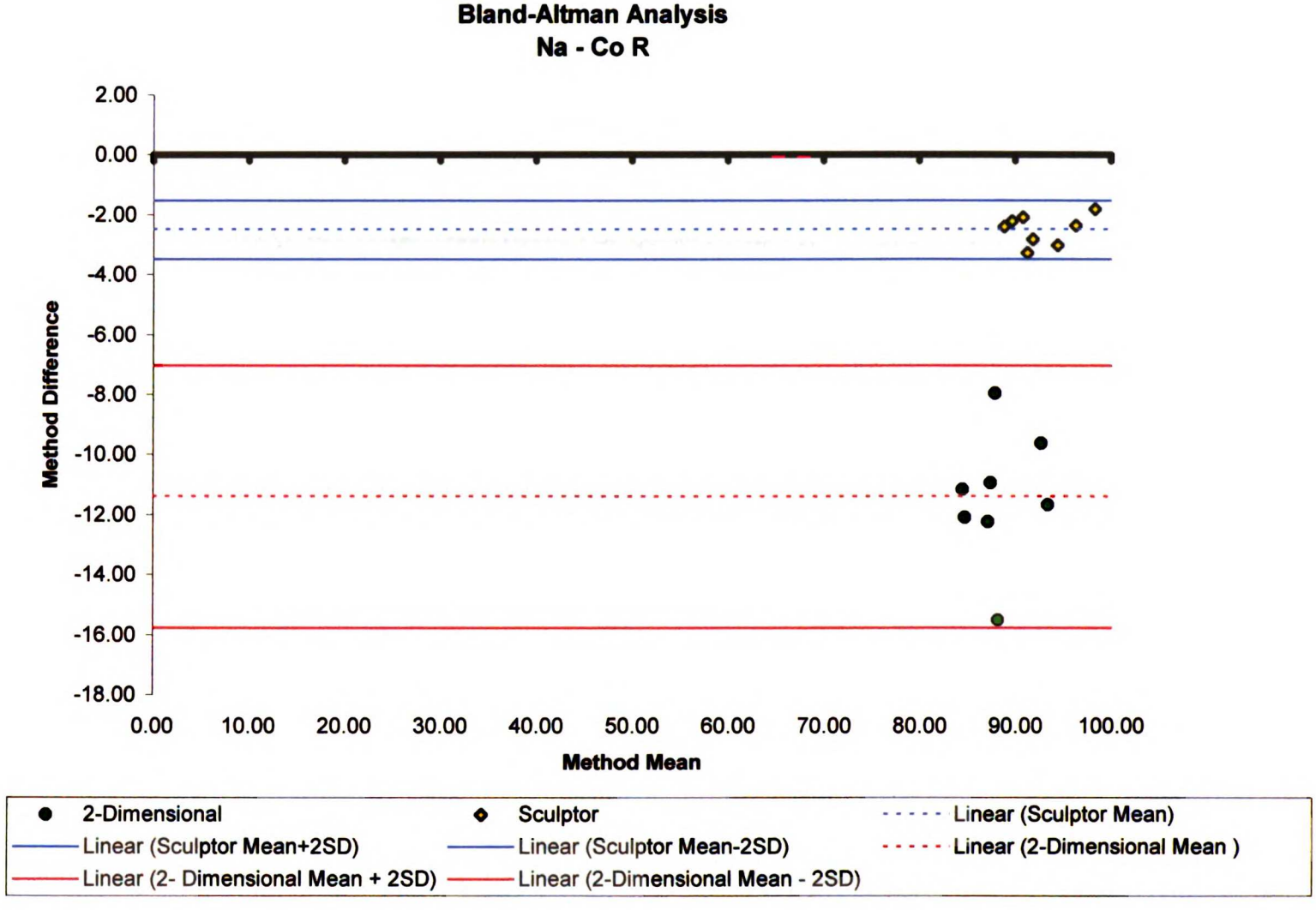
Bland-Altman Analysis
Na - Co R
Method Difference
2.00
0.00
-2.00
-4.00
-6.00
-8.00
-10.00
-12.00
-14.00
-16.00
-18.00
0.00
10.00
20.00
30.00
40.00
50.00
60.00
70.00
80.00
90.00
100.00
Method Mean
2-Dimensional
Sculptor
Linear (Sculptor Mean)
Linear (Sculptor Mean+2SD)
Linear (Sculptor Mean-2SD)
Linear (2-Dimensional Mean)
Linear (2- Dimensional Mean + 2SD)
Linear (2-Dimensional Mean - 2SD)

Figure 25.

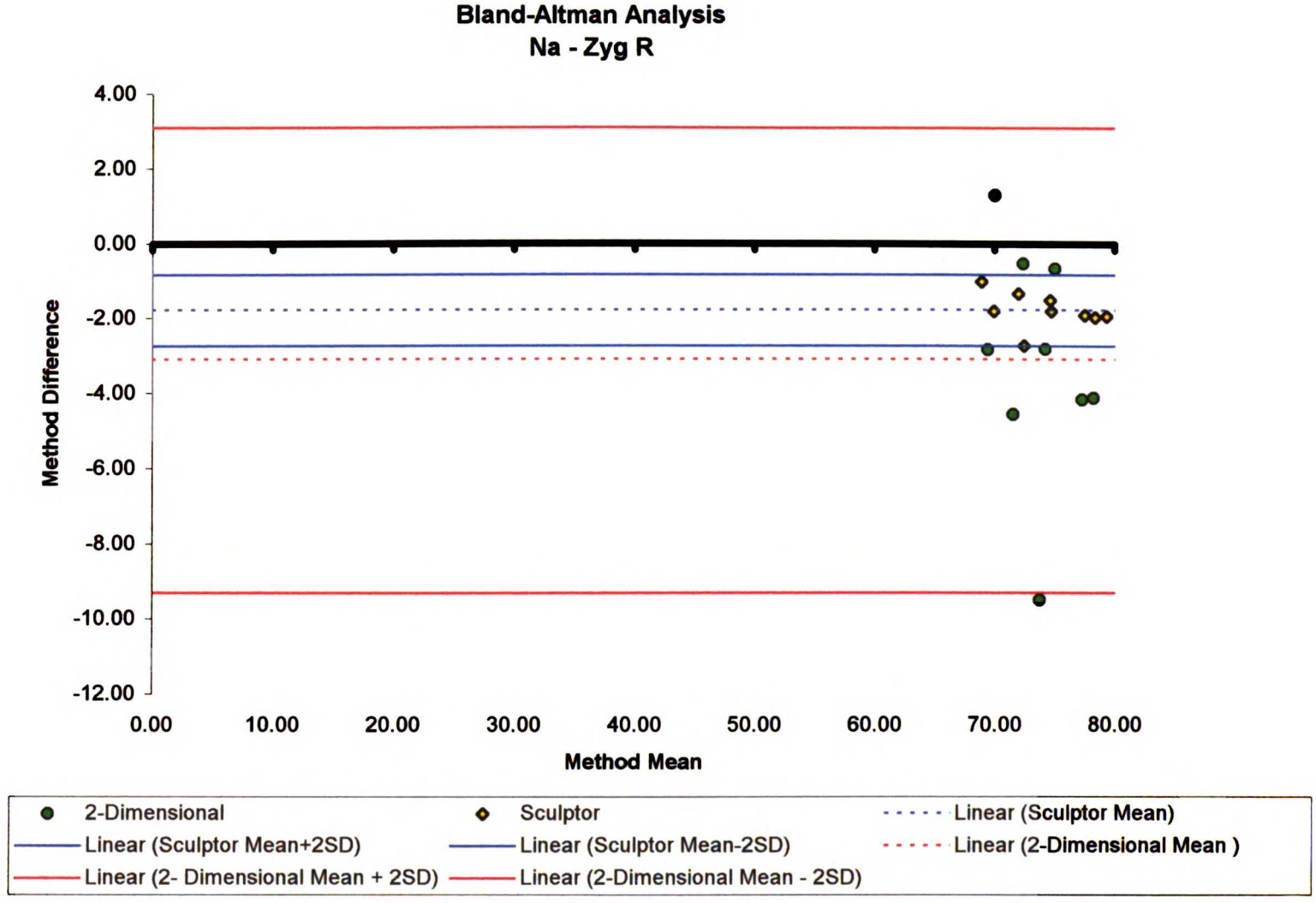
Bland-Altman Analysis
Na - Zyg R
Method Difference
4.00
2.00
0.00
-2.00
-4.00
-6.00
-8.00
-10.00
-12.00
0.00
10.00
20.00
30.00
40.00
50.00
60.00
70.00
80.00
Method Mean
2-Dimensional
Sculptor
Linear (Sculptor Mean)
Linear (Sculptor Mean+2SD)
Linear (Sculptor Mean-2SD)
Linear (2-Dimensional Mean)
Linear (2- Dimensional Mean + 2SD)
Linear (2-Dimensional Mean - 2SD)

Figure 26.

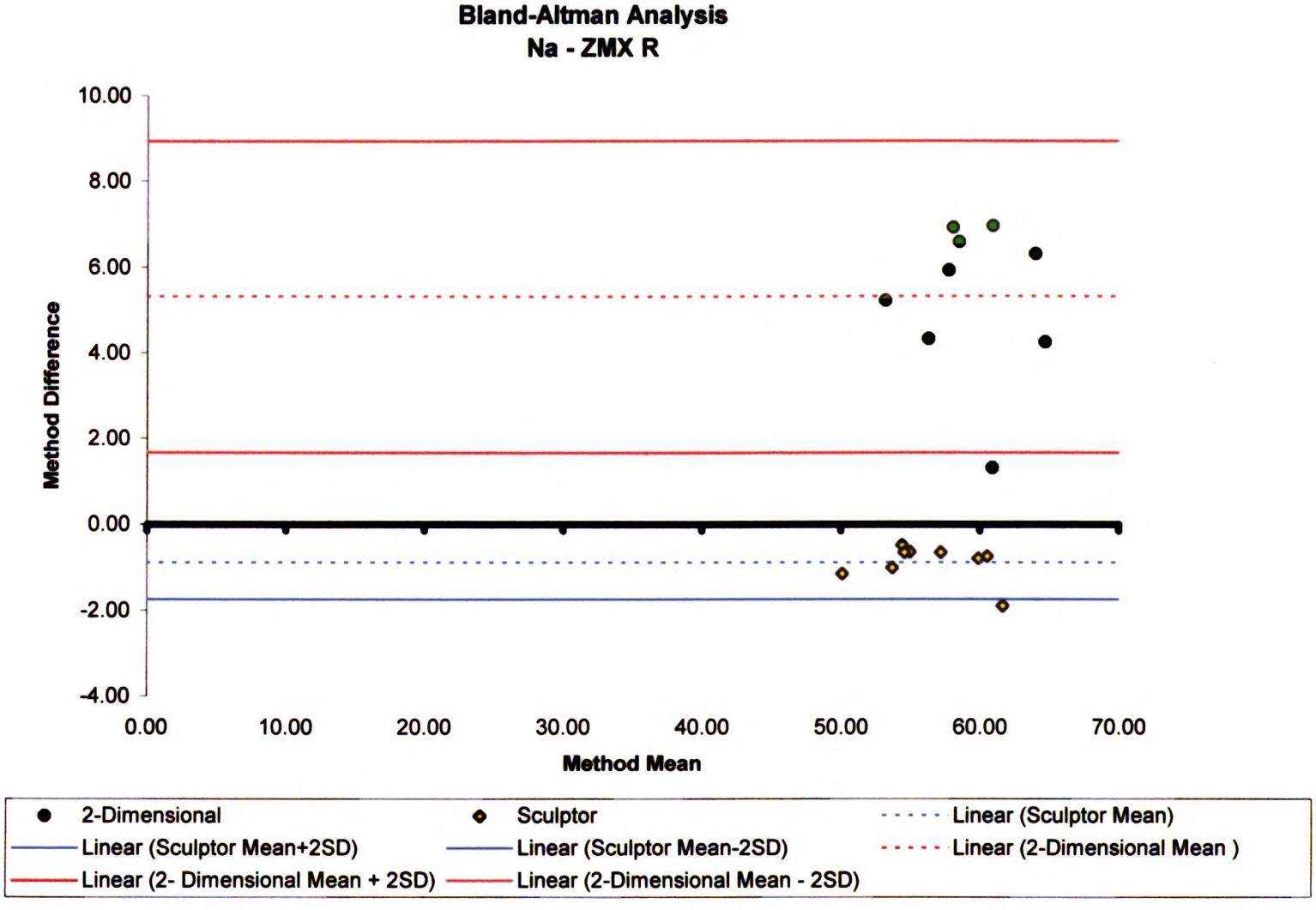
Bland-Altman Analysis
Na - ZMX R
Method Difference
10.00
8.00
6.00
4.00
2.00
0.00
-2.00
-4.00
0.00
10.00
20.00
30.00
40.00
50.00
60.00
70.00
Method Mean
2-Dimensional
Sculptor
Linear (Sculptor Mean)
Linear (Sculptor Mean+2SD)
Linear (Sculptor Mean-2SD)
Linear (2-Dimensional Mean)
Linear (2- Dimensional Mean + 2SD)
Linear (2-Dimensional Mean - 2SD)

Figure 27.

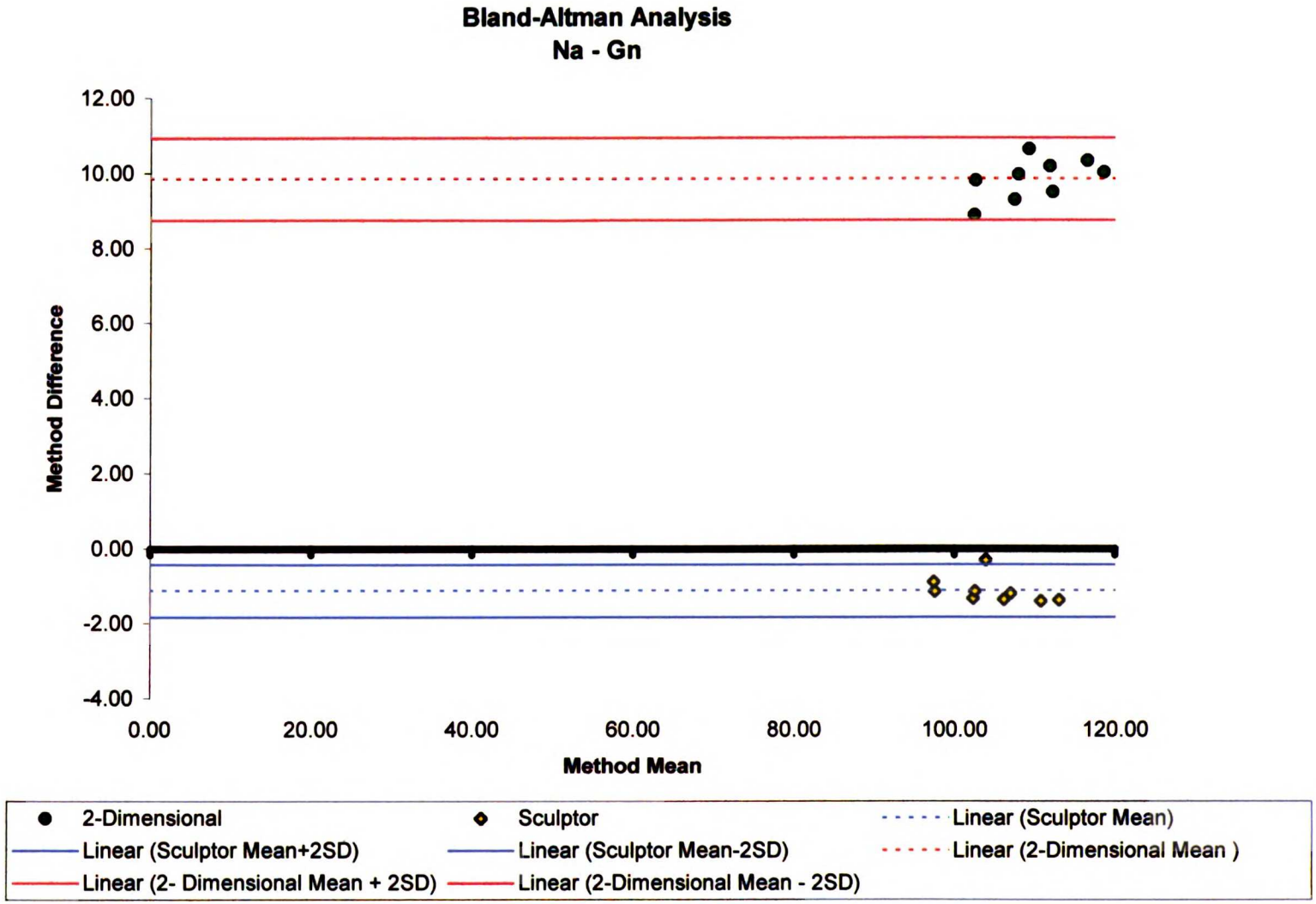
Bland-Altman Analysis
Na - Gn
12.00
10.00
8.00
6.00
4.00
2.00
0.00
-2.00
-4.00
Method Difference
0.00
20.00
40.00
60.00
80.00
100.00
120.00
Method Mean
2-Dimensional
Sculptor
Linear (Sculptor Mean)
Linear (Sculptor Mean+2SD)
Linear (Sculptor Mean-2SD)
Linear (2-Dimensional Mean)
Linear (2- Dimensional Mean + 2SD)
Linear (2-Dimensional Mean - 2SD)

Figure 28.

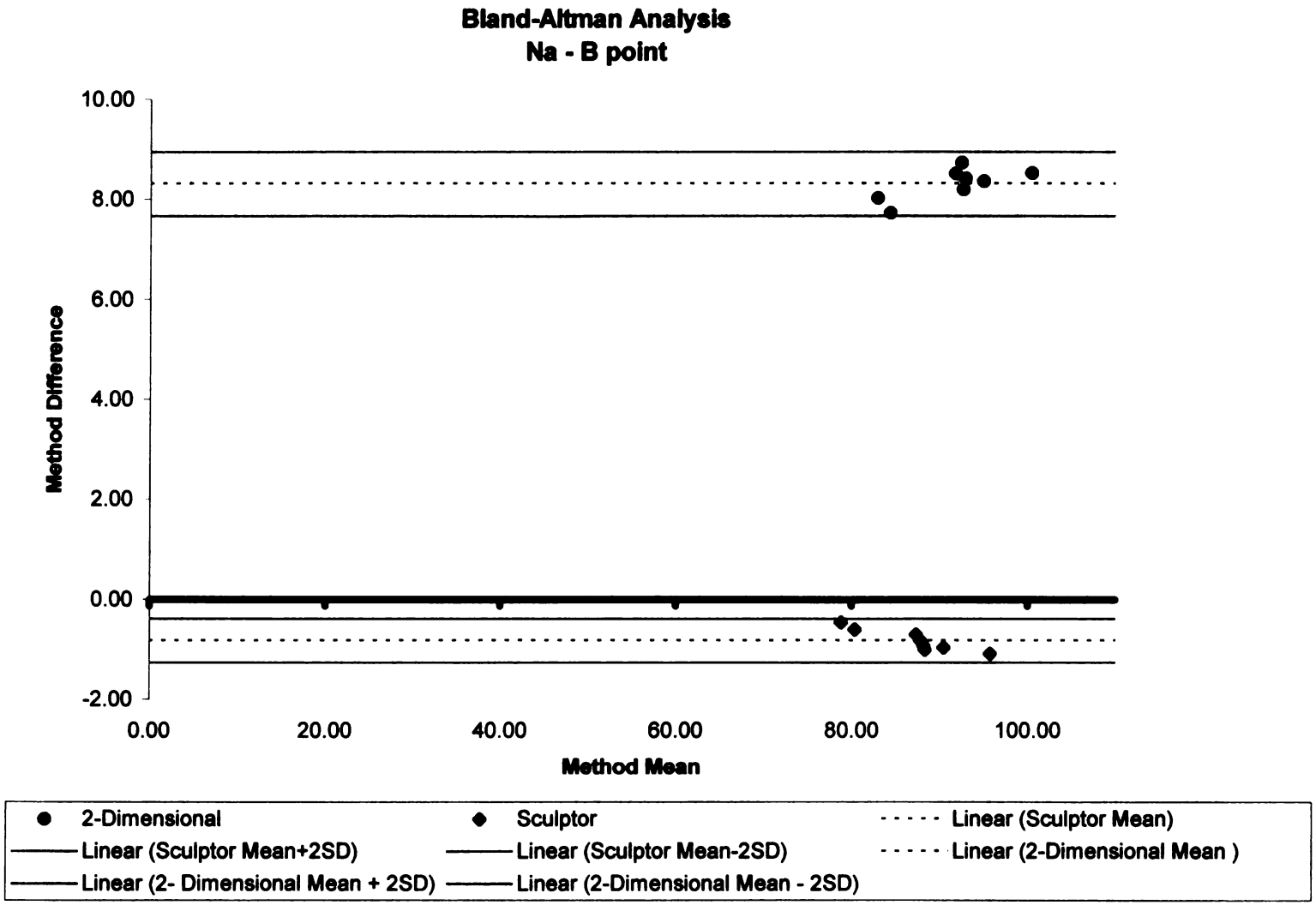
Bland-Altman Analysis
Na - B point
Method Difference
10.00
8.00
6.00
4.00
2.00
0.00
-2.00
0.00
20.00
40.00
60.00
80.00
100.00
Method Mean
2-Dimensional
Sculptor
Linear (Sculptor Mean)
Linear (Sculptor Mean+2SD)
Linear (Sculptor Mean-2SD)
Linear (2-Dimensional Mean)
Linear (2- Dimensional Mean + 2SD)
Linear (2-Dimensional Mean - 2SD)

Figure 29.

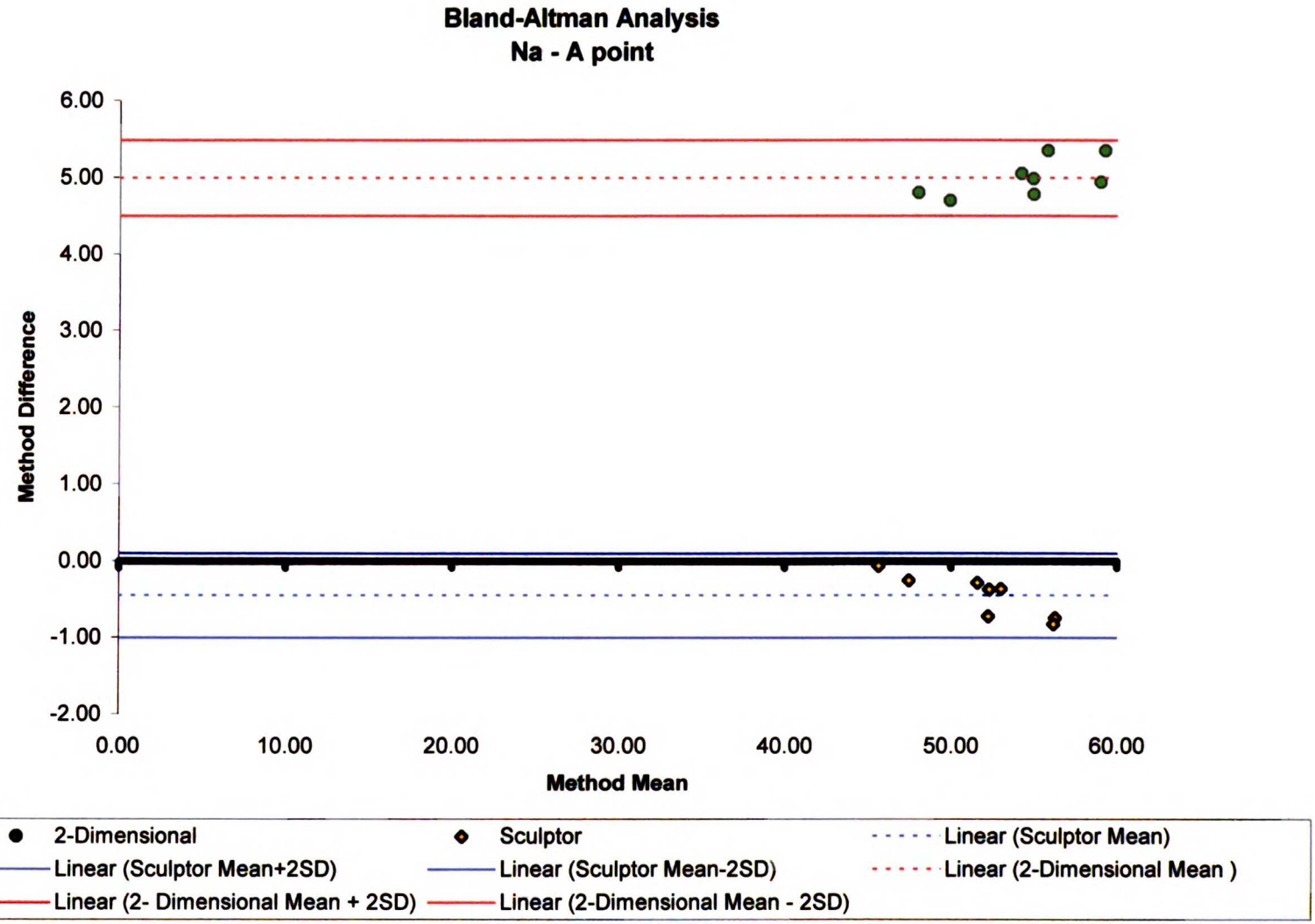
Bland-Altman Analysis
Na - A point
Method Difference
6.00
5.00
4.00
3.00
2.00
1.00
0.00
-1.00
-2.00
0.00
10.00
20.00
30.00
40.00
50.00
60.00
Method Mean
2-Dimensional
Sculptor
Linear (Sculptor Mean)
Linear (Sculptor Mean+2SD)
Linear (Sculptor Mean-2SD)
Linear (2-Dimensional Mean)
Linear (2- Dimensional Mean + 2SD)
Linear (2-Dimensional Mean - 2SD)

Figure 30.

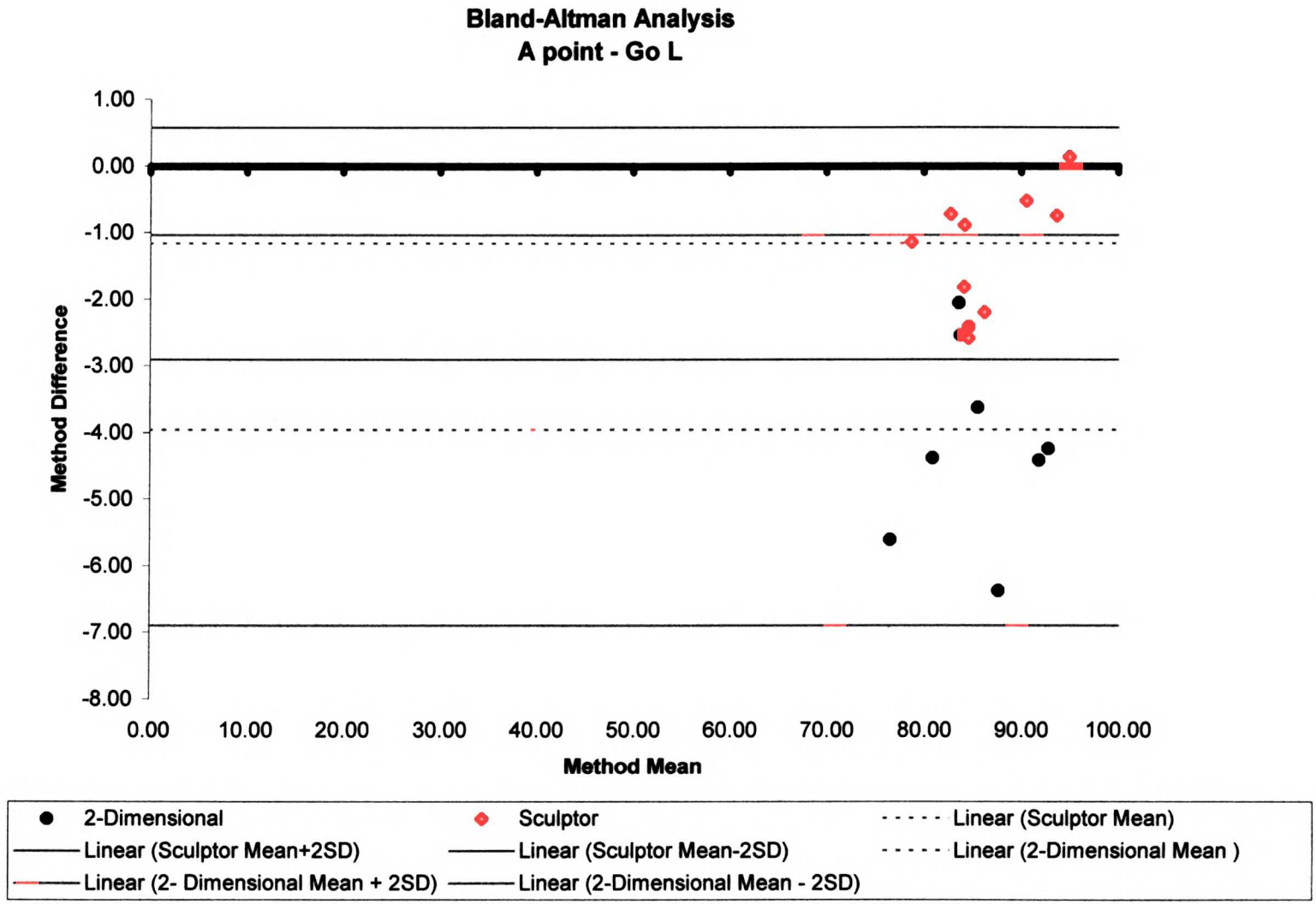
Bland-Altman Analysis
A point - Go L
Method Difference
1.00
0.00
-1.00
-2.00
-3.00
-4.00
-5.00
-6.00
-7.00
-8.00
0.00
10.00
20.00
30.00
40.00
50.00
60.00
70.00
80.00
90.00
100.00
Method Mean
2-Dimensional
Sculptor
Linear (Sculptor Mean)
Linear (Sculptor Mean+2SD)
Linear (Sculptor Mean-2SD)
Linear (2-Dimensional Mean)
Linear (2- Dimensional Mean + 2SD)
Linear (2-Dimensional Mean - 2SD)

Figure 31.

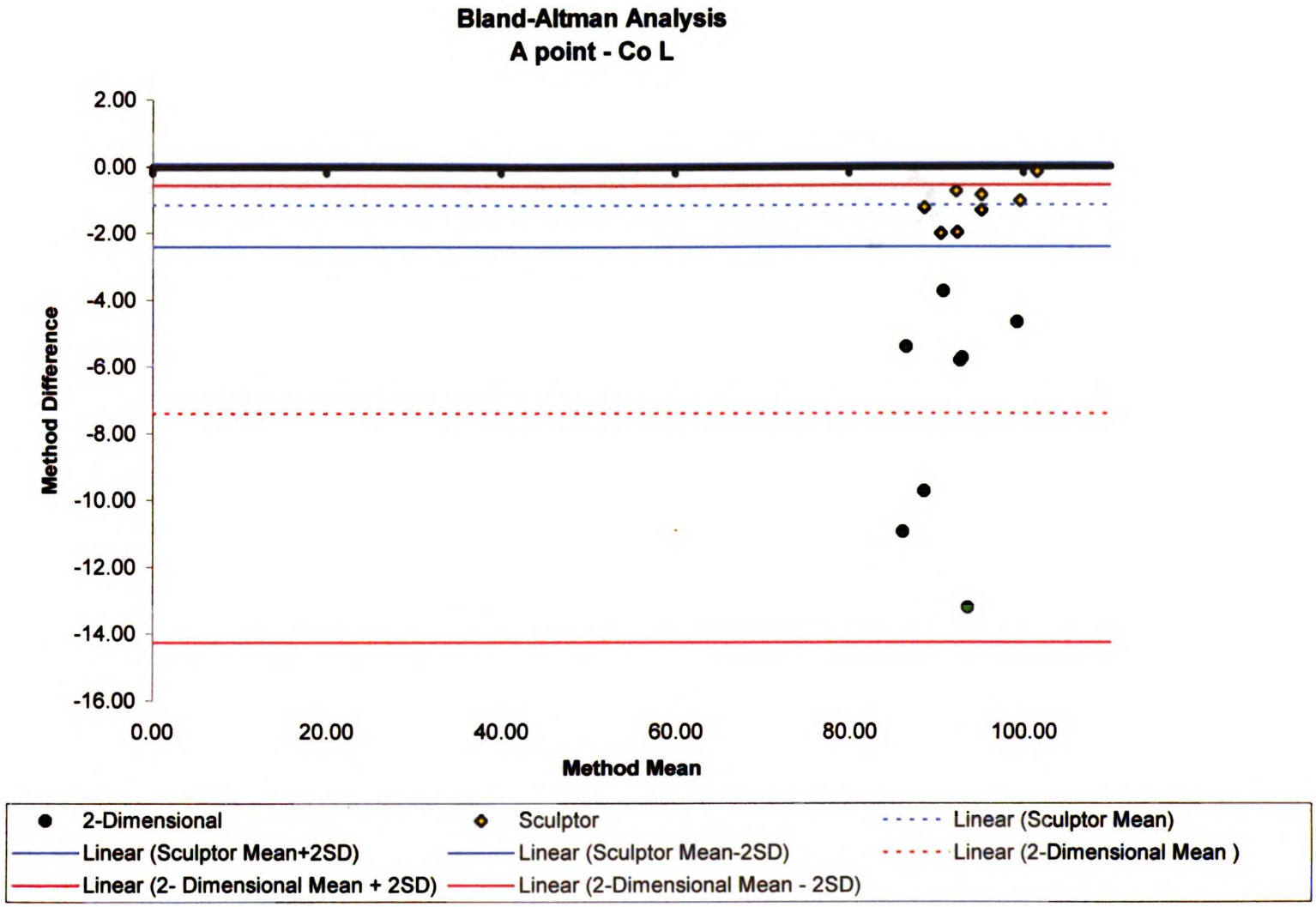
Bland-Altman Analysis
A point - Co L
Method Difference
2.00
0.00
-2.00
-4.00
-6.00
-8.00
-10.00
-12.00
-14.00
-16.00
0.00
20.00
40.00
60.00
80.00
100.00
Method Mean
2-Dimensional
Sculptor
Linear (Sculptor Mean)
Linear (Sculptor Mean+2SD)
Linear (Sculptor Mean-2SD)
Linear (2-Dimensional Mean)
Linear (2- Dimensional Mean + 2SD)
Linear (2-Dimensional Mean - 2SD)

Figure 32.

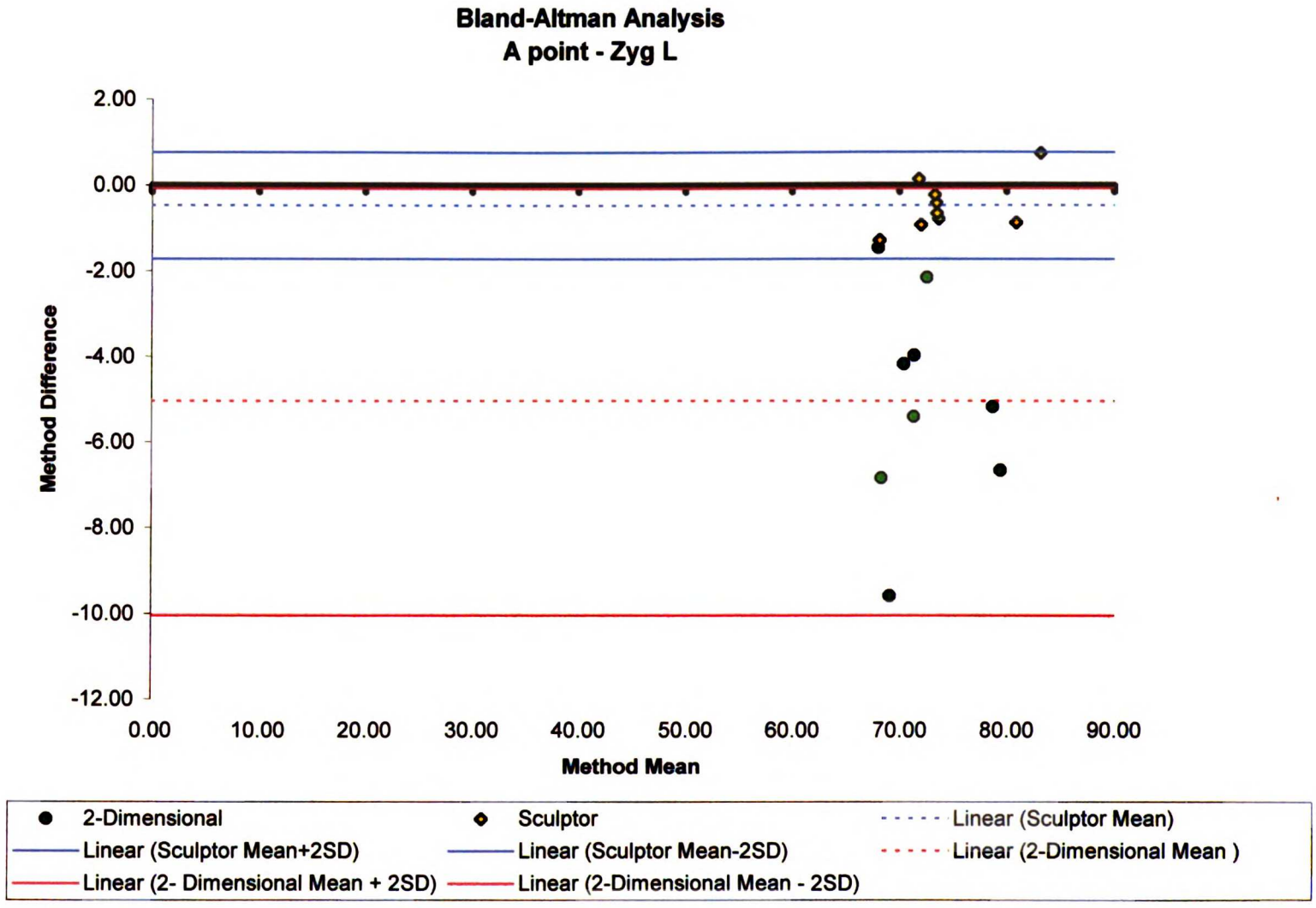
Bland-Altman Analysis
A point - Zyg L
Method Difference
2.00
0.00
-2.00
-4.00
-6.00
-8.00
-10.00
-12.00
0.00
10.00
20.00
30.00
40.00
50.00
60.00
70.00
80.00
90.00
Method Mean
2-Dimensional
Sculptor
Linear (Sculptor Mean)
Linear (Sculptor Mean+2SD)
Linear (Sculptor Mean-2SD)
Linear (2-Dimensional Mean)
Linear (2- Dimensional Mean + 2SD)
Linear (2-Dimensional Mean - 2SD)

Figure 33.

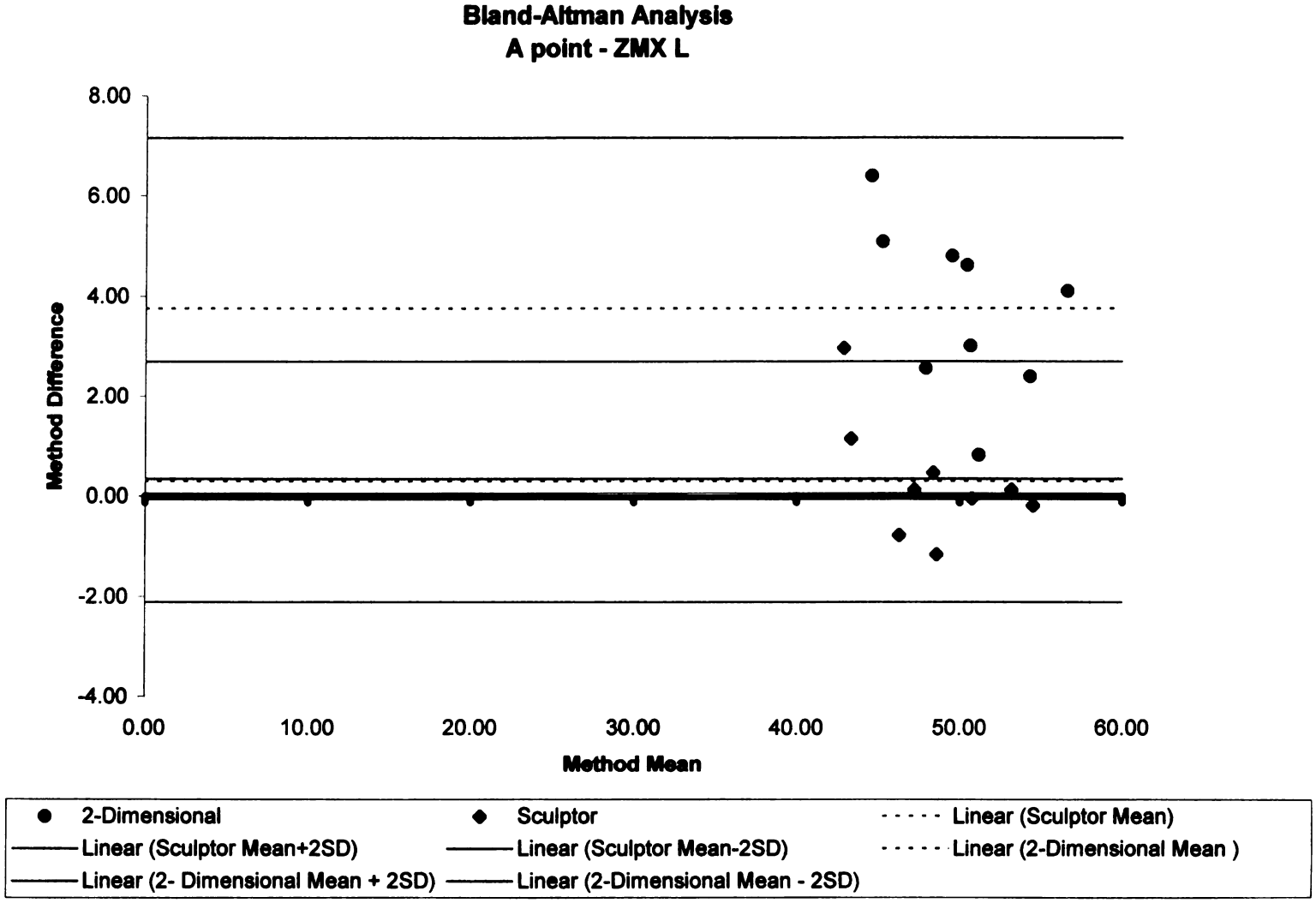
Bland-Altman Analysis
A point - ZMX L
8.00
6.00
4.00
2.00
0.00
-2.00
-4.00
Method Difference
0.00
10.00
20.00
30.00
40.00
50.00
60.00
Method Mean
2-Dimensional
Sculptor
Linear (Sculptor Mean)
Linear (Sculptor Mean+2SD)
Linear (Sculptor Mean-2SD)
Linear (2-Dimensional Mean)
Linear (2- Dimensional Mean + 2SD)
Linear (2-Dimensional Mean - 2SD)

Figure 34.

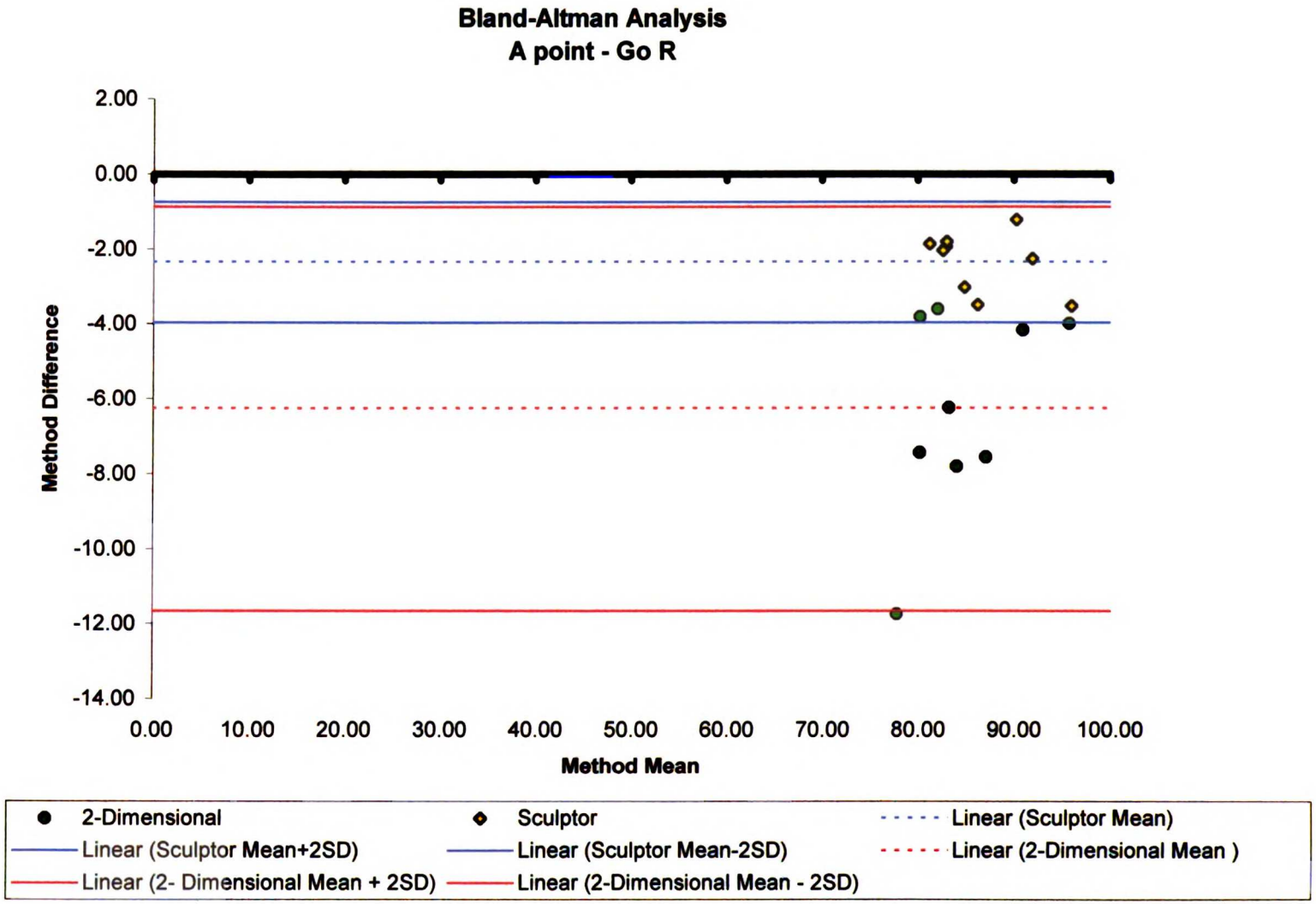
Bland-Altman Analysis
A point - Go R
Method Difference
2.00
0.00
-2.00
-4.00
-6.00
-8.00
-10.00
-12.00
-14.00
0.00
10.00
20.00
30.00
40.00
50.00
60.00
70.00
80.00
90.00
100.00
Method Mean
2-Dimensional
Sculptor
Linear (Sculptor Mean)
Linear (Sculptor Mean+2SD)
Linear (Sculptor Mean-2SD)
Linear (2-Dimensional Mean)
Linear (2- Dimensional Mean + 2SD)
Linear (2-Dimensional Mean - 2SD)

Figure 35.

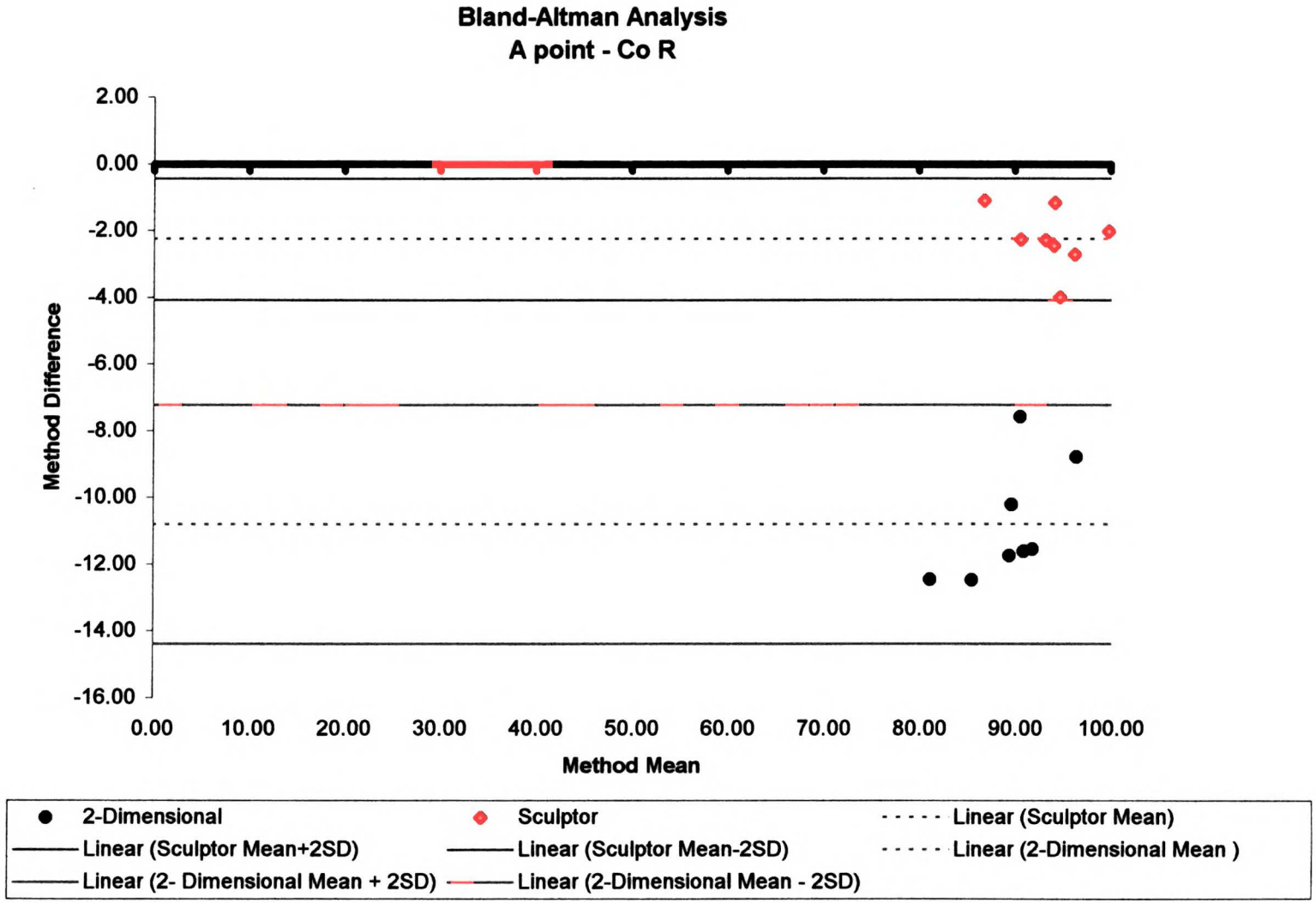
Bland-Altman Analysis
A point - Co R
Method Difference
2.00
0.00
-2.00
-4.00
-6.00
-8.00
-10.00
-12.00
-14.00
-16.00
0.00
10.00
20.00
30.00
40.00
50.00
60.00
70.00
80.00
90.00
100.00
Method Mean
2-Dimensional
Sculptor
Linear (Sculptor Mean)
Linear (Sculptor Mean+2SD)
Linear (Sculptor Mean-2SD)
Linear (2-Dimensional Mean)
Linear (2- Dimensional Mean + 2SD)
Linear (2-Dimensional Mean - 2SD)

Figure 36.

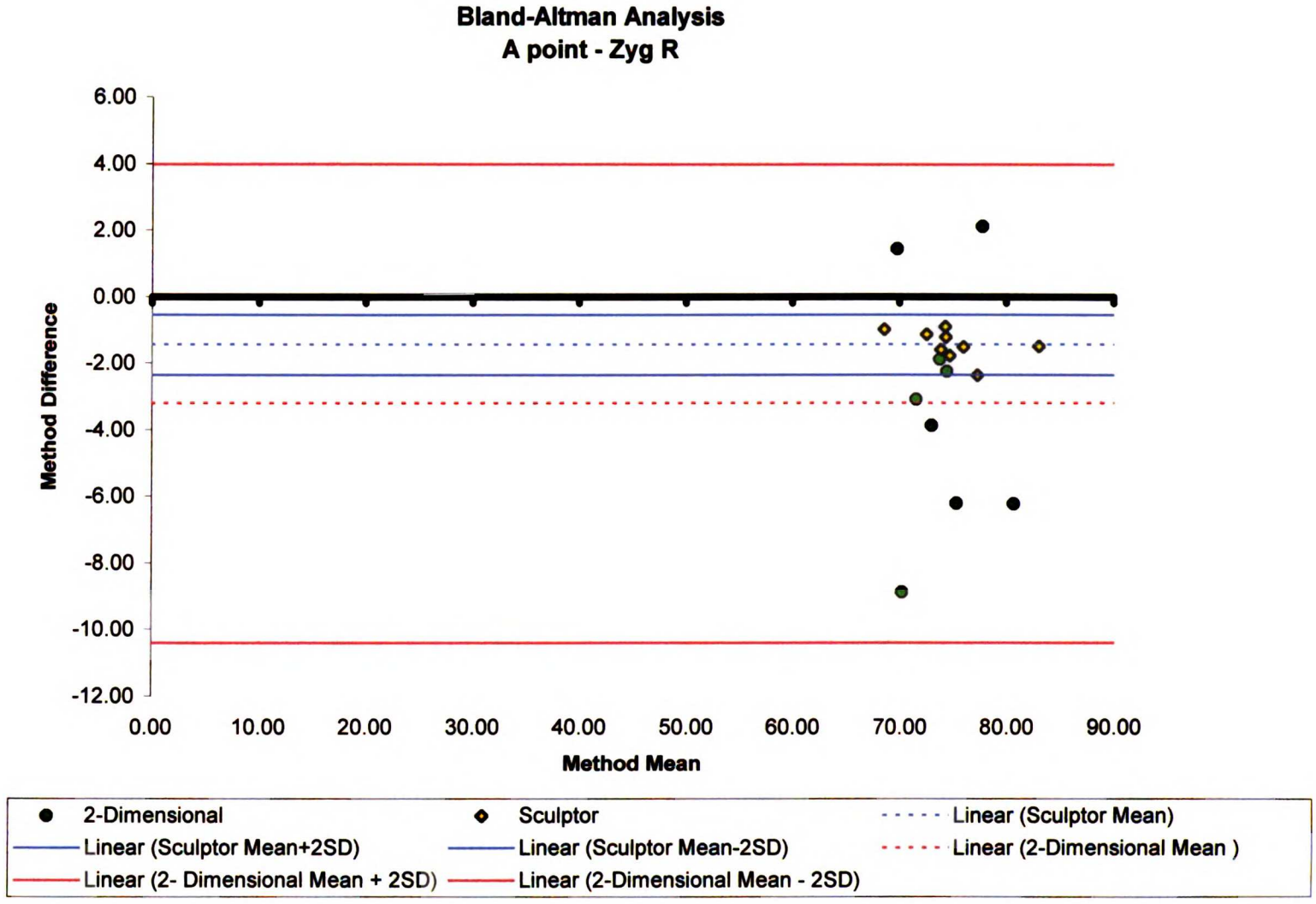
Bland-Altman Analysis
A point - Zyg R
Method Difference
6.00
4.00
2.00
0.00
-2.00
-4.00
-6.00
-8.00
-10.00
-12.00
0.00
10.00
20.00
30.00
40.00
50.00
60.00
70.00
80.00
90.00
Method Mean
2-Dimensional
Sculptor
Linear (Sculptor Mean)
Linear (Sculptor Mean+2SD)
Linear (Sculptor Mean-2SD)
Linear (2-Dimensional Mean)
Linear (2- Dimensional Mean + 2SD)
Linear (2-Dimensional Mean - 2SD)

Figure 37.

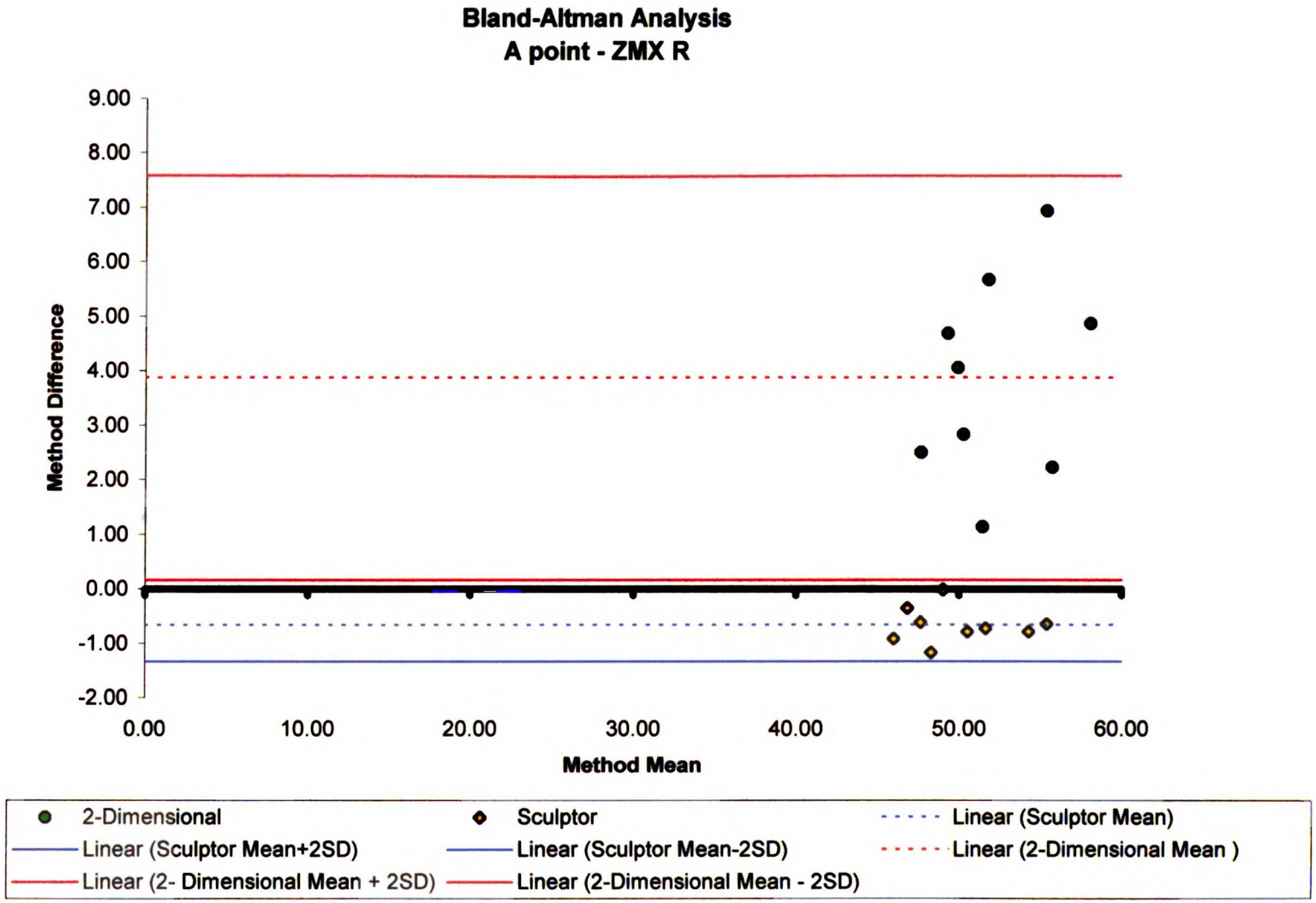
Bland-Altman Analysis
A point - ZMX R
Method Difference
9.00
8.00
7.00
6.00
5.00
4.00
3.00
2.00
1.00
0.00
-1.00
-2.00
0.00
10.00
20.00
30.00
40.00
50.00
60.00
Method Mean
2-Dimensional
Sculptor
Linear (Sculptor Mean)
Linear (Sculptor Mean+2SD)
Linear (Sculptor Mean-2SD)
Linear (2-Dimensional Mean)
Linear (2- Dimensional Mean + 2SD)
Linear (2-Dimensional Mean - 2SD)

Figure 38.

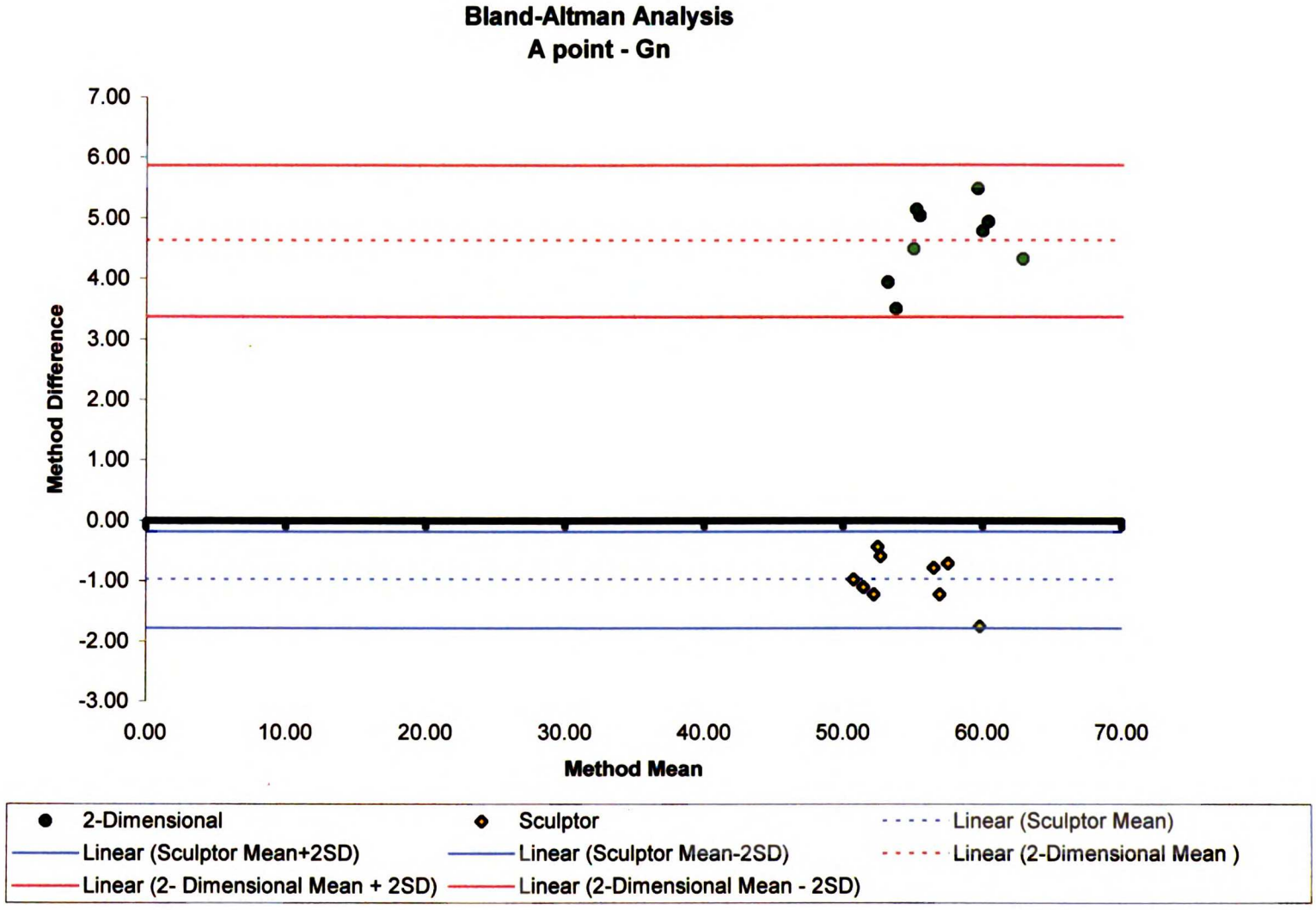
Bland-Altman Analysis
A point - Gn
Method Difference
7.00
6.00
5.00
4.00
3.00
2.00
1.00
0.00
-1.00
-2.00
-3.00
0.00
10.00
20.00
30.00
40.00
50.00
60.00
70.00
Method Mean
2-Dimensional
Sculptor
Linear (Sculptor Mean)
Linear (Sculptor Mean+2SD)
Linear (Sculptor Mean-2SD)
Linear (2-Dimensional Mean)
Linear (2- Dimensional Mean + 2SD)
Linear (2-Dimensional Mean - 2SD)

Figure 39.

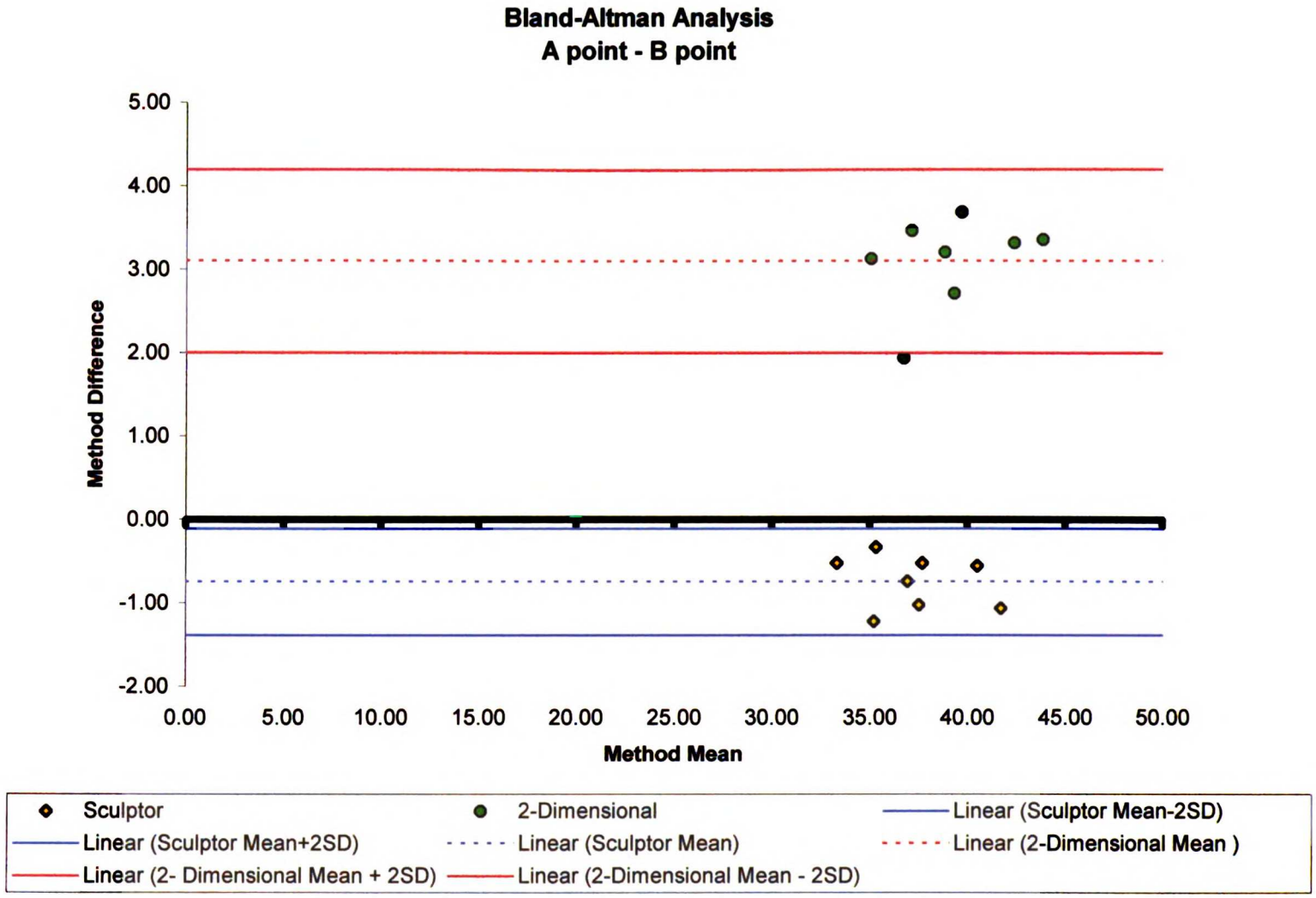
Bland-Altman Analysis
A point - B point
Method Difference
5.00
4.00
3.00
2.00
1.00
0.00
-1.00
-2.00
0.00
5.00
10.00
15.00
20.00
25.00
30.00
35.00
40.00
45.00
50.00
Method Mean
Sculptor
2-Dimensional
Linear (Sculptor Mean-2SD)
Linear (Sculptor Mean+2SD)
Linear (Sculptor Mean)
Linear (2-Dimensional Mean)
Linear (2- Dimensional Mean + 2SD)
Linear (2-Dimensional Mean - 2SD)

Figure 40.

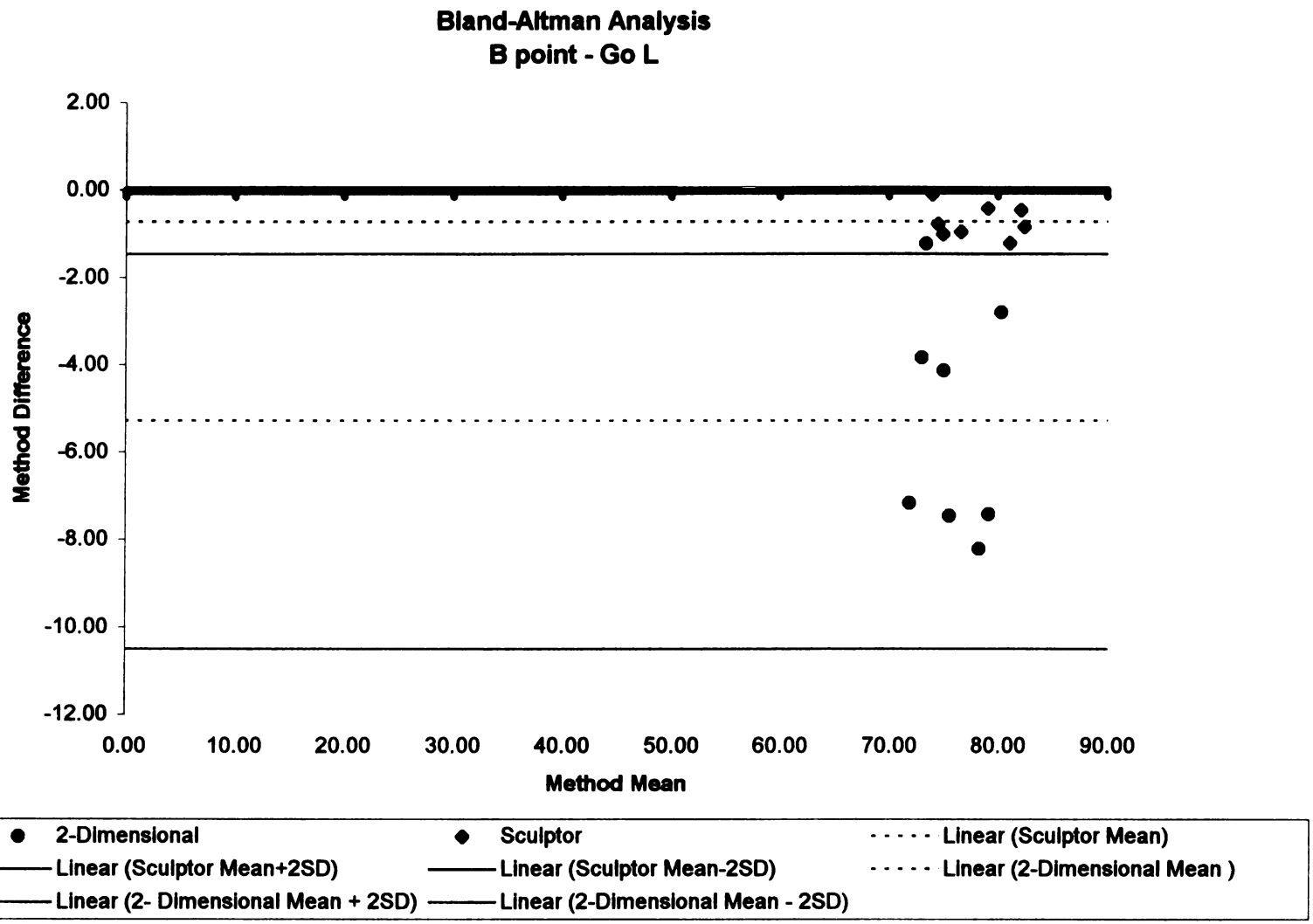
Bland-Altman Analysis
B point - Go L
2.00
0.00
-2.00
-4.00
-6.00
-8.00
-10.00
-12.00
Method Difference
0.00
10.00
20.00
30.00
40.00
50.00
60.00
70.00
80.00
90.00
Method Mean
2-Dimensional
Sculptor
Linear (Sculptor Mean)
Linear (Sculptor Mean+2SD)
Linear (Sculptor Mean-2SD)
Linear (2-Dimensional Mean)
Linear (2- Dimensional Mean + 2SD)
Linear (2-Dimensional Mean - 2SD)

Figure 41.

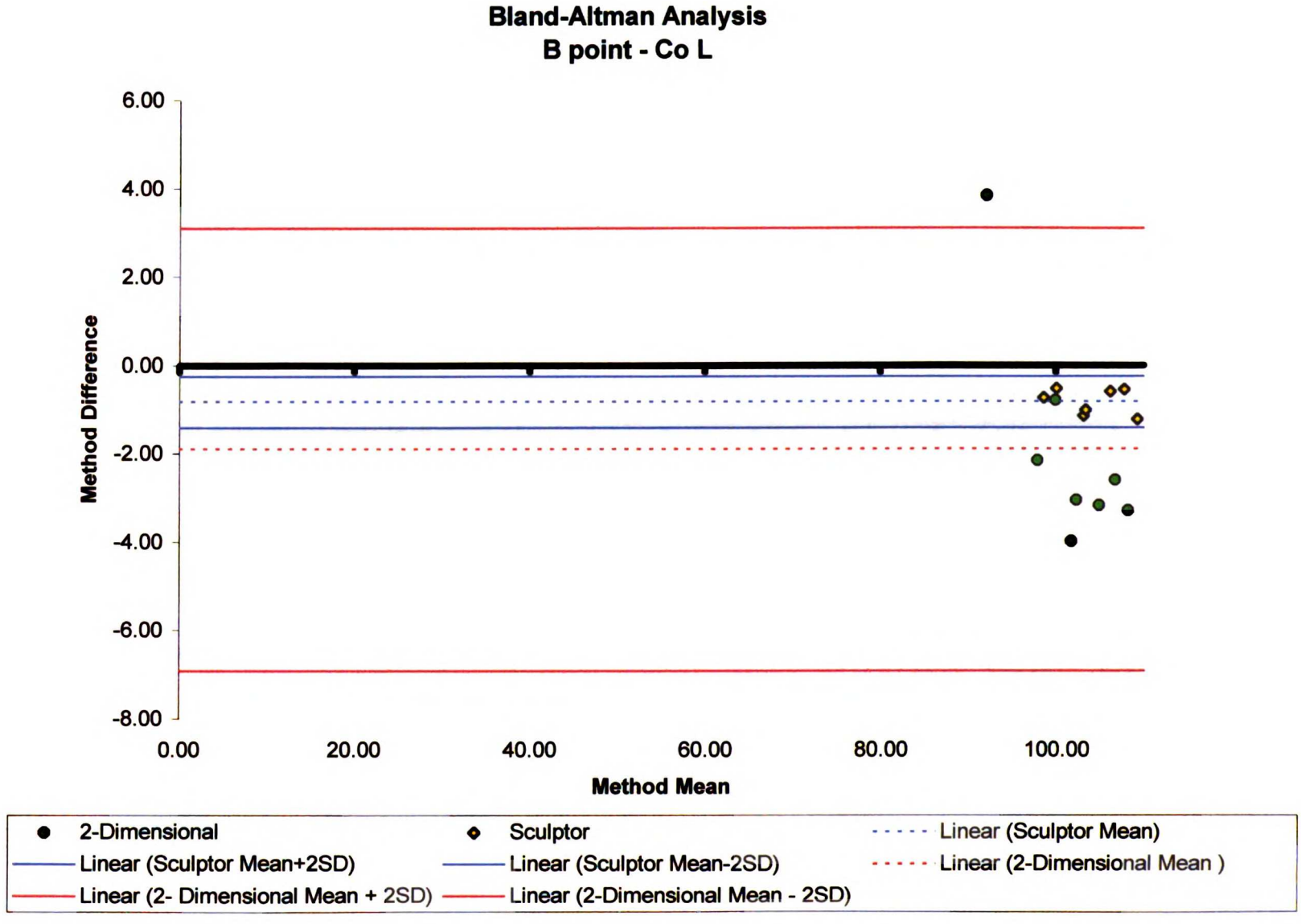
Bland-Altman Analysis
B point - Co L
Method Difference
6.00
4.00
2.00
0.00
-2.00
-4.00
-6.00
-8.00
0.00
20.00
40.00
60.00
80.00
100.00
Method Mean
2-Dimensional
Sculptor
Linear (Sculptor Mean)
Linear (Sculptor Mean+2SD)
Linear (Sculptor Mean-2SD)
Linear (2-Dimensional Mean)
Linear (2- Dimensional Mean + 2SD)
Linear (2-Dimensional Mean - 2SD)

Figure 42.

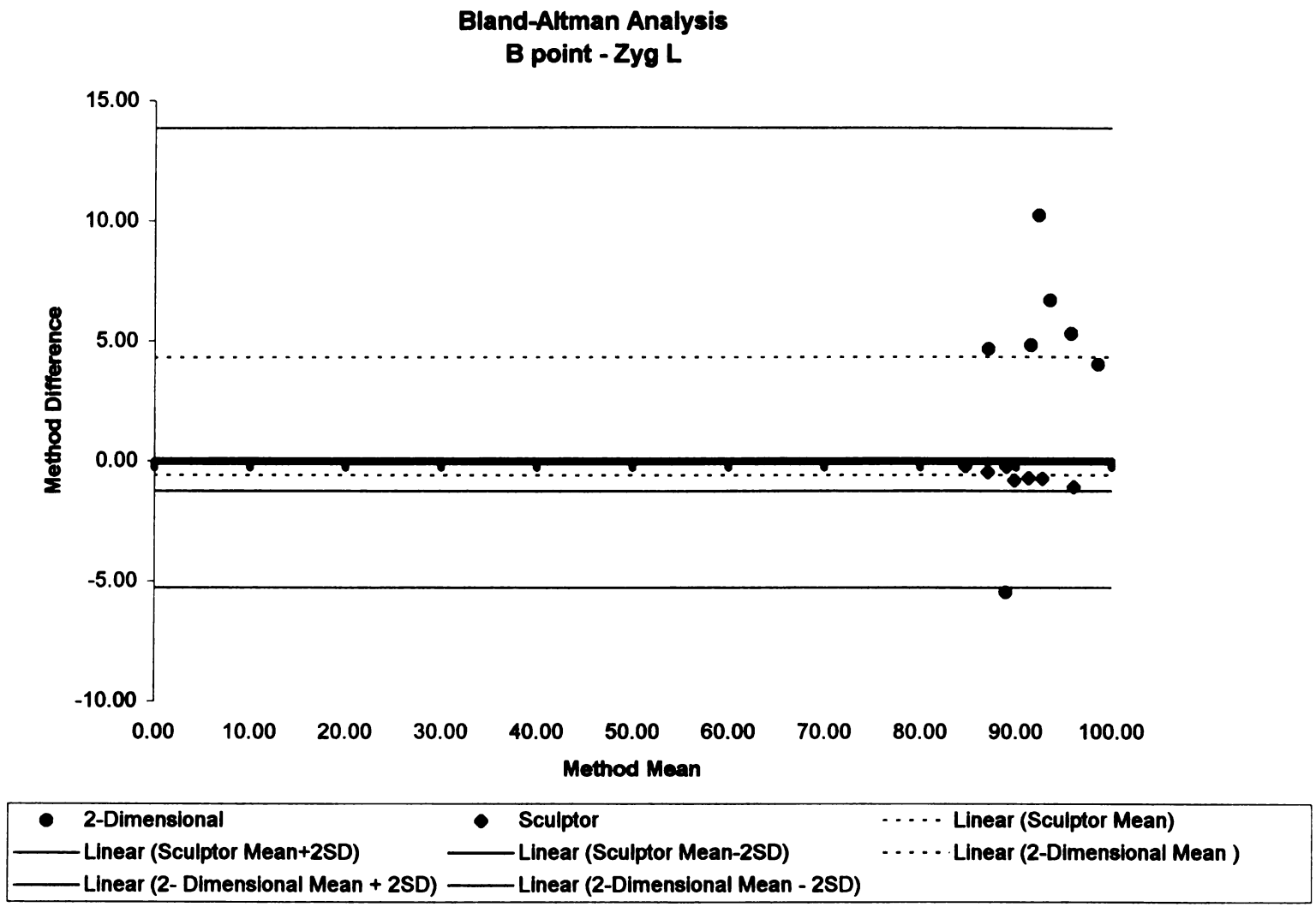
Bland-Altman Analysis
B point - Zyg L
15.00
10.00
5.00
0.00
-5.00
-10.00
Method Difference
0.00
10.00
20.00
30.00
40.00
50.00
60.00
70.00
80.00
90.00
100.00
Method Mean
2-Dimensional
Sculptor
Linear (Sculptor Mean)
Linear (Sculptor Mean+2SD)
Linear (Sculptor Mean-2SD)
Linear (2-Dimensional Mean)
Linear (2- Dimensional Mean + 2SD)
Linear (2-Dimensional Mean - 2SD)

Figure 43.

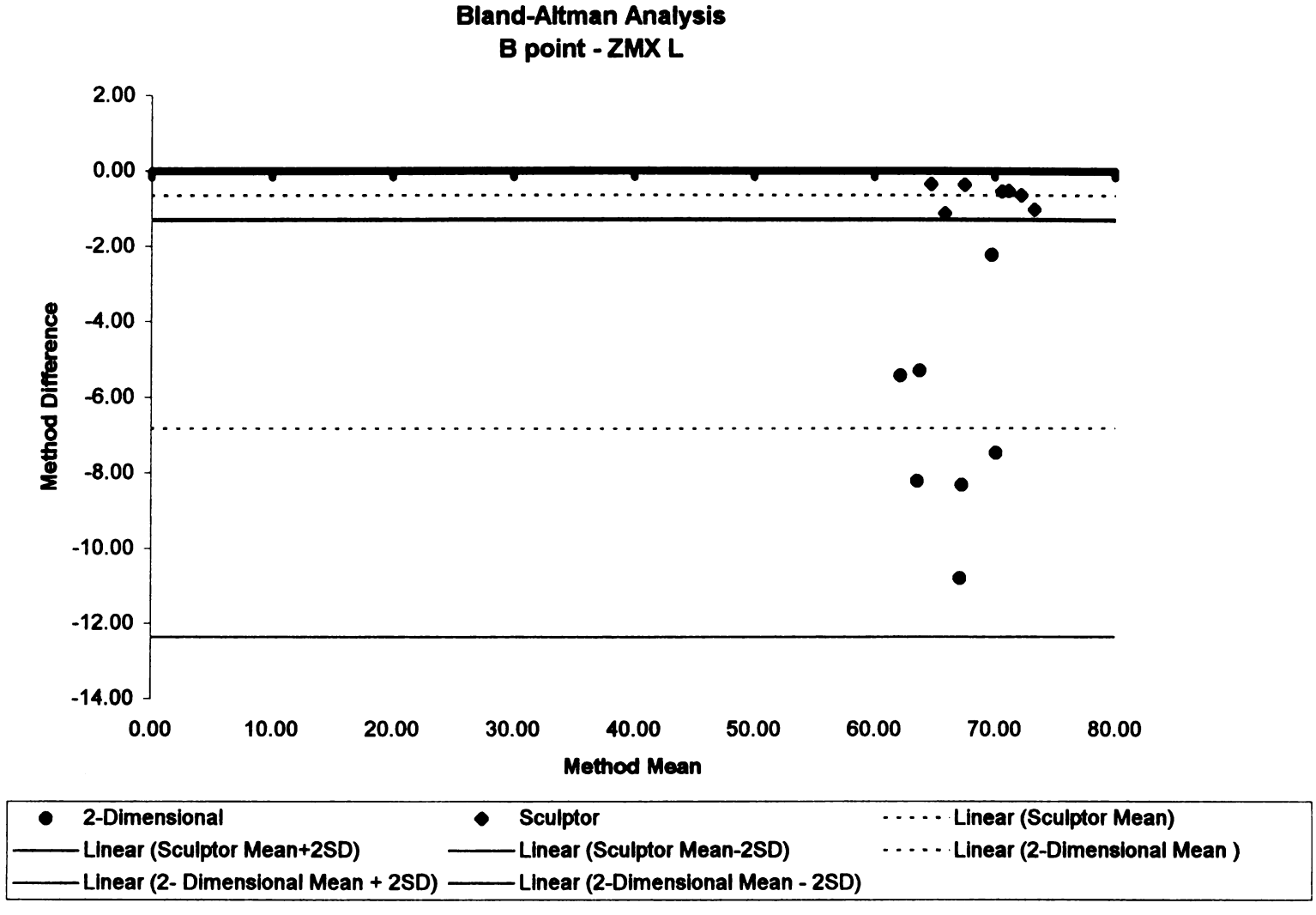
Bland-Altman Analysis
B point - ZMX L
2.00
0.00
-2.00
-4.00
-6.00
-8.00
-10.00
-12.00
-14.00
Method Difference
0.00
10.00
20.00
30.00
40.00
50.00
60.00
70.00
80.00
Method Mean
2-Dimensional
Sculptor
Linear (Sculptor Mean)
Linear (Sculptor Mean+2SD)
Linear (Sculptor Mean-2SD)
Linear (2-Dimensional Mean)
Linear (2- Dimensional Mean + 2SD)
Linear (2-Dimensional Mean - 2SD)

Figure 44.

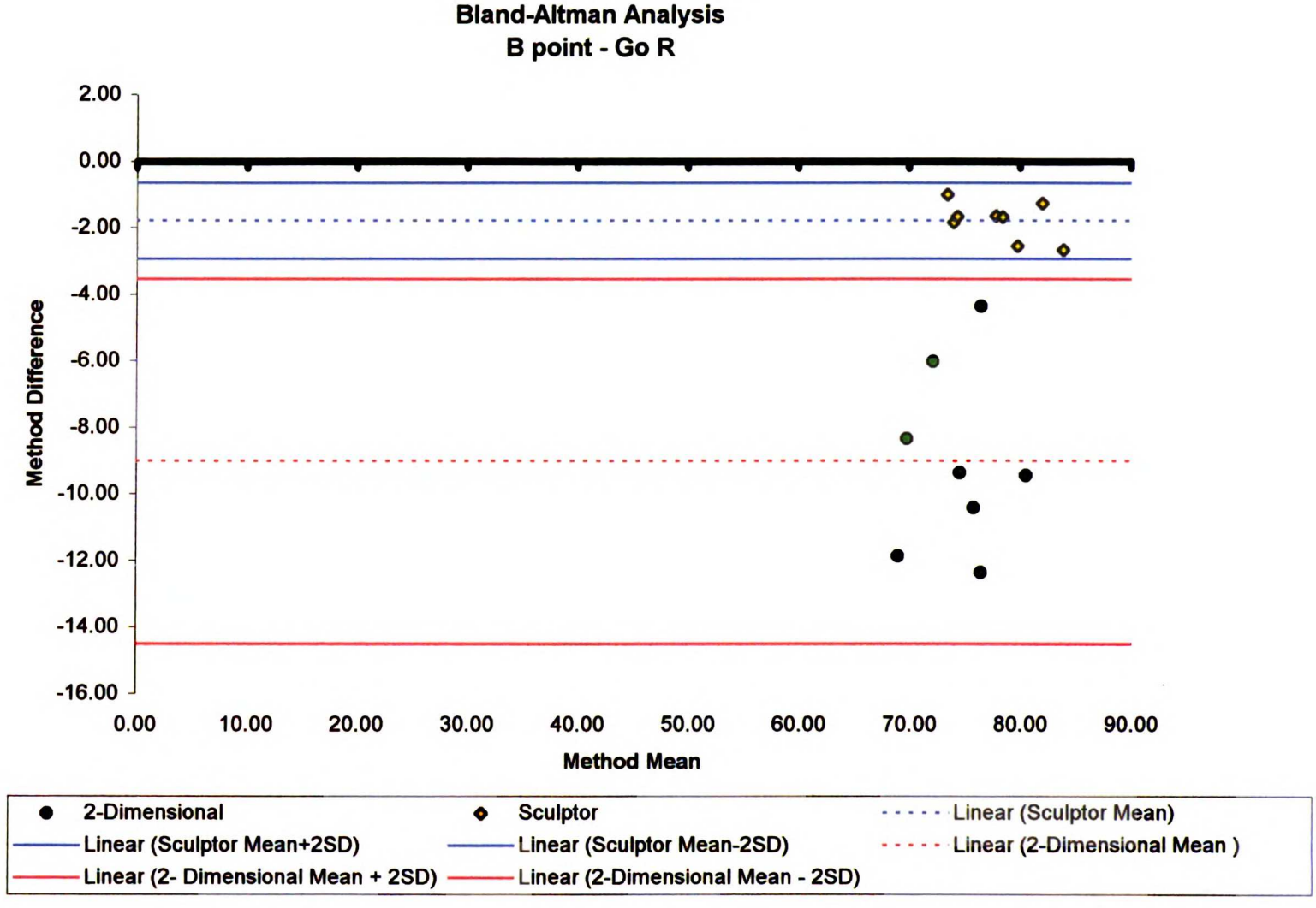
Bland-Altman Analysis
B point - Go R
2.00
0.00
-2.00
-4.00
-6.00
-8.00
-10.00
-12.00
-14.00
-16.00
Method Difference
0.00
10.00
20.00
30.00
40.00
50.00
60.00
70.00
80.00
90.00
Method Mean
2-Dimensional
Sculptor
Linear (Sculptor Mean)
Linear (Sculptor Mean+2SD)
Linear (Sculptor Mean-2SD)
Linear (2-Dimensional Mean)
Linear (2- Dimensional Mean + 2SD)
Linear (2-Dimensional Mean - 2SD)

Figure 45.

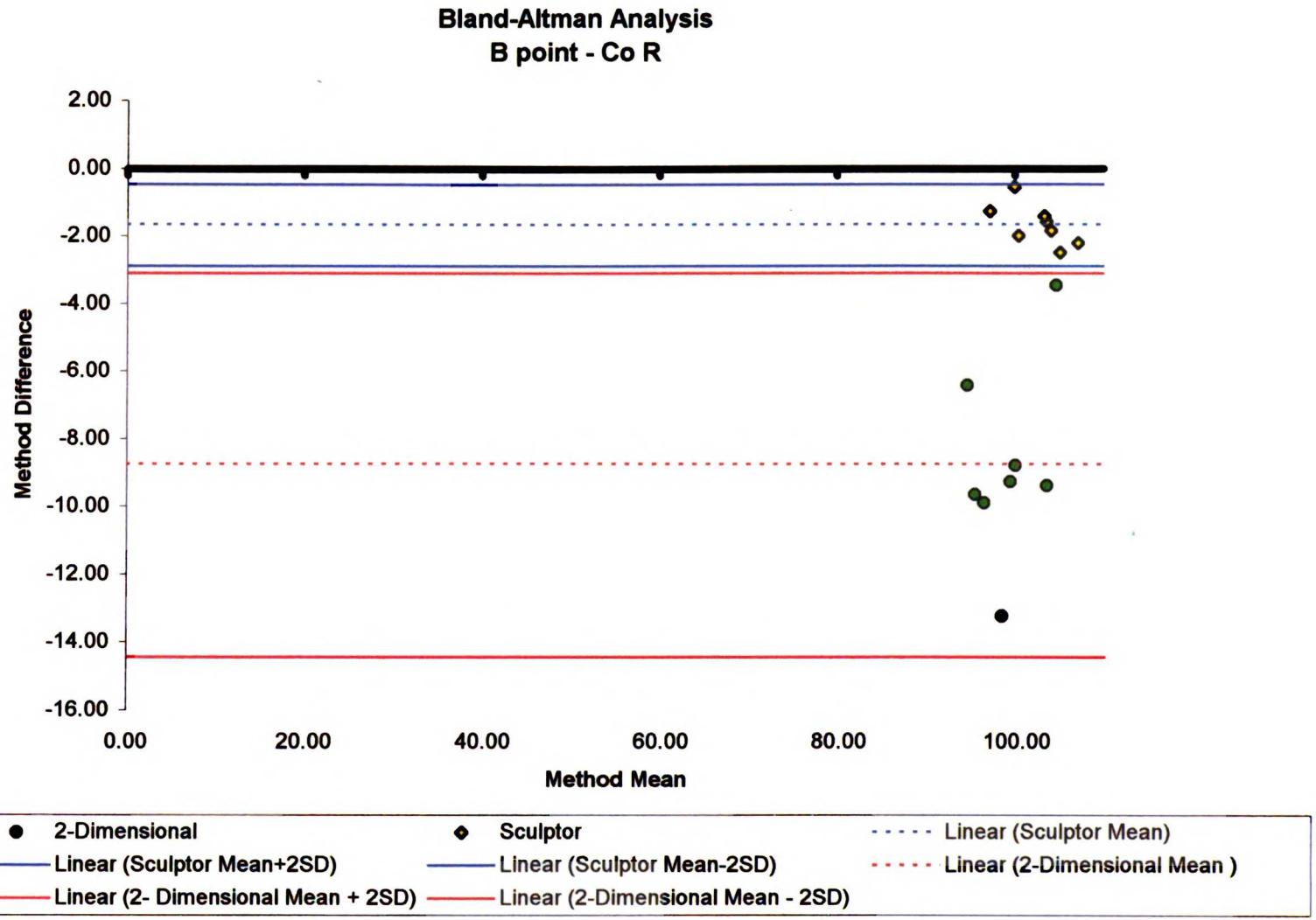
Bland-Altman Analysis
B point - Co R
Method Difference
2.00
0.00
-2.00
-4.00
-6.00
-8.00
-10.00
-12.00
-14.00
-16.00
0.00
20.00
40.00
60.00
80.00
100.00
Method Mean
2-Dimensional
Sculptor
Linear (Sculptor Mean)
Linear (Sculptor Mean+2SD)
Linear (Sculptor Mean-2SD)
Linear (2-Dimensional Mean)
Linear (2- Dimensional Mean + 2SD)
Linear (2-Dimensional Mean - 2SD)

Figure 46.

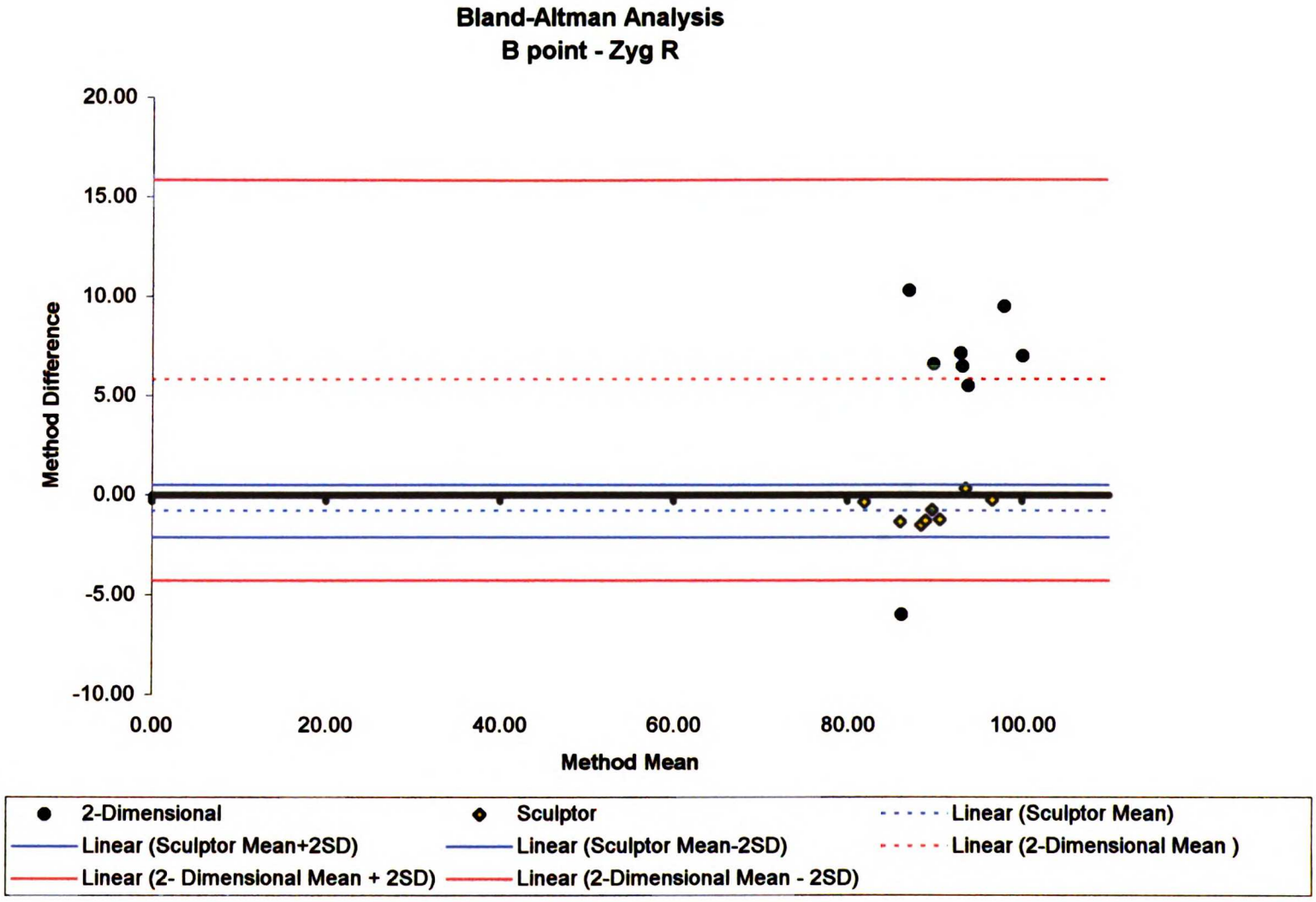
Bland-Altman Analysis
B point - Zyg R
Method Difference
20.00
15.00
10.00
5.00
0.00
-5.00
-10.00
0.00
20.00
40.00
60.00
80.00
100.00
Method Mean
2-Dimensional
Sculptor
Linear (Sculptor Mean)
Linear (Sculptor Mean+2SD)
Linear (Sculptor Mean-2SD)
Linear (2-Dimensional Mean)
Linear (2- Dimensional Mean + 2SD)
Linear (2-Dimensional Mean - 2SD)

Figure 47.

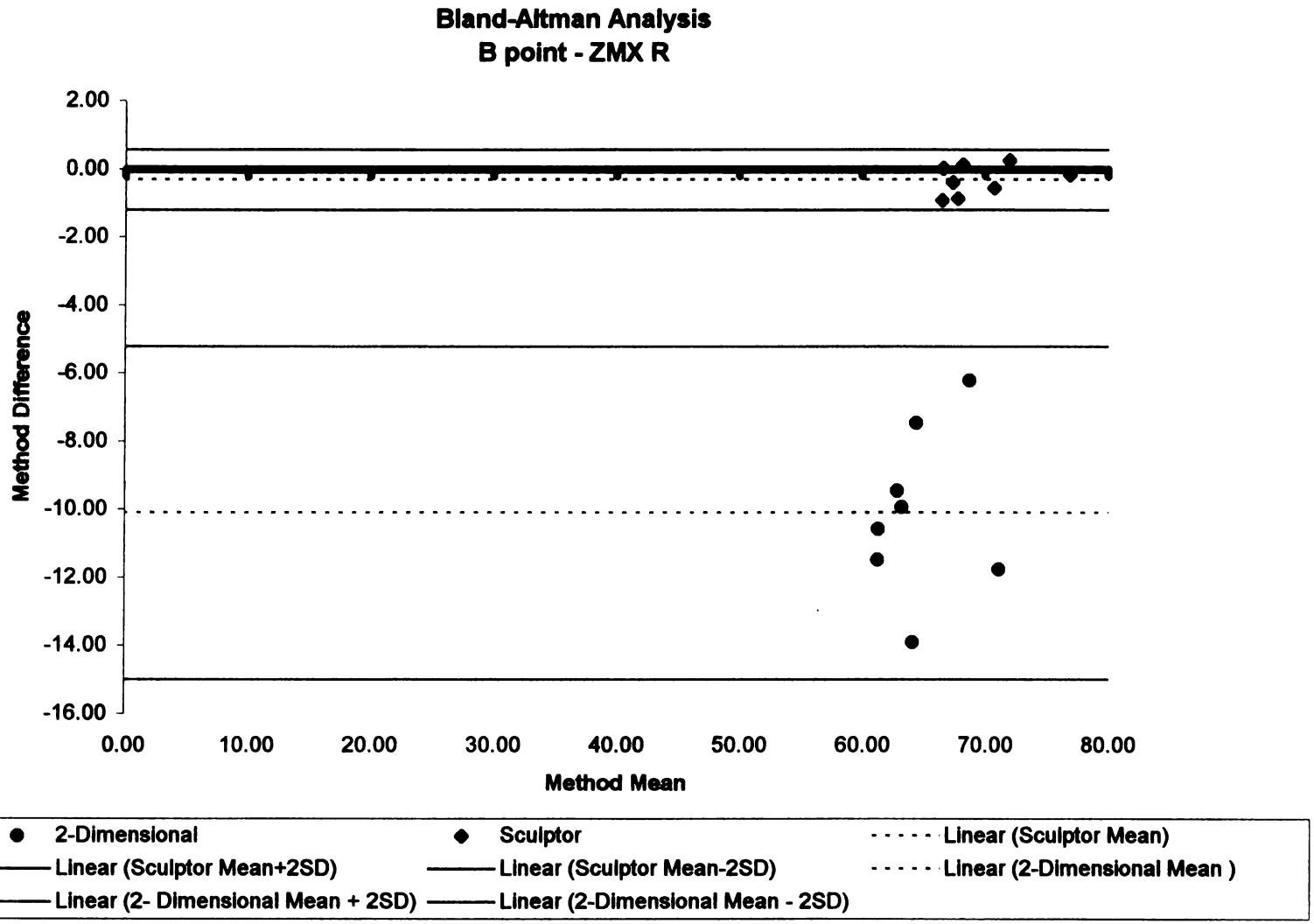
Bland-Altman Analysis
B point - ZMX R
Method Difference
2.00
0.00
-2.00
-4.00
-6.00
-8.00
-10.00
-12.00
-14.00
-16.00
0.00
10.00
20.00
30.00
40.00
50.00
60.00
70.00
80.00
Method Mean
2-Dimensional
Sculptor
Linear (Sculptor Mean)
Linear (Sculptor Mean+2SD)
Linear (Sculptor Mean-2SD)
Linear (2-Dimensional Mean)
Linear (2- Dimensional Mean + 2SD)
Linear (2-Dimensional Mean - 2SD)

Figure 48.

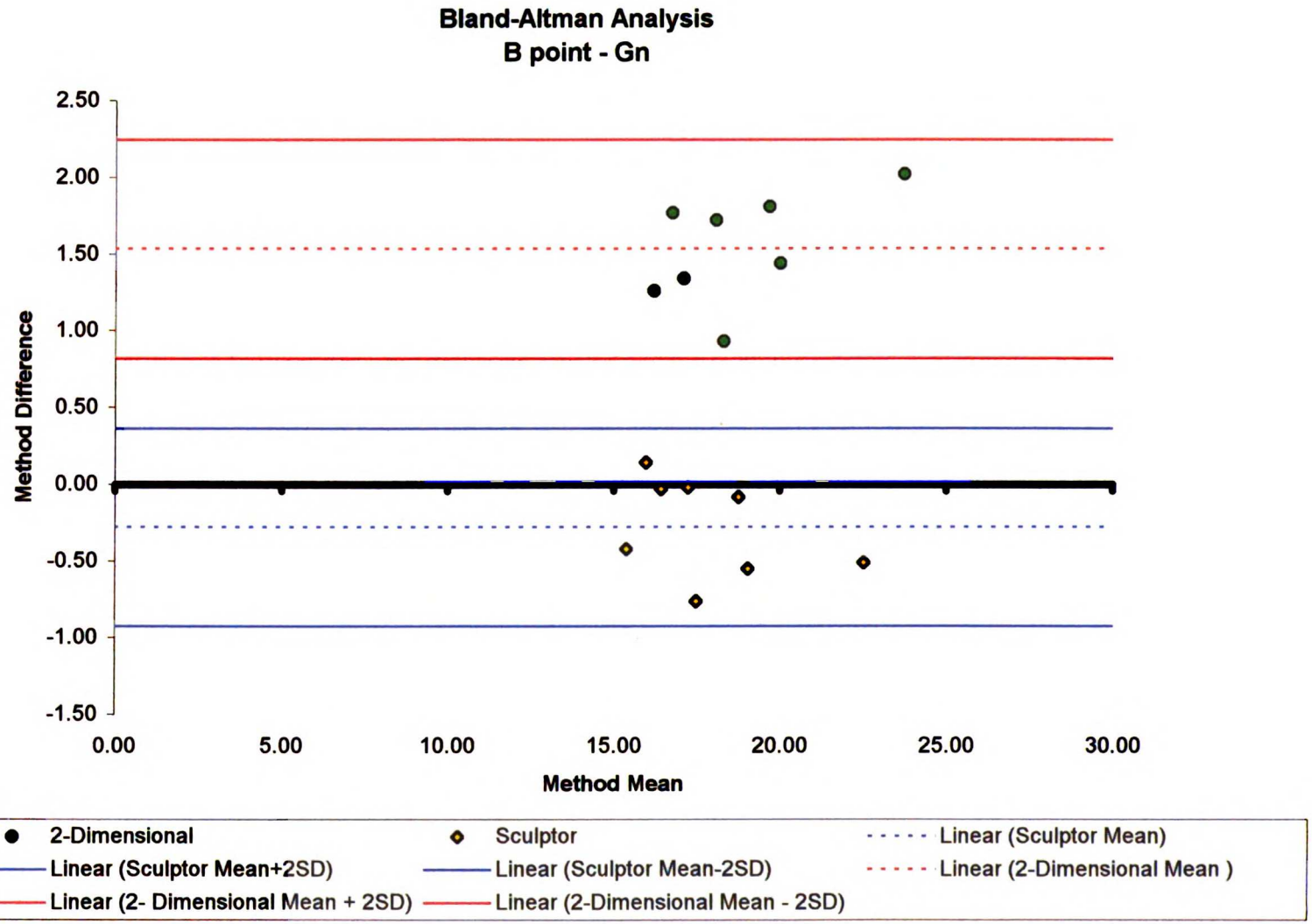
Bland-Altman Analysis
B point - Gn
Method Difference
2.50
2.00
1.50
1.00
0.50
0.00
-0.50
-1.00
-1.50
0.00
5.00
10.00
15.00
20.00
25.00
30.00
Method Mean
2-Dimensional
Sculptor
Linear (Sculptor Mean)
Linear (Sculptor Mean+2SD)
Linear (Sculptor Mean-2SD)
Linear (2-Dimensional Mean)
Linear (2- Dimensional Mean + 2SD)
Linear (2-Dimensional Mean - 2SD)

Figure 49.

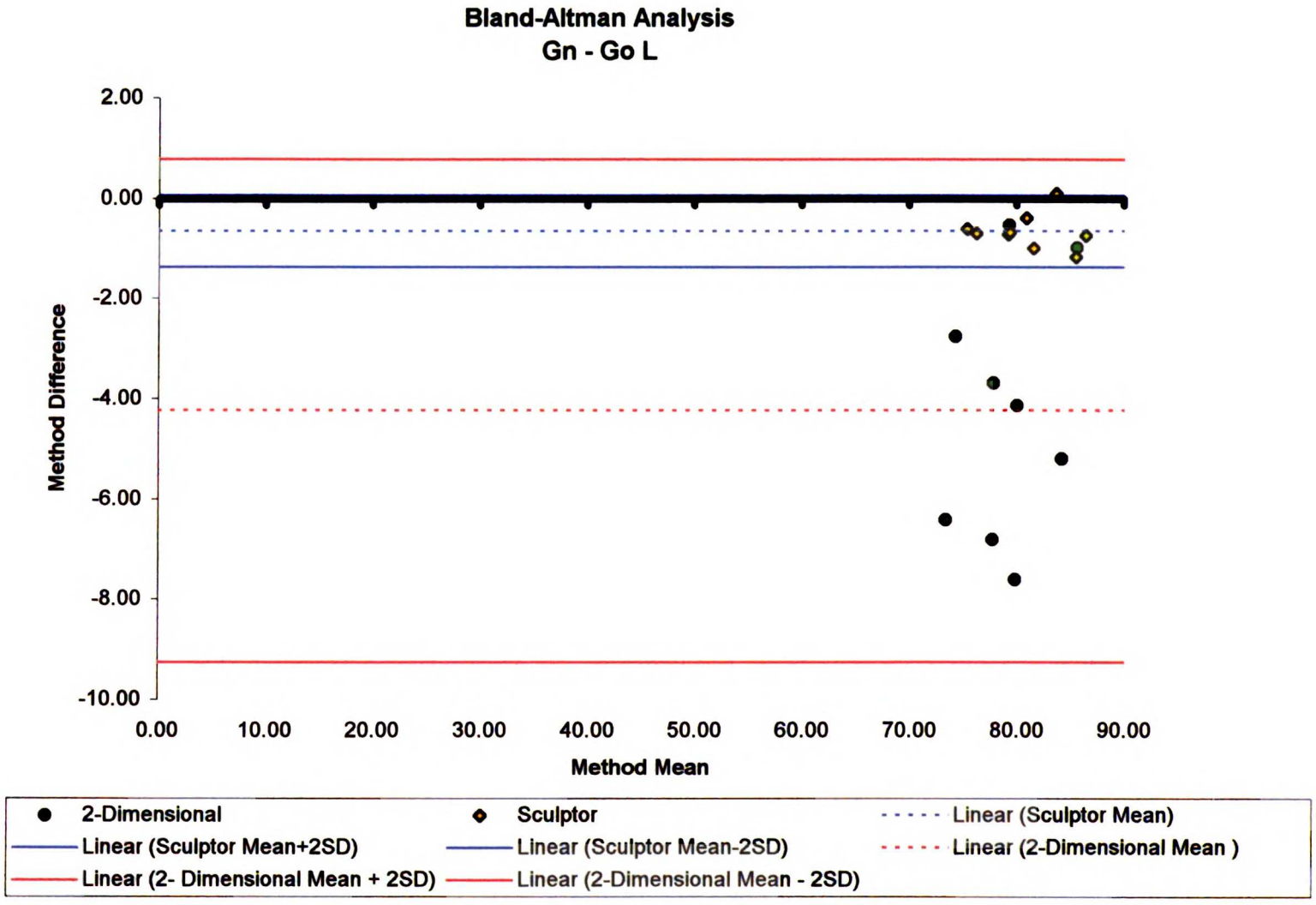
Bland-Altman Analysis
Gn - Go L
Method Difference
2.00
0.00
-2.00
-4.00
-6.00
-8.00
-10.00
0.00
10.00
20.00
30.00
40.00
50.00
60.00
70.00
80.00
90.00
Method Mean
2-Dimensional
Sculptor
Linear (Sculptor Mean)
Linear (Sculptor Mean+2SD)
Linear (Sculptor Mean-2SD)
Linear (2-Dimensional Mean)
Linear (2- Dimensional Mean + 2SD)
Linear (2-Dimensional Mean - 2SD)

Figure 50.

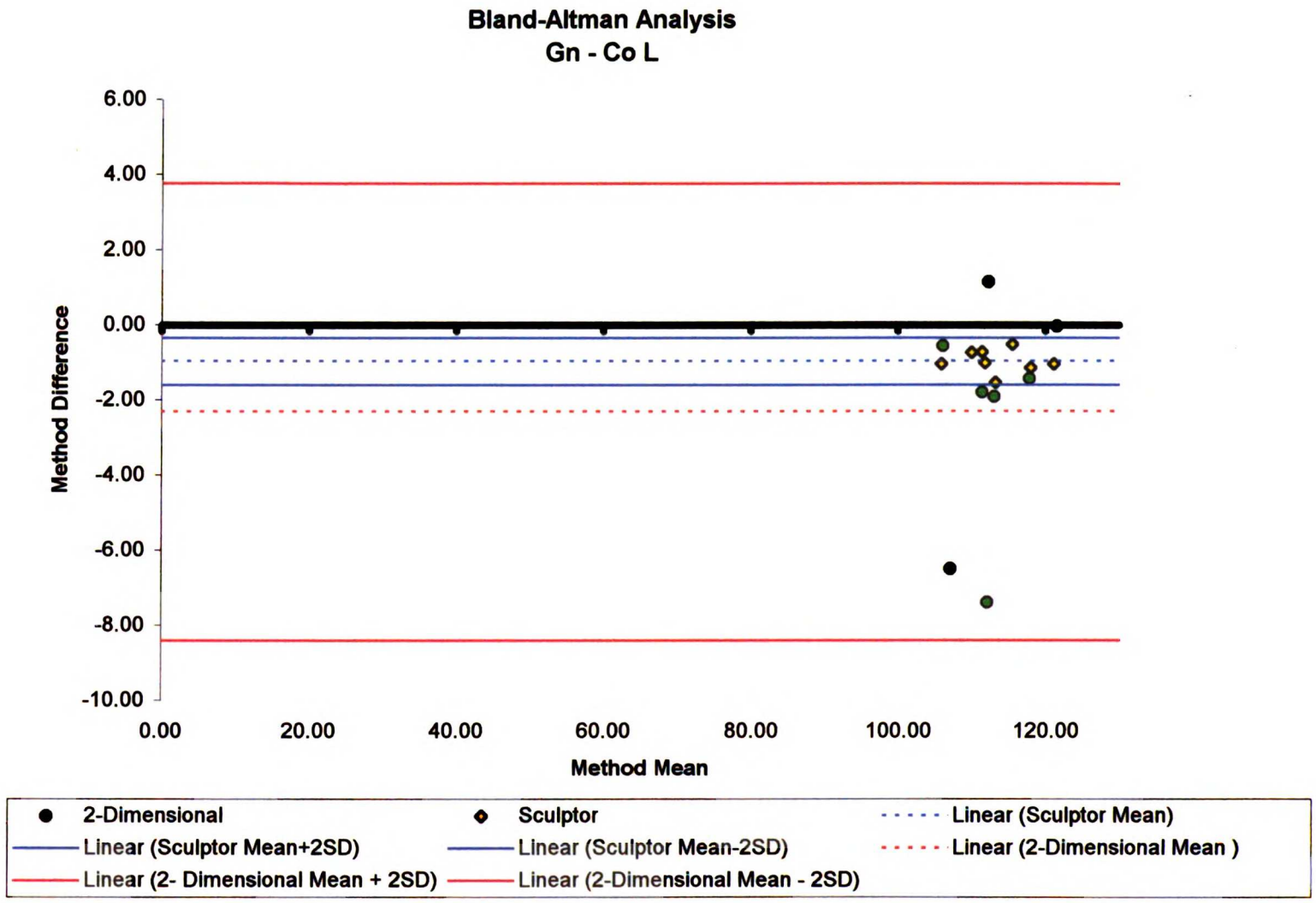
Bland-Altman Analysis
Gn - Co L
Method Difference
6.00
4.00
2.00
0.00
-2.00
-4.00
-6.00
-8.00
-10.00
0.00
20.00
40.00
60.00
80.00
100.00
120.00
Method Mean
2-Dimensional
Sculptor
Linear (Sculptor Mean)
Linear (Sculptor Mean+2SD)
Linear (Sculptor Mean-2SD)
Linear (2-Dimensional Mean)
Linear (2- Dimensional Mean + 2SD)
Linear (2-Dimensional Mean - 2SD)

Figure 51.

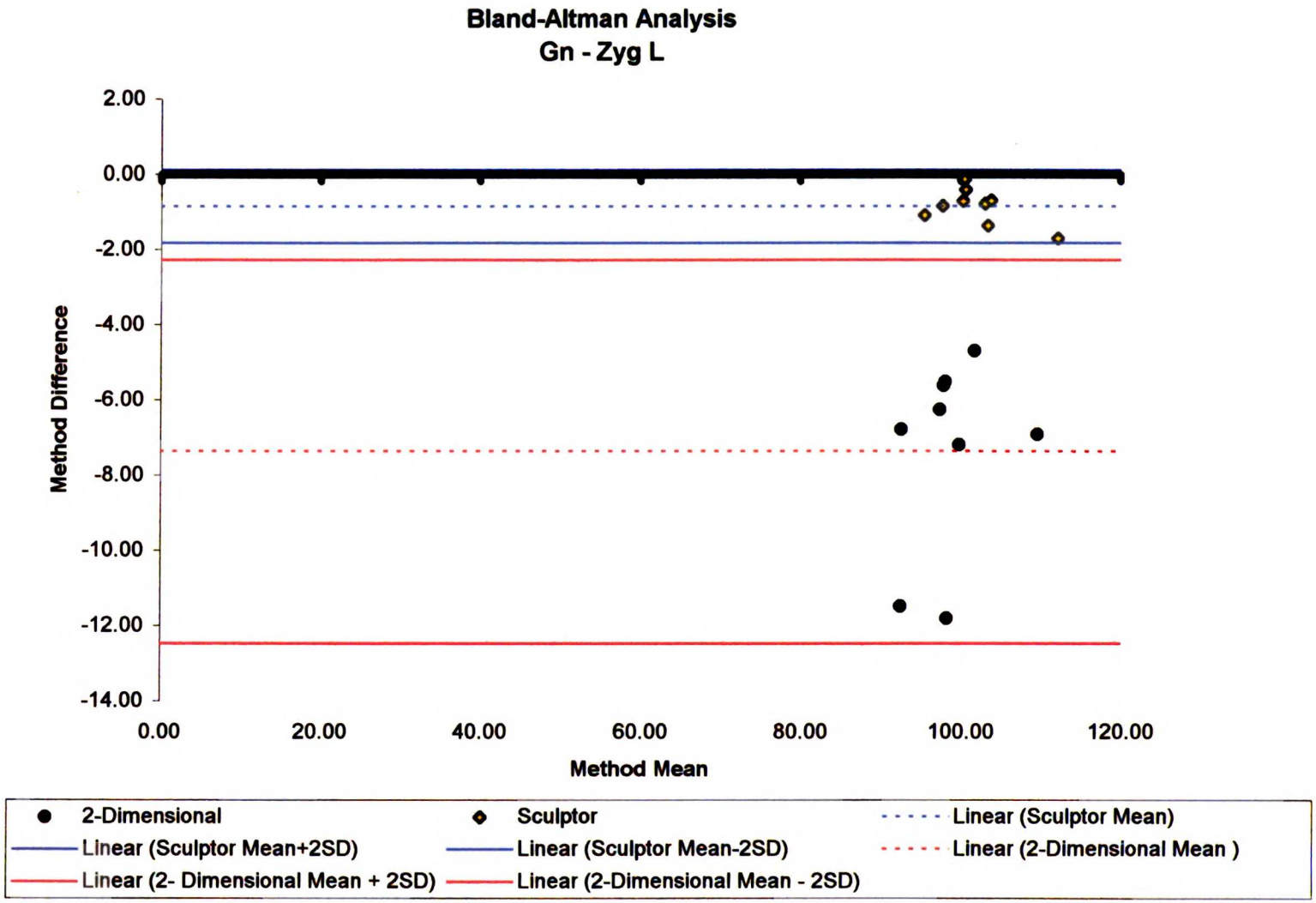
Bland-Altman Analysis
Gn - Zyg L
Method Difference
2.00
0.00
-2.00
-4.00
-6.00
-8.00
-10.00
-12.00
-14.00
0.00
20.00
40.00
60.00
80.00
100.00
120.00
Method Mean
2-Dimensional
Sculptor
Linear (Sculptor Mean)
Linear (Sculptor Mean+2SD)
Linear (Sculptor Mean-2SD)
Linear (2-Dimensional Mean)
Linear (2- Dimensional Mean + 2SD)
Linear (2-Dimensional Mean - 2SD)

Figure 52.

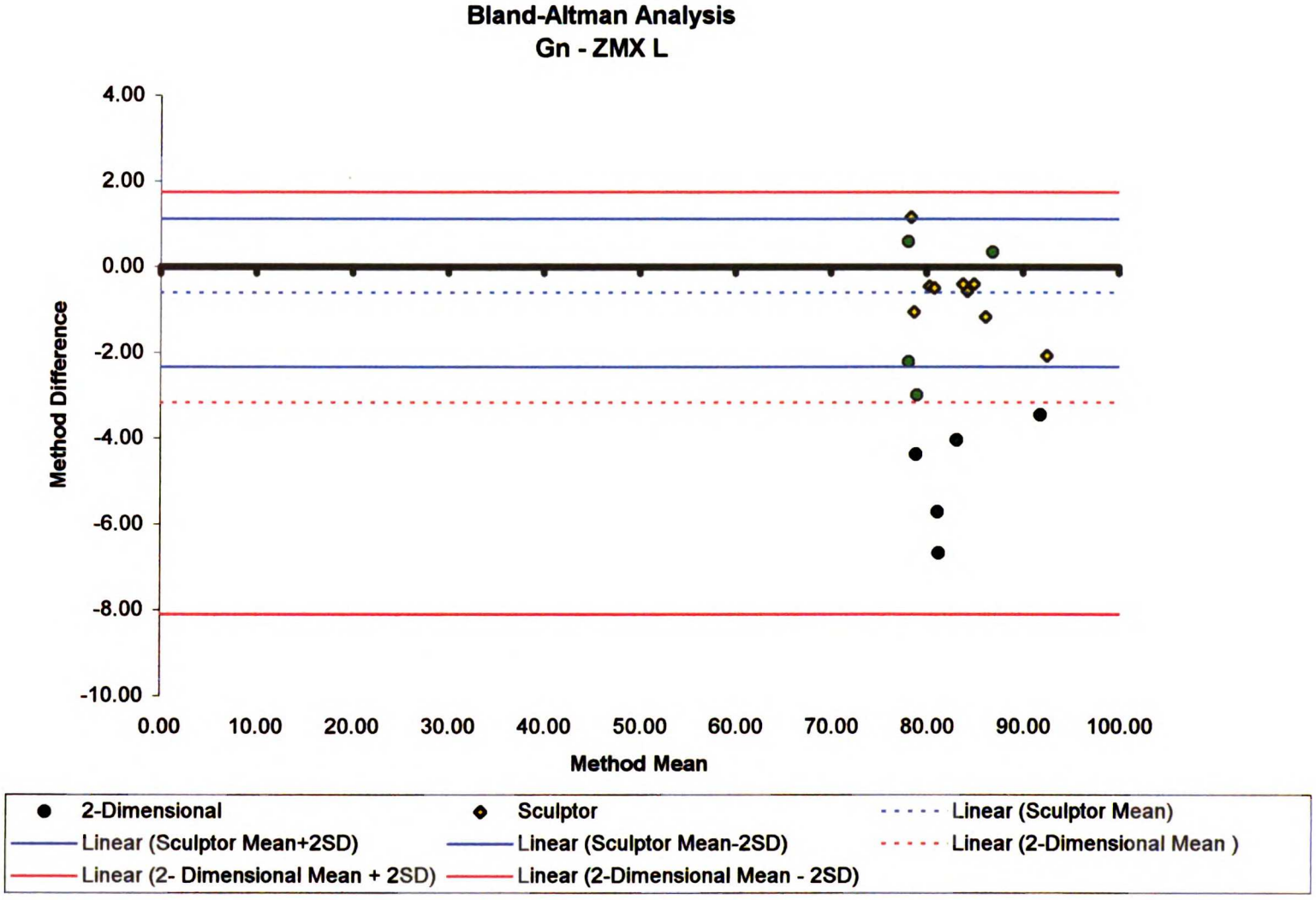
Bland-Altman Analysis
Gn - ZMX L
Method Difference
4.00
2.00
0.00
-2.00
-4.00
-6.00
-8.00
-10.00
0.00
10.00
20.00
30.00
40.00
50.00
60.00
70.00
80.00
90.00
100.00
Method Mean
2-Dimensional
Sculptor
Linear (Sculptor Mean)
Linear (Sculptor Mean+2SD)
Linear (Sculptor Mean-2SD)
Linear (2-Dimensional Mean)
Linear (2- Dimensional Mean + 2SD)
Linear (2-Dimensional Mean - 2SD)

Figure 53.

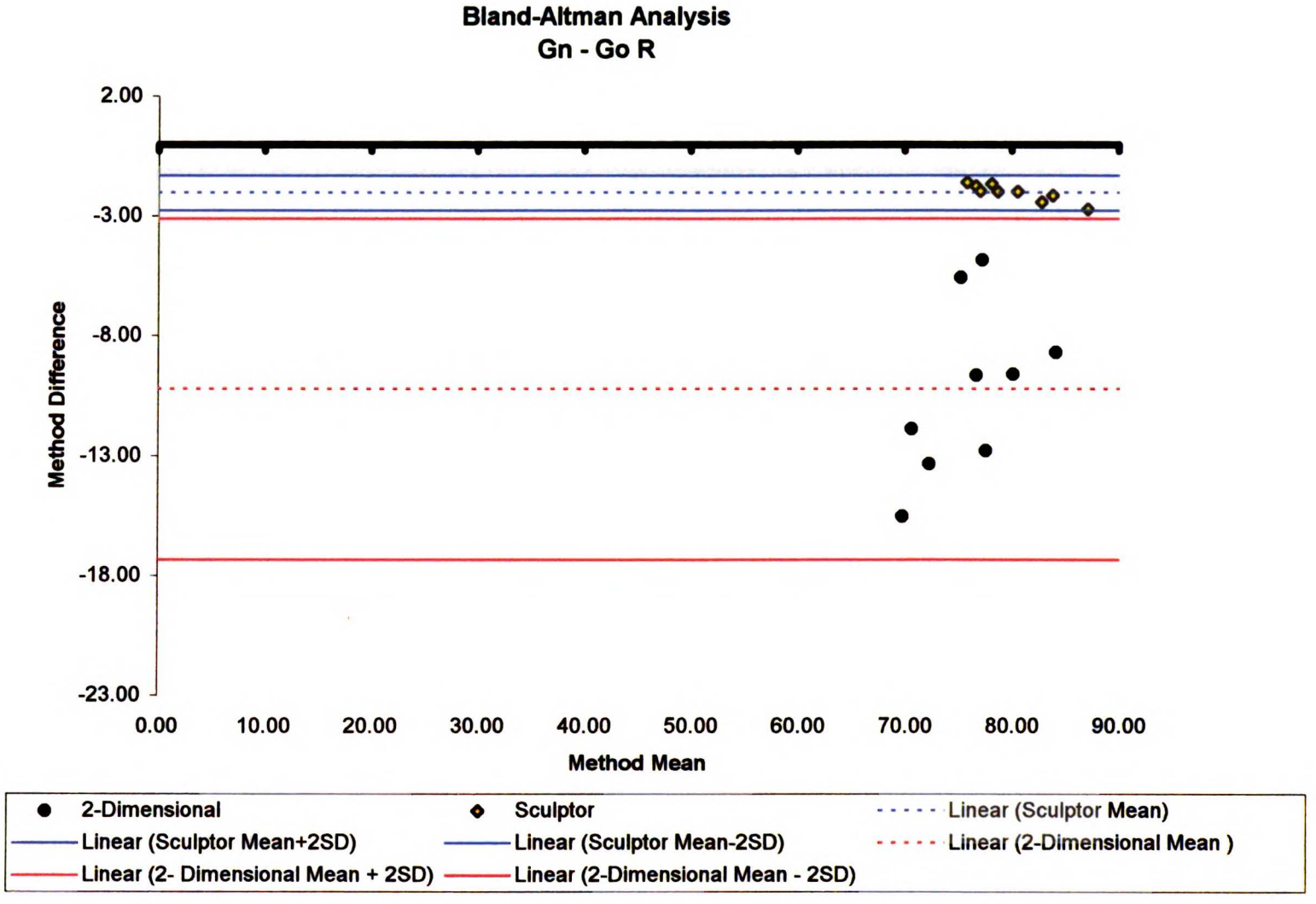
Bland-Altman Analysis
Gn - Go R
2.00
-3.00
-8.00
-13.00
-18.00
-23.00
Method Difference
0.00
10.00
20.00
30.00
40.00
50.00
60.00
70.00
80.00
90.00
Method Mean
2-Dimensional
Sculptor
Linear (Sculptor Mean)
Linear (Sculptor Mean+2SD)
Linear (Sculptor Mean-2SD)
Linear (2-Dimensional Mean)
Linear (2- Dimensional Mean + 2SD)
Linear (2-Dimensional Mean - 2SD)

Figure 54.

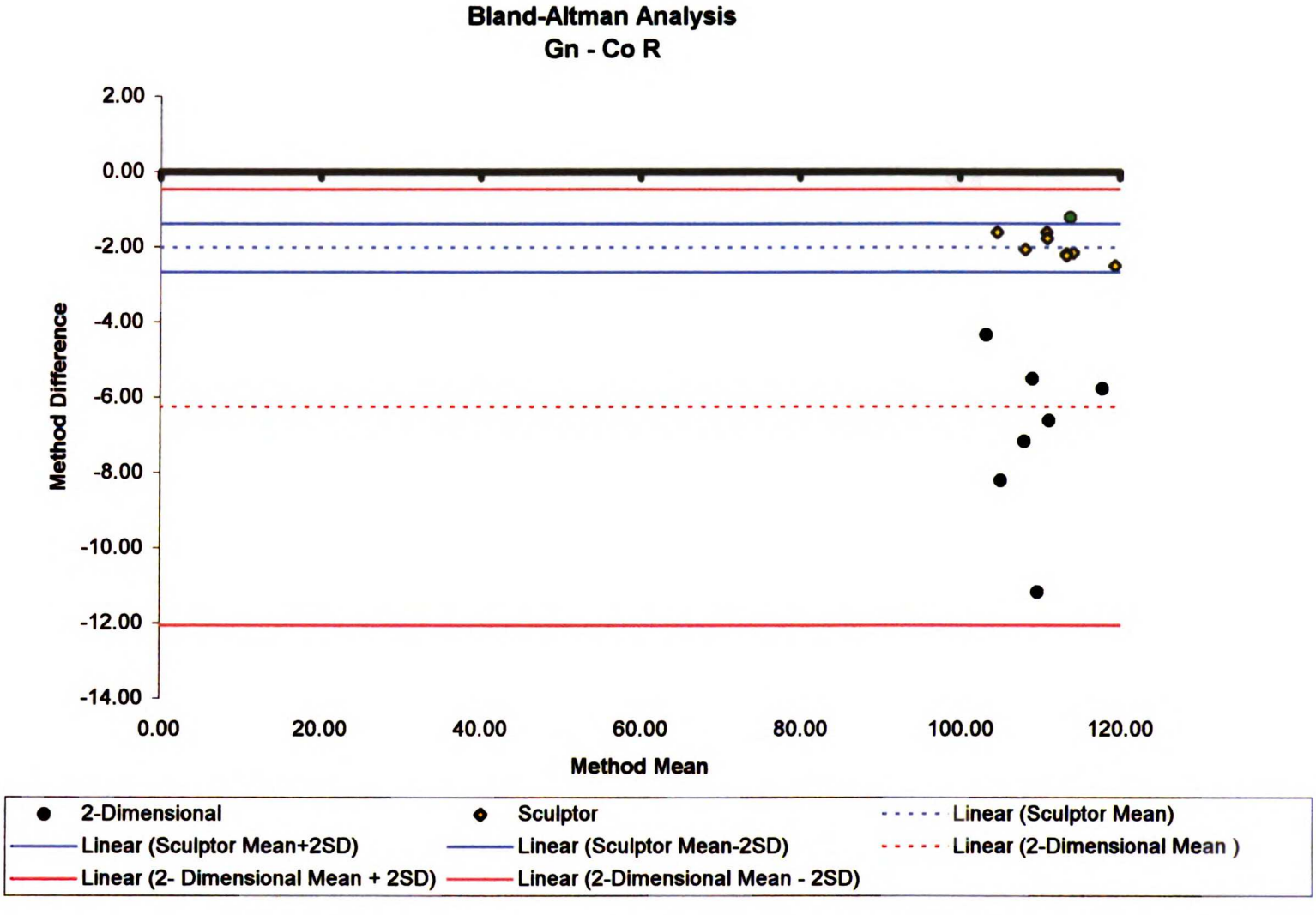
Bland-Altman Analysis
Gn - Co R
Method Difference
2.00
0.00
-2.00
-4.00
-6.00
-8.00
-10.00
-12.00
-14.00
0.00
20.00
40.00
60.00
80.00
100.00
120.00
Method Mean
2-Dimensional
Sculptor
Linear (Sculptor Mean)
Linear (Sculptor Mean+2SD)
Linear (Sculptor Mean-2SD)
Linear (2-Dimensional Mean)
Linear (2- Dimensional Mean + 2SD)
Linear (2-Dimensional Mean - 2SD)

Figure 55.

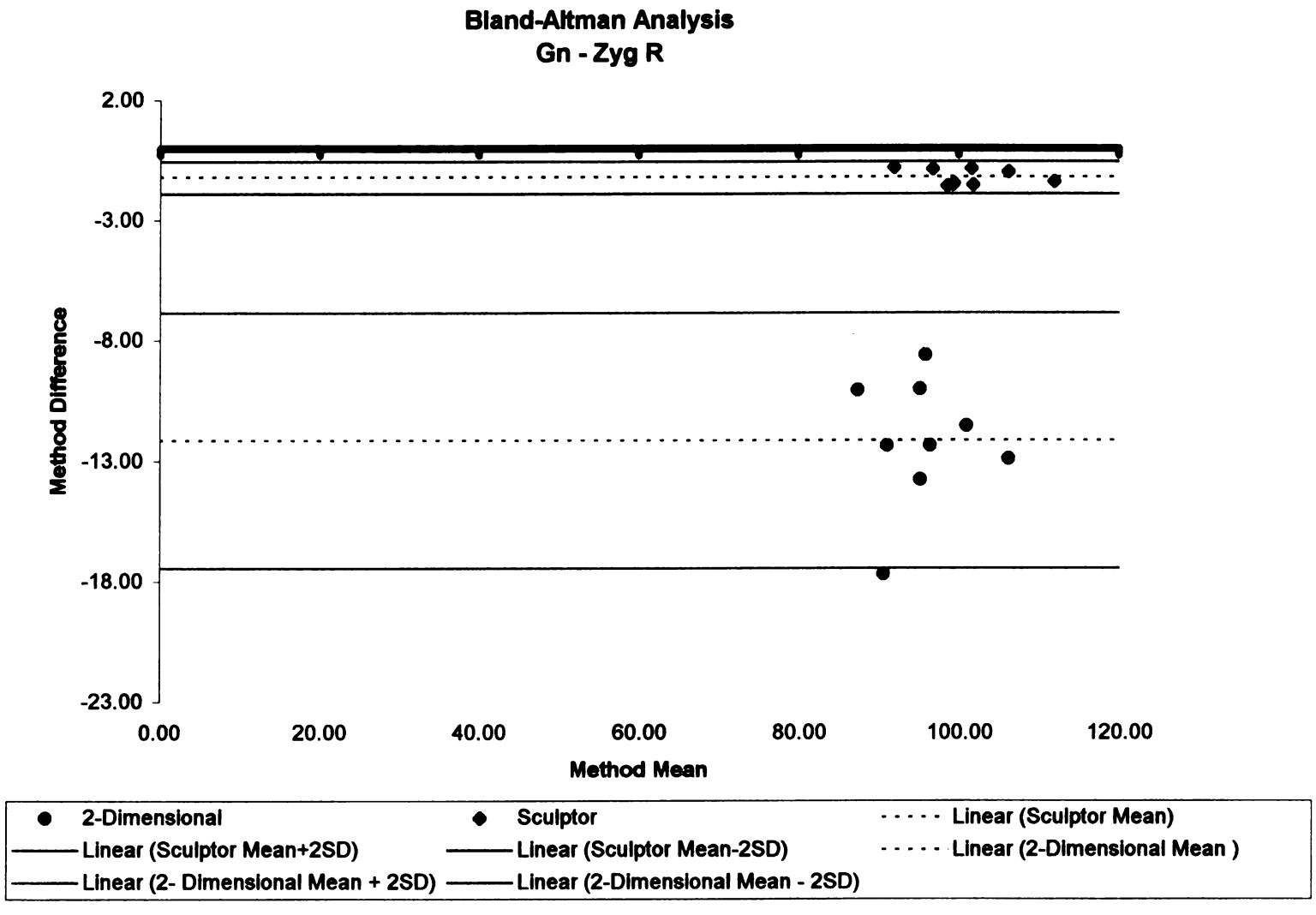
Bland-Altman Analysis
Gn - Zyg R
2.00
-3.00
-8.00
-13.00
-18.00
-23.00
Method Difference
0.00
20.00
40.00
60.00
80.00
100.00
120.00
Method Mean
2-Dimensional
Sculptor
Linear (Sculptor Mean)
Linear (Sculptor Mean+2SD)
Linear (Sculptor Mean-2SD)
Linear (2-Dimensional Mean)
Linear (2- Dimensional Mean + 2SD)
Linear (2-Dimensional Mean - 2SD)

Figure 56.

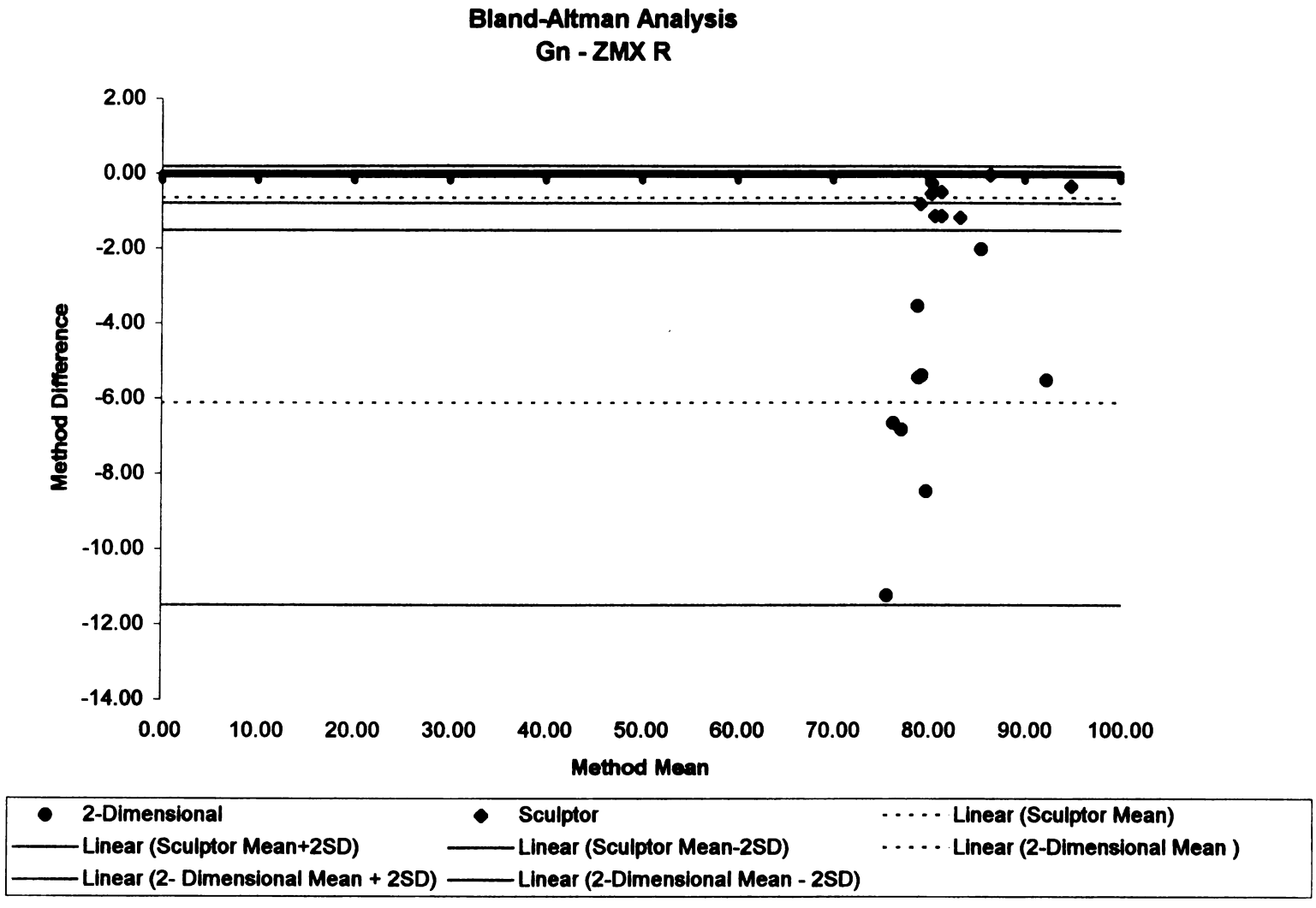
Bland-Altman Analysis
Gn - ZMX R
Method Difference
2.00
0.00
-2.00
-4.00
-6.00
-8.00
-10.00
-12.00
-14.00
0.00
10.00
20.00
30.00
40.00
50.00
60.00
70.00
80.00
90.00
100.00
Method Mean
2-Dimensional
Sculptor
Linear (Sculptor Mean)
Linear (Sculptor Mean+2SD)
Linear (Sculptor Mean-2SD)
Linear (2-Dimensional Mean)
Linear (2- Dimensional Mean + 2SD)
Linear (2-Dimensional Mean - 2SD)

Figure 57.

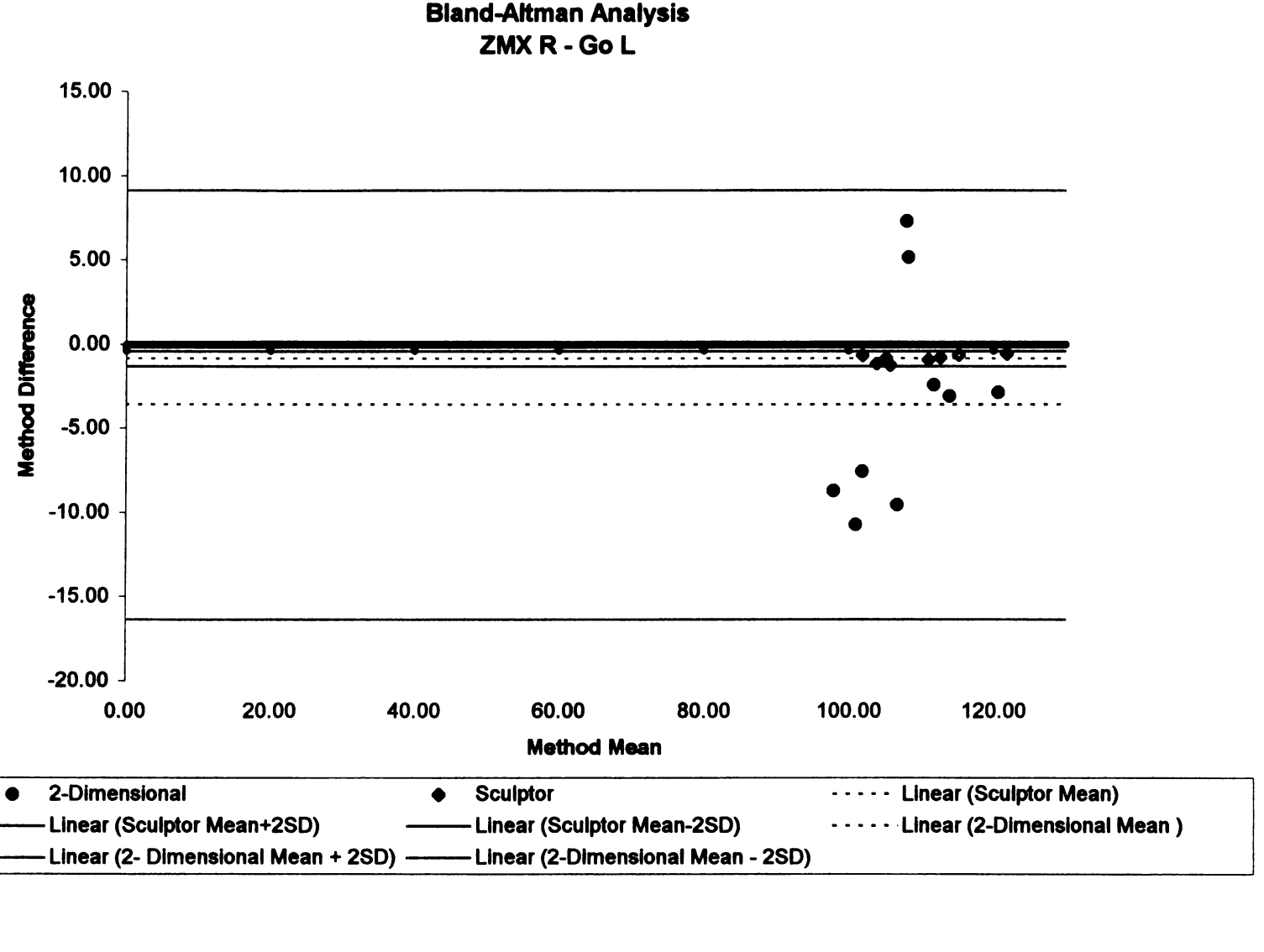
Bland-Altman Analysis
ZMX R - Go L
15.00
10.00
5.00
0.00
-5.00
-10.00
-15.00
-20.00
Method Difference
0.00
20.00
40.00
60.00
80.00
100.00
120.00
Method Mean
2-Dimensional
Sculptor
Linear (Sculptor Mean)
Linear (Sculptor Mean+2SD)
Linear (Sculptor Mean-2SD)
Linear (2-Dimensional Mean)
Linear (2- Dimensional Mean + 2SD)
Linear (2-Dimensional Mean - 2SD)

Figure 58.

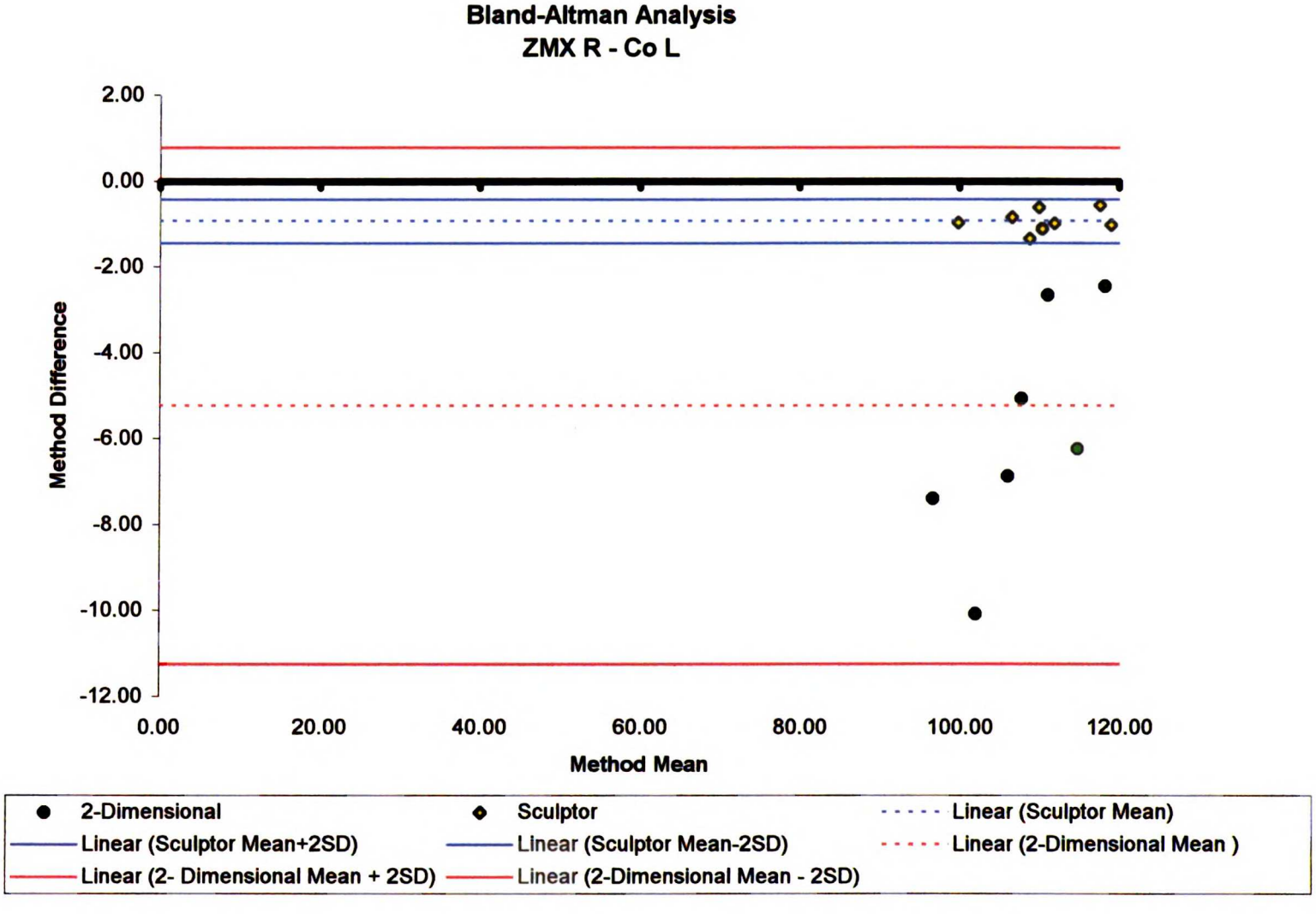
Bland-Altman Analysis
ZMX R - Co L
Method Difference
2.00
0.00
-2.00
-4.00
-6.00
-8.00
-10.00
-12.00
0.00
20.00
40.00
60.00
80.00
100.00
120.00
Method Mean
2-Dimensional
Sculptor
Linear (Sculptor Mean)
Linear (Sculptor Mean+2SD)
Linear (Sculptor Mean-2SD)
Linear (2-Dimensional Mean)
Linear (2- Dimensional Mean + 2SD)
Linear (2-Dimensional Mean - 2SD)

Figure 59.

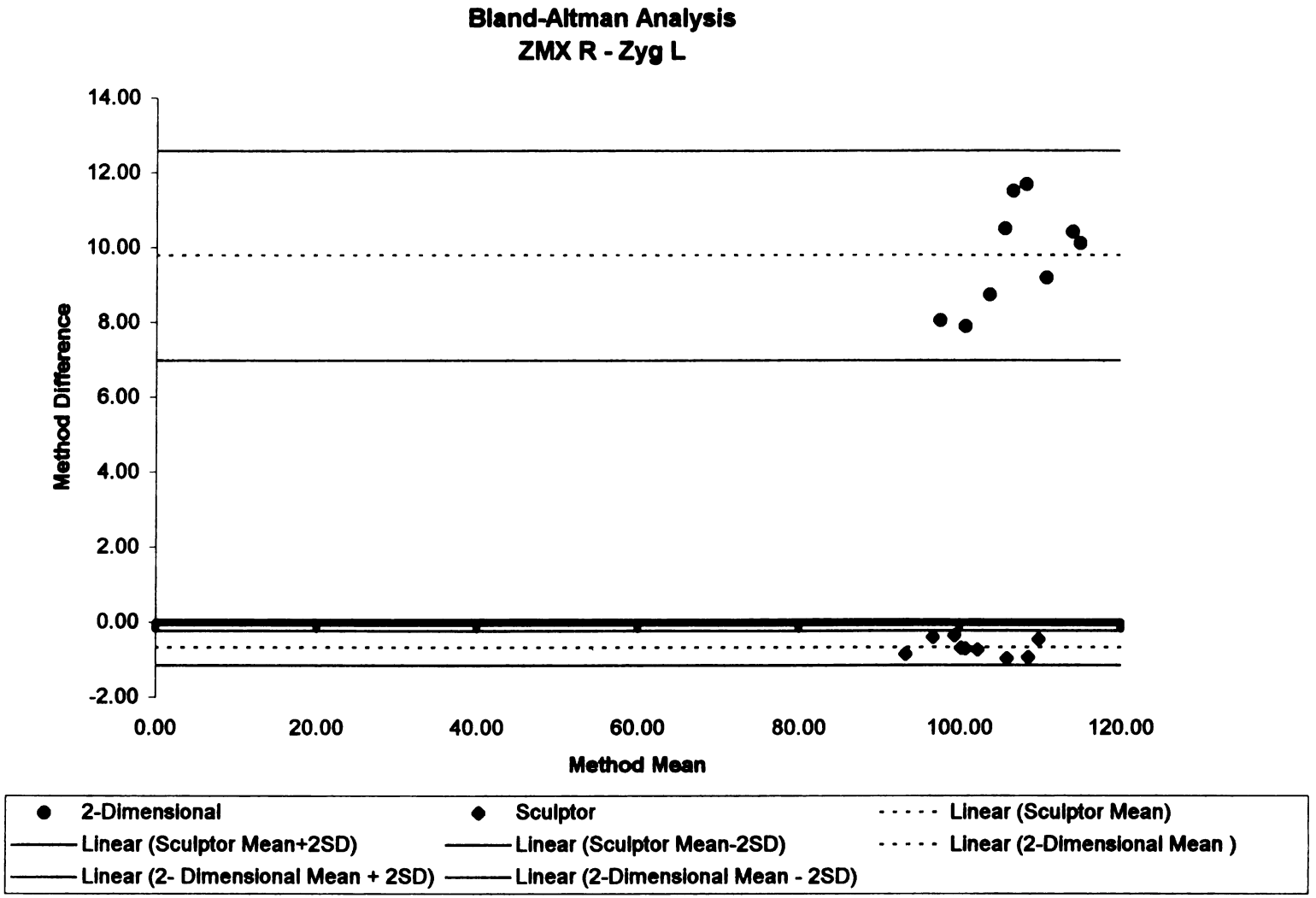
Bland-Altman Analysis
ZMX R - Zyg L
14.00
12.00
10.00
8.00
6.00
4.00
2.00
0.00
-2.00
Method Difference
0.00
20.00
40.00
60.00
80.00
100.00
120.00
Method Mean
2-Dimensional
Sculptor
Linear (Sculptor Mean)
Linear (Sculptor Mean+2SD)
Linear (Sculptor Mean-2SD)
Linear (2-Dimensional Mean)
Linear (2- Dimensional Mean + 2SD)
Linear (2-Dimensional Mean - 2SD)

Figure 60.

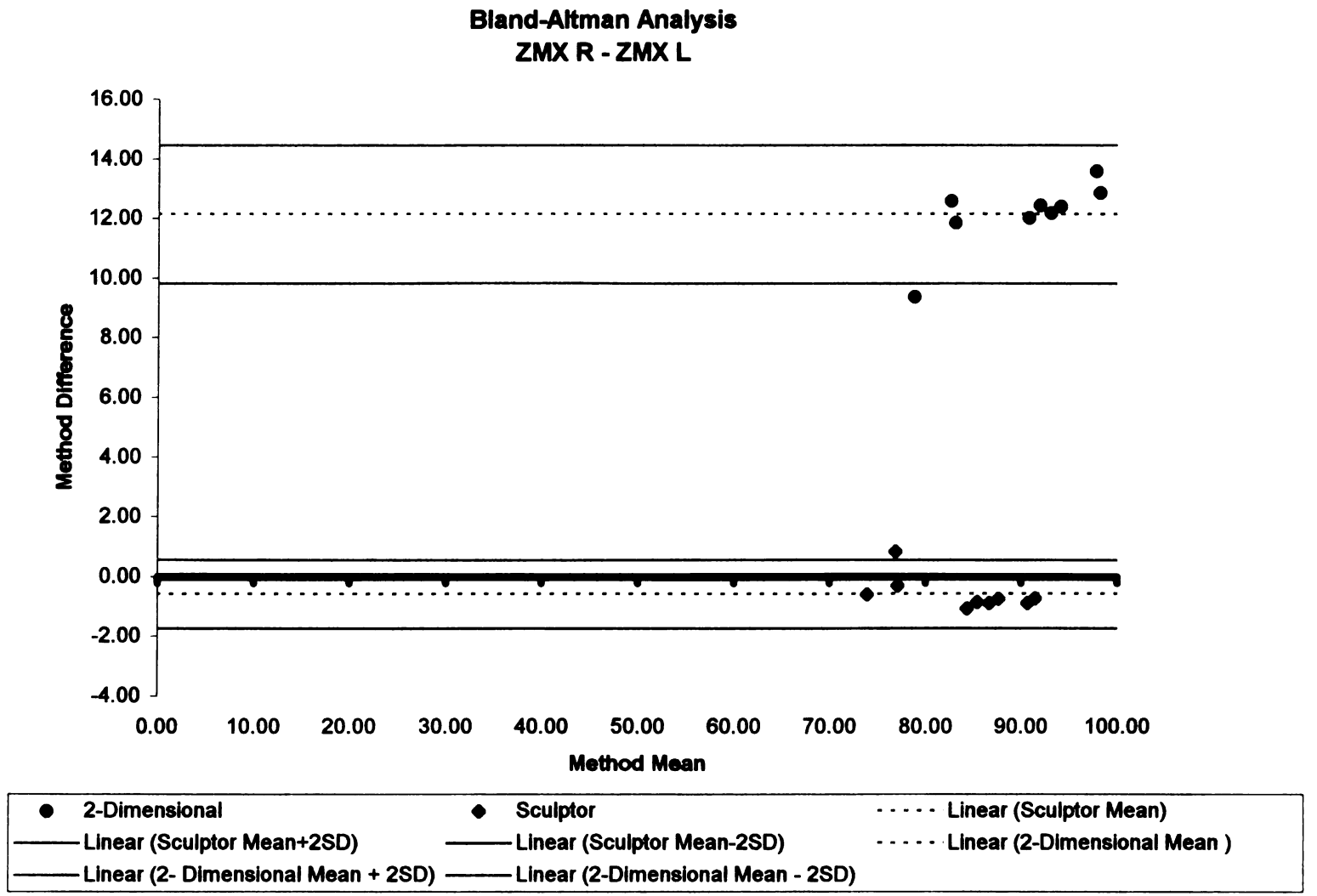
Bland-Altman Analysis
ZMX R - ZMX L
16.00
14.00
12.00
10.00
8.00
6.00
4.00
2.00
0.00
-2.00
-4.00
Method Difference
0.00
10.00
20.00
30.00
40.00
50.00
60.00
70.00
80.00
90.00
100.00
Method Mean
2-Dimensional
Sculptor
Linear (Sculptor Mean)
Linear (Sculptor Mean+2SD)
Linear (Sculptor Mean-2SD)
Linear (2-Dimensional Mean)
Linear (2- Dimensional Mean + 2SD)
Linear (2-Dimensional Mean - 2SD)

Figure 61.

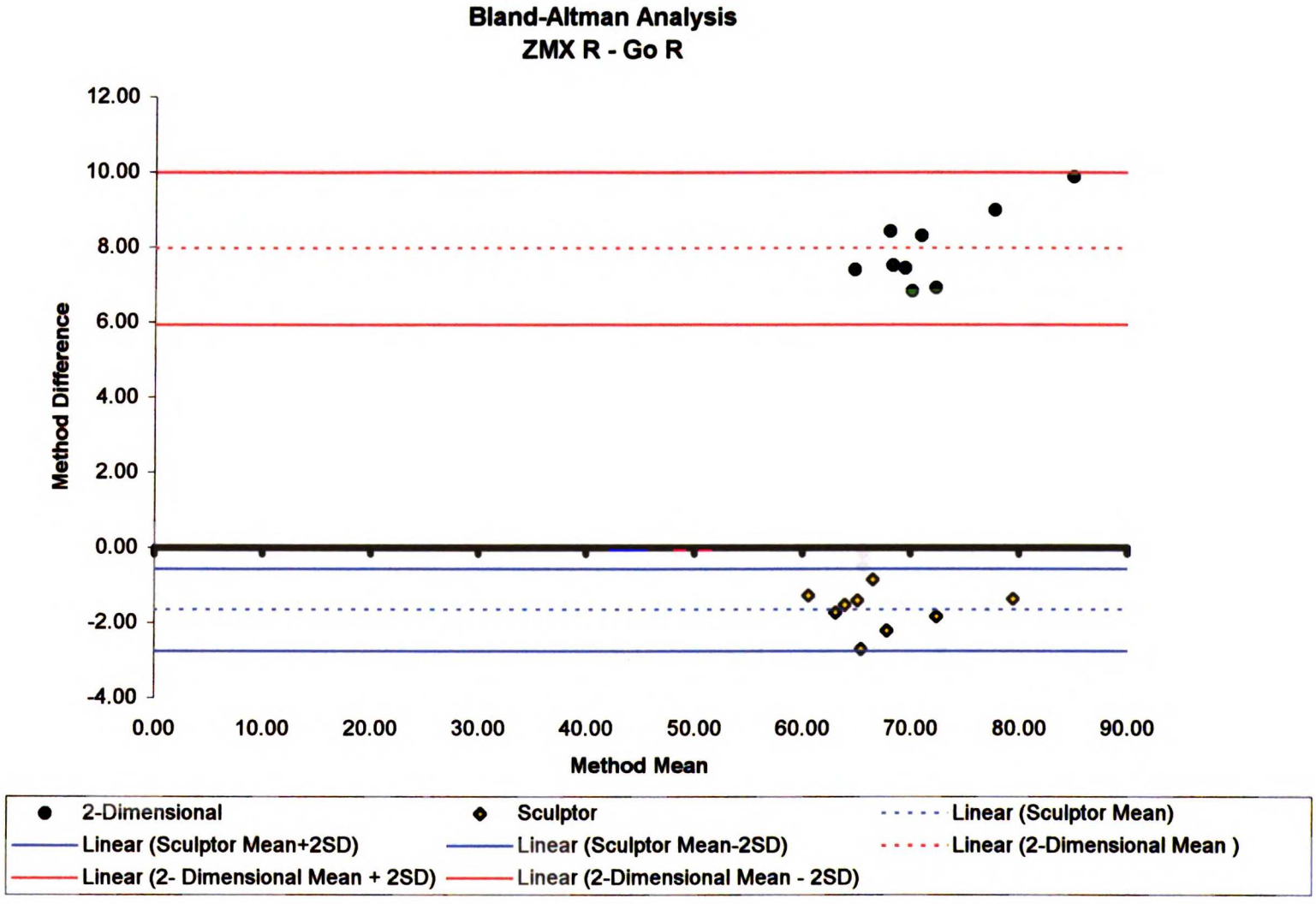
Bland-Altman Analysis
ZMX R - Go R
12.00
10.00
8.00
6.00
4.00
2.00
0.00
-2.00
-4.00
Method Difference
0.00
10.00
20.00
30.00
40.00
50.00
60.00
70.00
80.00
90.00
Method Mean
2-Dimensional
Sculptor
Linear (Sculptor Mean)
Linear (Sculptor Mean+2SD)
Linear (Sculptor Mean-2SD)
Linear (2-Dimensional Mean)
Linear (2- Dimensional Mean + 2SD)
Linear (2-Dimensional Mean - 2SD)

Figure 62.

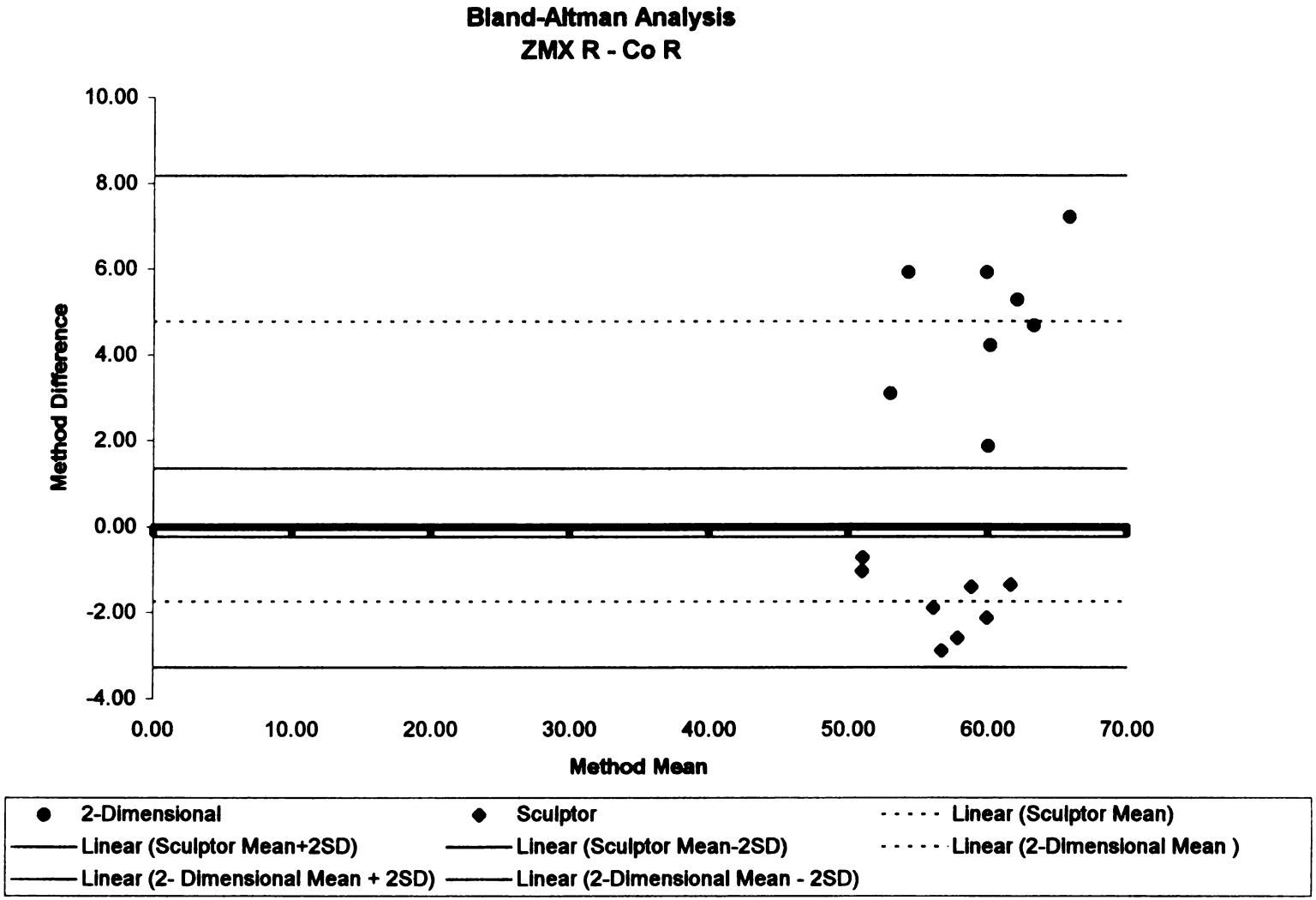
Bland-Altman Analysis
ZMX R - Co R
Method Difference
10.00
8.00
6.00
4.00
2.00
0.00
-2.00
-4.00
0.00
10.00
20.00
30.00
40.00
50.00
60.00
70.00
Method Mean
2-Dimensional
Sculptor
Linear (Sculptor Mean)
Linear (Sculptor Mean+2SD)
Linear (Sculptor Mean-2SD)
Linear (2-Dimensional Mean)
Linear (2- Dimensional Mean + 2SD)
Linear (2-Dimensional Mean - 2SD)

Figure 63.

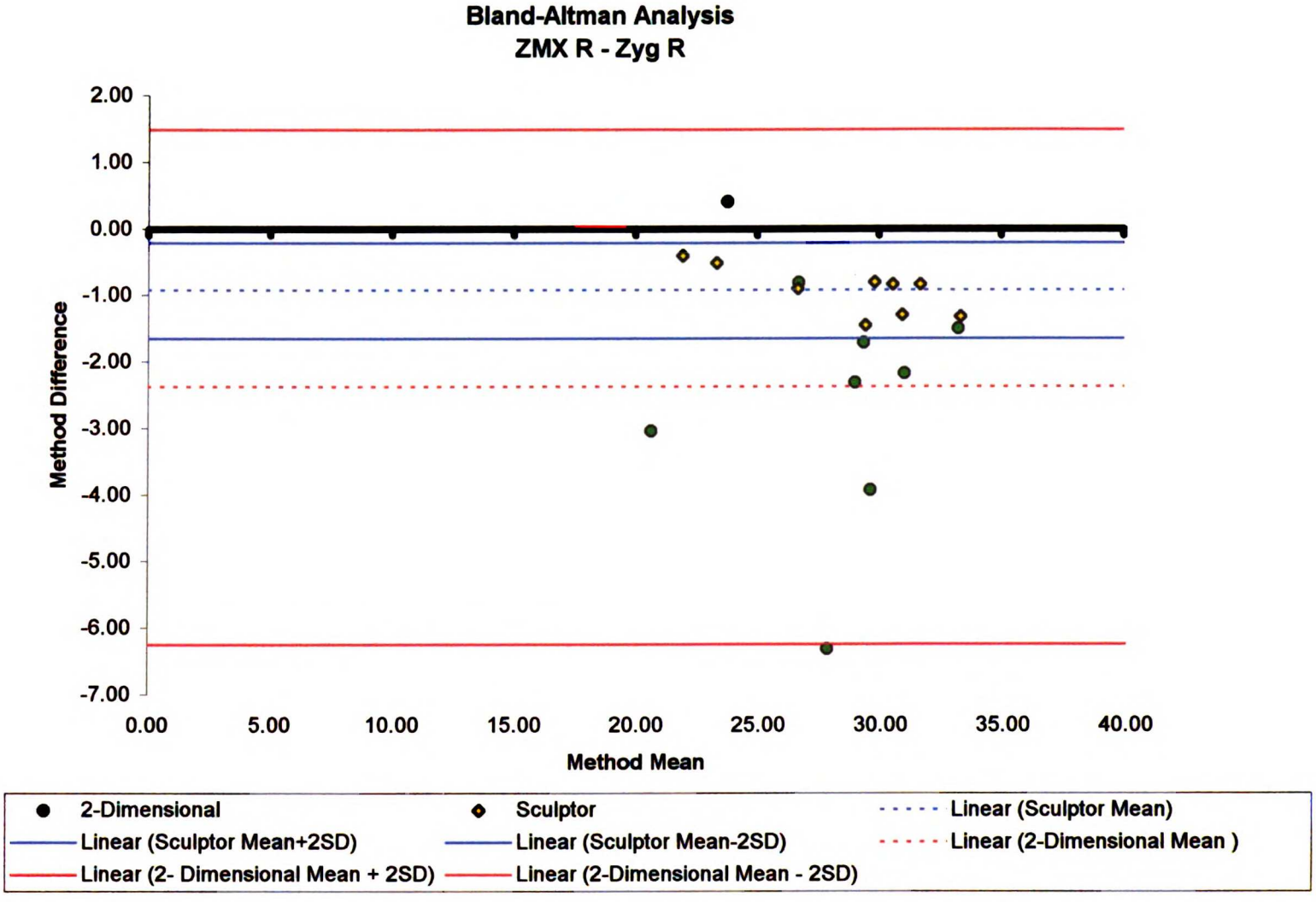
Bland-Altman Analysis
ZMX R - Zyg R
Method Difference
2.00
1.00
0.00
-1.00
-2.00
-3.00
-4.00
-5.00
-6.00
-7.00
0.00
5.00
10.00
15.00
20.00
25.00
30.00
35.00
40.00
Method Mean
2-Dimensional
Sculptor
Linear (Sculptor Mean)
Linear (Sculptor Mean+2SD)
Linear (Sculptor Mean-2SD)
Linear (2-Dimensional Mean)
Linear (2- Dimensional Mean + 2SD)
Linear (2-Dimensional Mean - 2SD)

Figure 64.

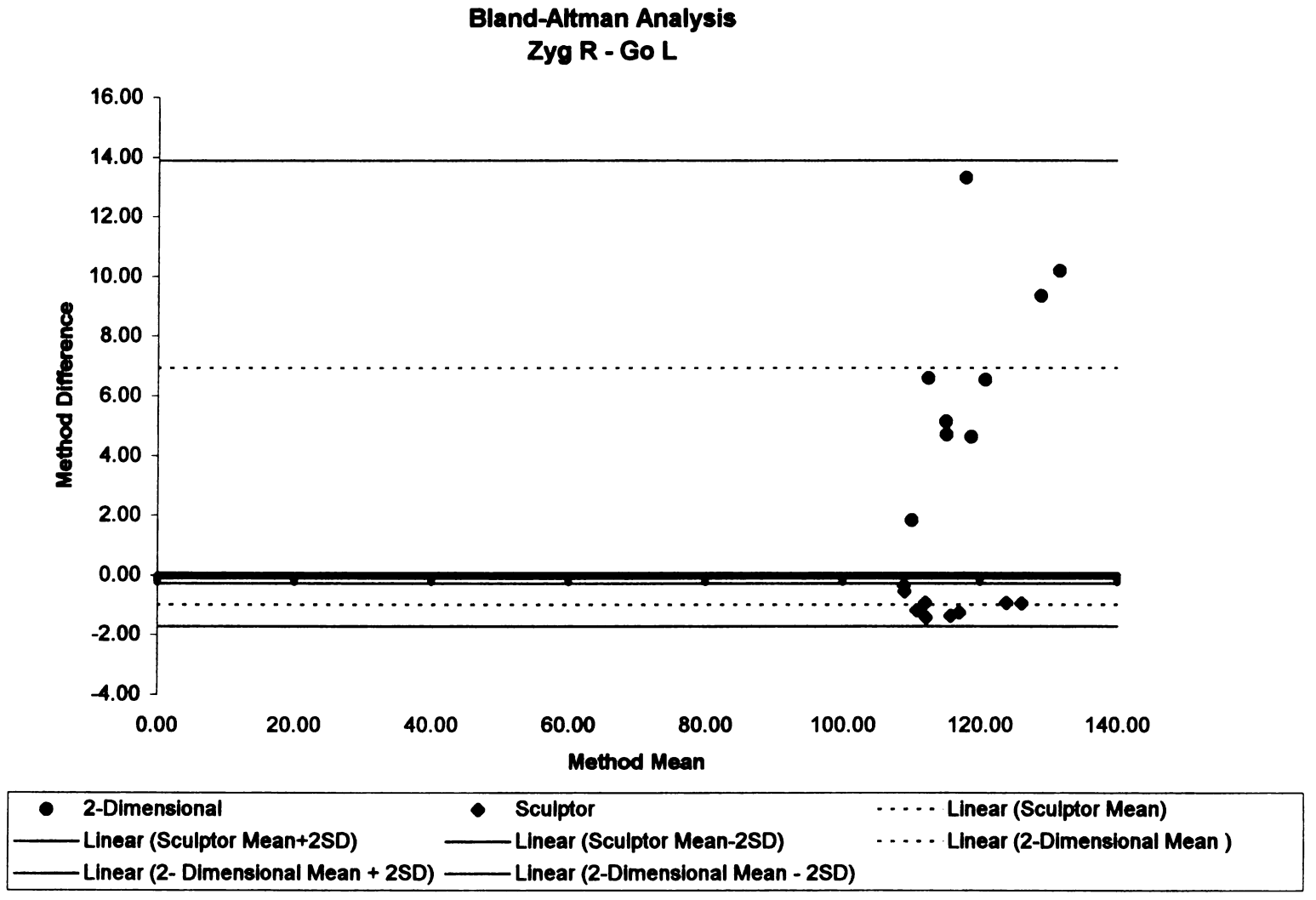
Bland-Altman Analysis
Zyg R - Go L
Method Difference
16.00
14.00
12.00
10.00
8.00
6.00
4.00
2.00
0.00
-2.00
-4.00
0.00
20.00
40.00
60.00
80.00
100.00
120.00
140.00
Method Mean
2-Dimensional
Sculptor
Linear (Sculptor Mean)
Linear (Sculptor Mean+2SD)
Linear (Sculptor Mean-2SD)
Linear (2-Dimensional Mean)
Linear (2- Dimensional Mean + 2SD)
Linear (2-Dimensional Mean - 2SD)

Figure 65.

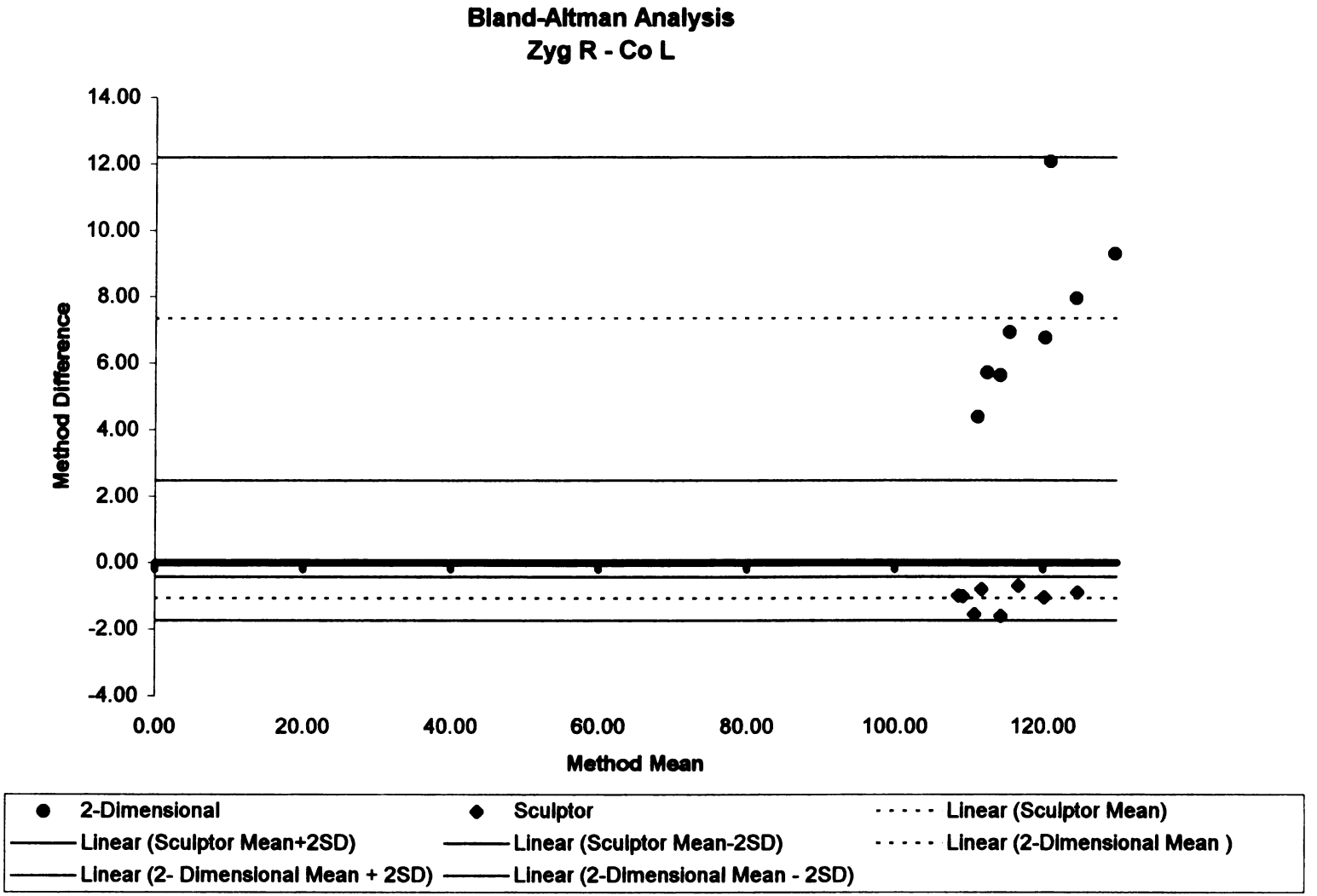
Bland-Altman Analysis
Zyg R - Co L
Method Difference
14.00
12.00
10.00
8.00
6.00
4.00
2.00
0.00
-2.00
-4.00
0.00
20.00
40.00
60.00
80.00
100.00
120.00
Method Mean
2-Dimensional
Sculptor
Linear (Sculptor Mean)
Linear (Sculptor Mean+2SD)
Linear (Sculptor Mean-2SD)
Linear (2-Dimensional Mean)
Linear (2- Dimensional Mean + 2SD)
Linear (2-Dimensional Mean - 2SD)

Figure 66.

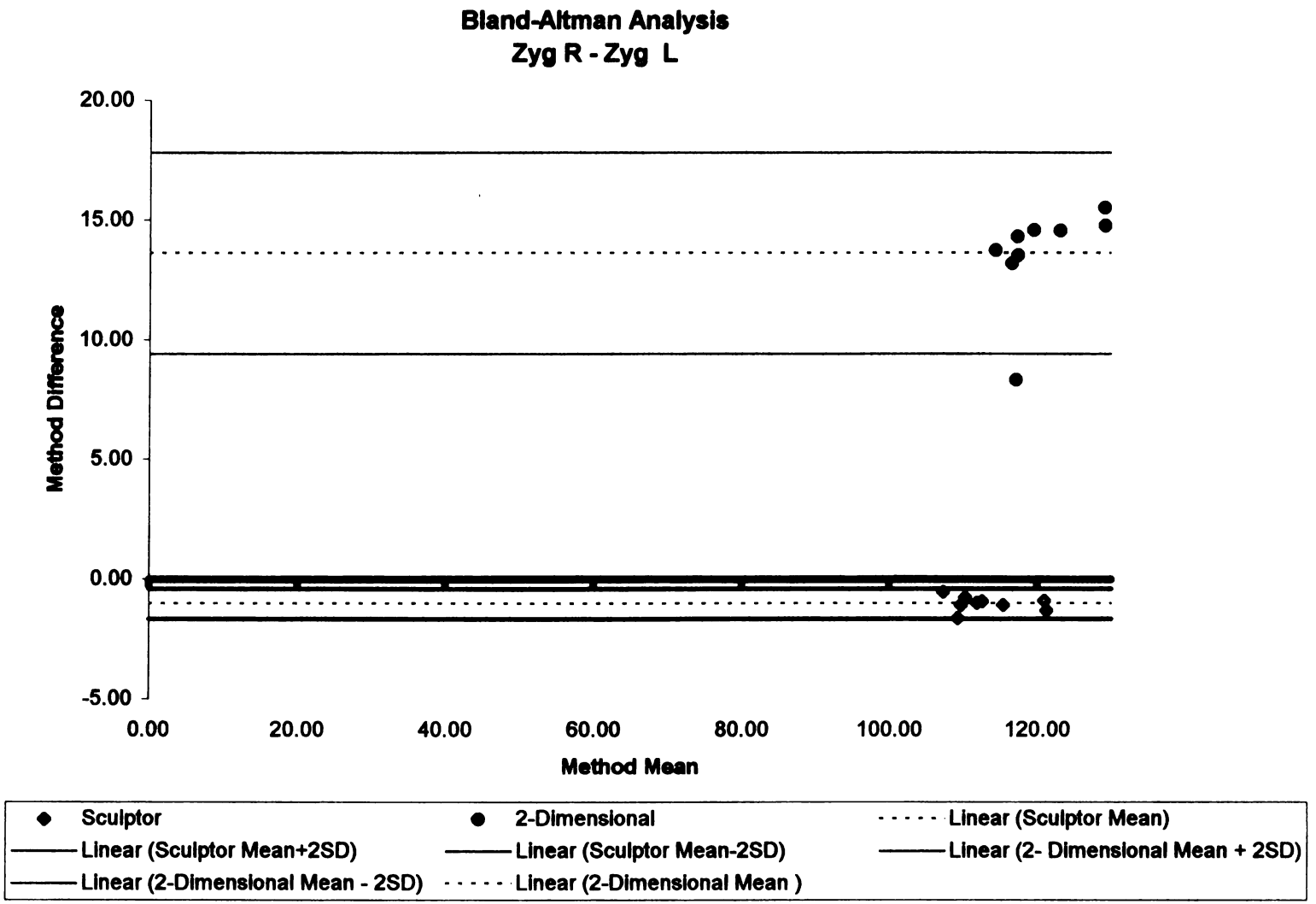
Bland-Altman Analysis
Zyg R - Zyg L
20.00
15.00
10.00
5.00
0.00
-5.00
Method Difference
0.00
20.00
40.00
60.00
80.00
100.00
120.00
Method Mean
Sculptor
2-Dimensional
Linear (Sculptor Mean)
Linear (Sculptor Mean+2SD)
Linear (Sculptor Mean-2SD)
Linear (2- Dimensional Mean + 2SD)
Linear (2-Dimensional Mean - 2SD)
Linear (2-Dimensional Mean)

Figure 67.

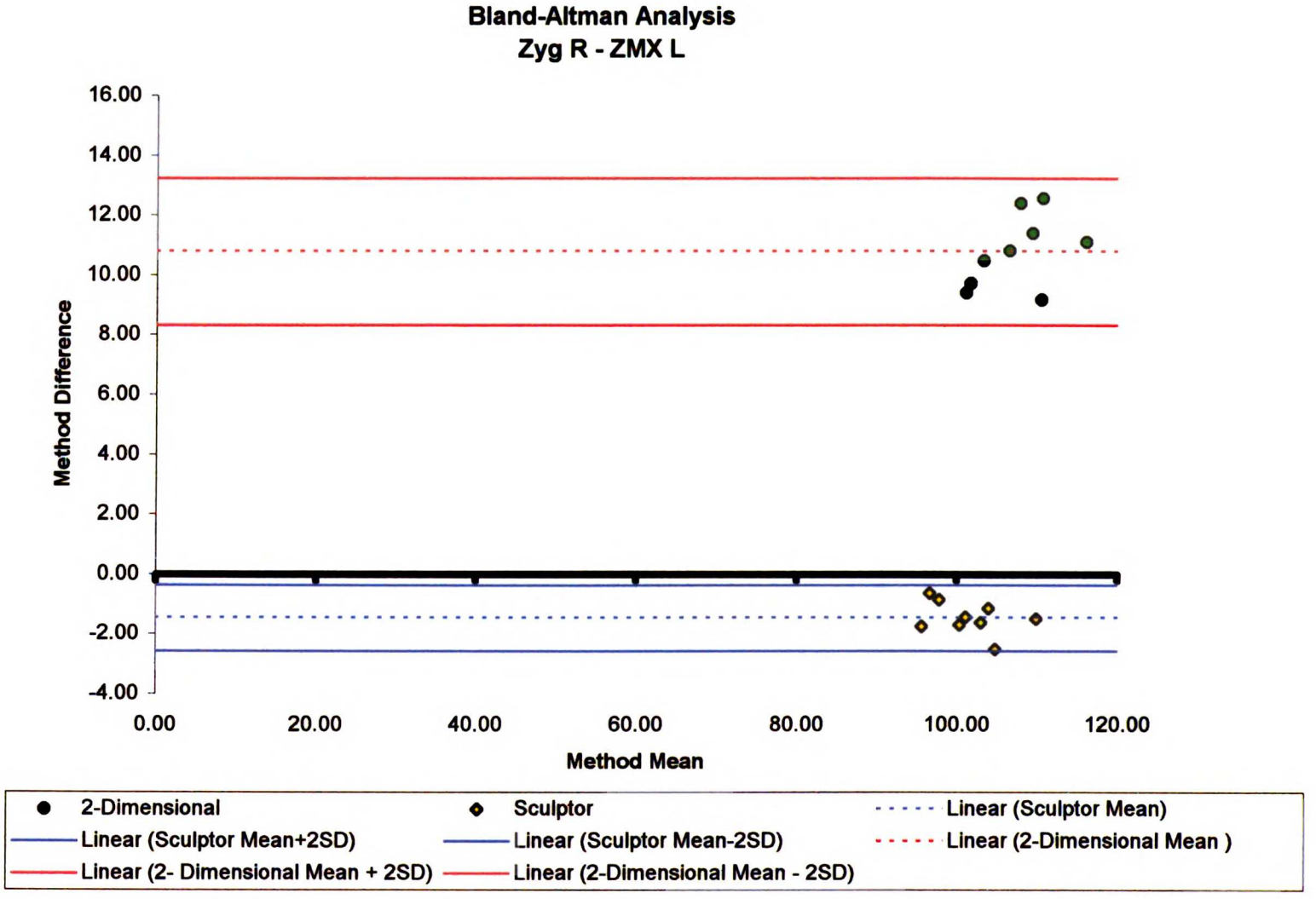
Bland-Altman Analysis
Zyg R - ZMX L
Method Difference
16.00
14.00
12.00
10.00
8.00
6.00
4.00
2.00
0.00
-2.00
-4.00
0.00
20.00
40.00
60.00
80.00
100.00
120.00
Method Mean
2-Dimensional
Sculptor
Linear (Sculptor Mean)
Linear (Sculptor Mean+2SD)
Linear (Sculptor Mean-2SD)
Linear (2-Dimensional Mean)
Linear (2- Dimensional Mean + 2SD)
Linear (2-Dimensional Mean - 2SD)

Figure 68.

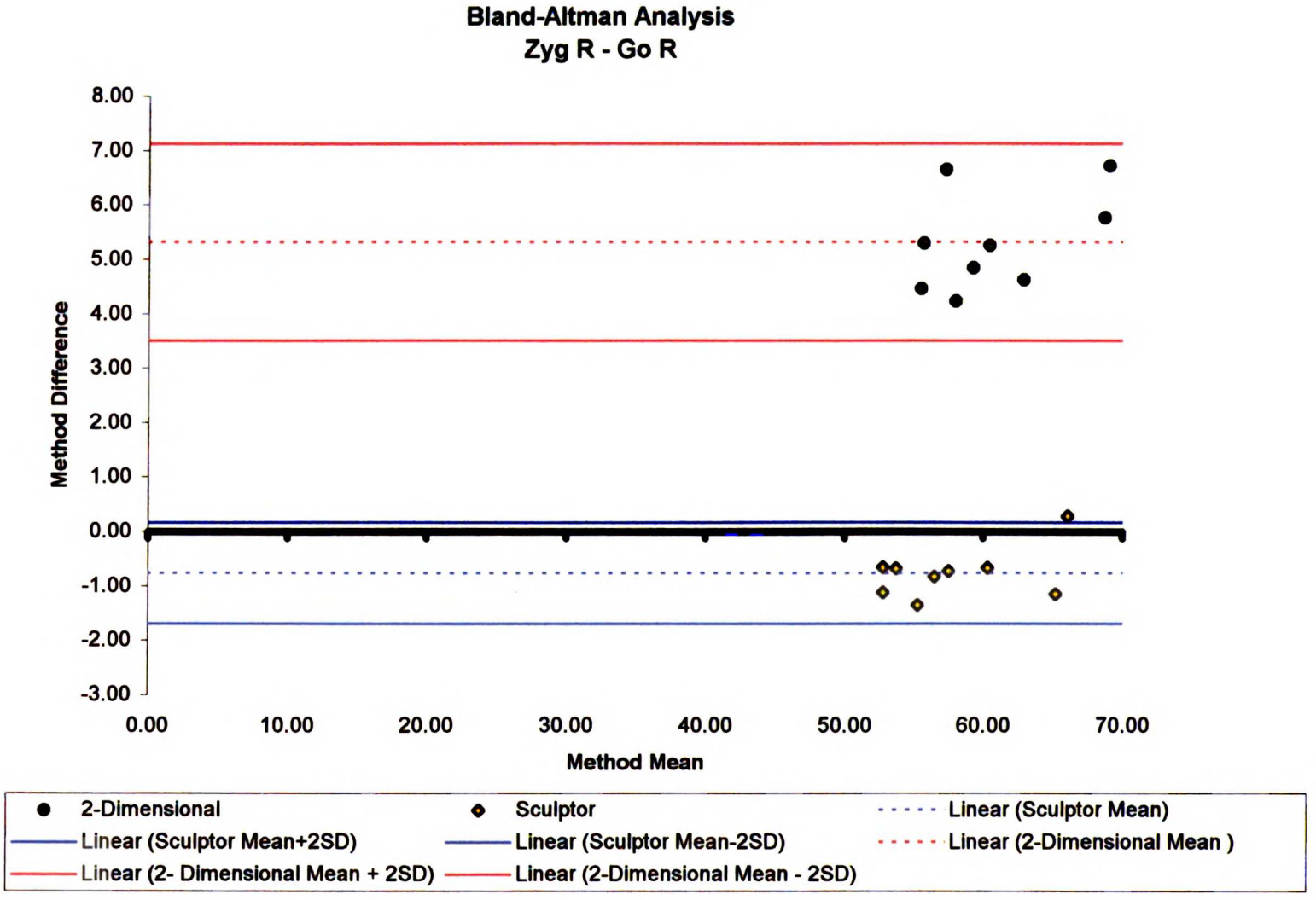
Bland-Altman Analysis
Zyg R - Go R
8.00
7.00
6.00
5.00
4.00
3.00
2.00
1.00
0.00
-1.00
-2.00
-3.00
Method Difference
0.00
10.00
20.00
30.00
40.00
50.00
60.00
70.00
Method Mean
2-Dimensional
Sculptor
Linear (Sculptor Mean)
Linear (Sculptor Mean+2SD)
Linear (Sculptor Mean-2SD)
Linear (2-Dimensional Mean)
Linear (2- Dimensional Mean + 2SD)
Linear (2-Dimensional Mean - 2SD)

Figure 69.

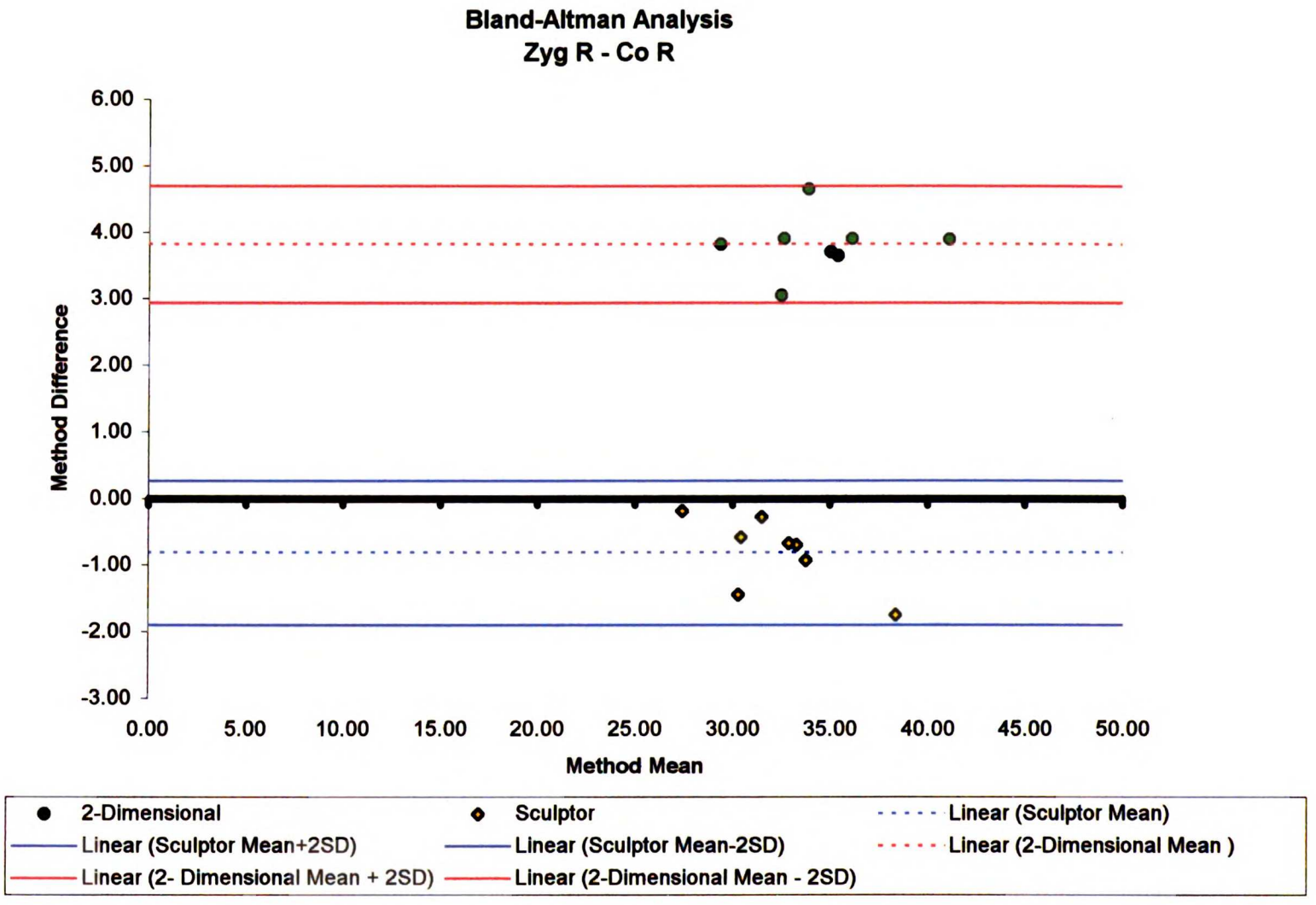
Bland-Altman Analysis
Zyg R - Co R
Method Difference
6.00
5.00
4.00
3.00
2.00
1.00
0.00
-1.00
-2.00
-3.00
0.00
5.00
10.00
15.00
20.00
25.00
30.00
35.00
40.00
45.00
50.00
Method Mean
2-Dimensional
Sculptor
Linear (Sculptor Mean)
Linear (Sculptor Mean+2SD)
Linear (Sculptor Mean-2SD)
Linear (2-Dimensional Mean)
Linear (2- Dimensional Mean + 2SD)
Linear (2-Dimensional Mean - 2SD)

Figure 70.

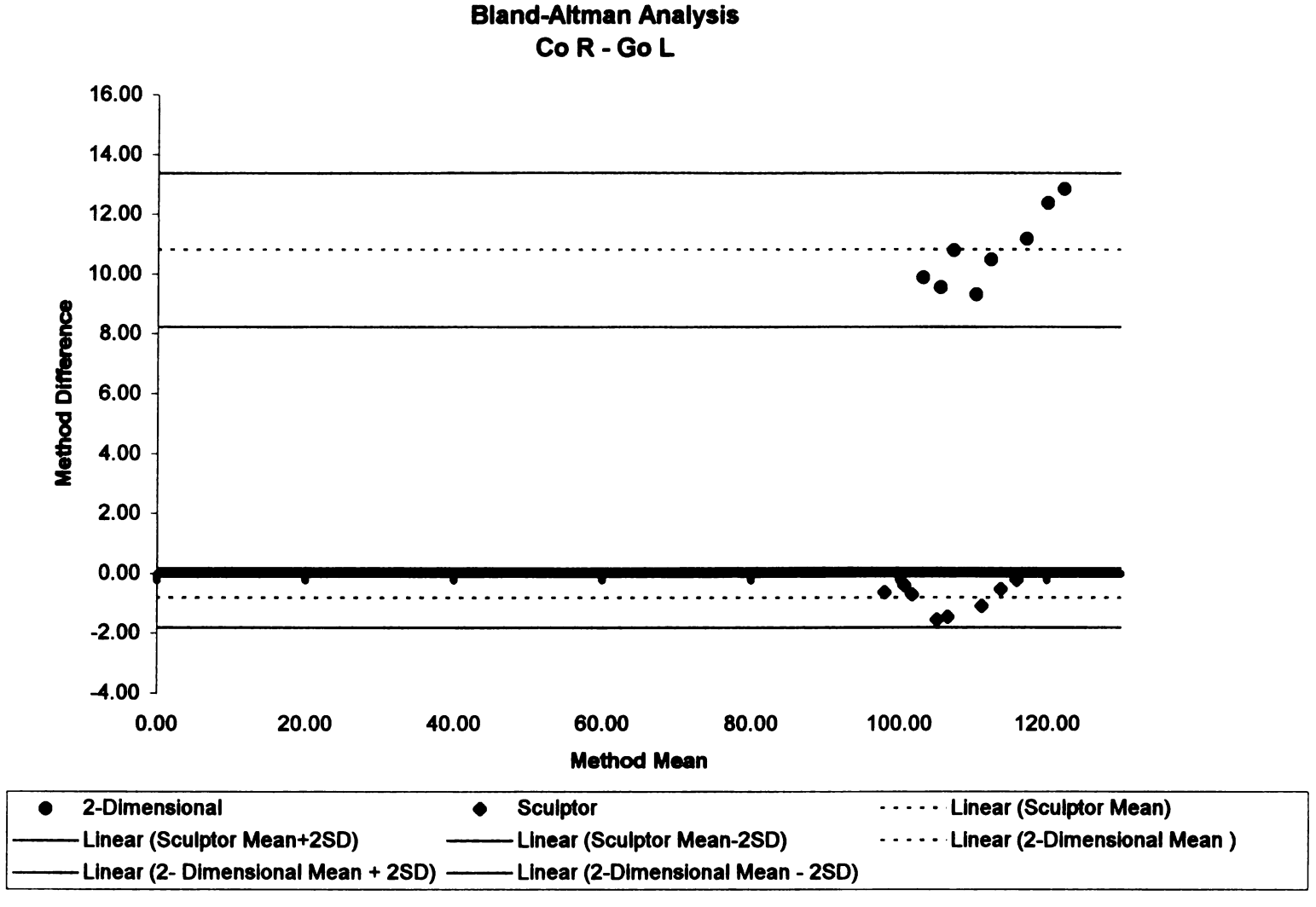
Bland-Altman Analysis
Co R - Go L
16.00
14.00
12.00
10.00
8.00
6.00
4.00
2.00
0.00
-2.00
-4.00
Method Difference
0.00
20.00
40.00
60.00
80.00
100.00
120.00
Method Mean
2-Dimensional
Sculptor
Linear (Sculptor Mean)
Linear (Sculptor Mean+2SD)
Linear (Sculptor Mean-2SD)
Linear (2-Dimensional Mean)
Linear (2- Dimensional Mean + 2SD)
Linear (2-Dimensional Mean - 2SD)

Figure 71.

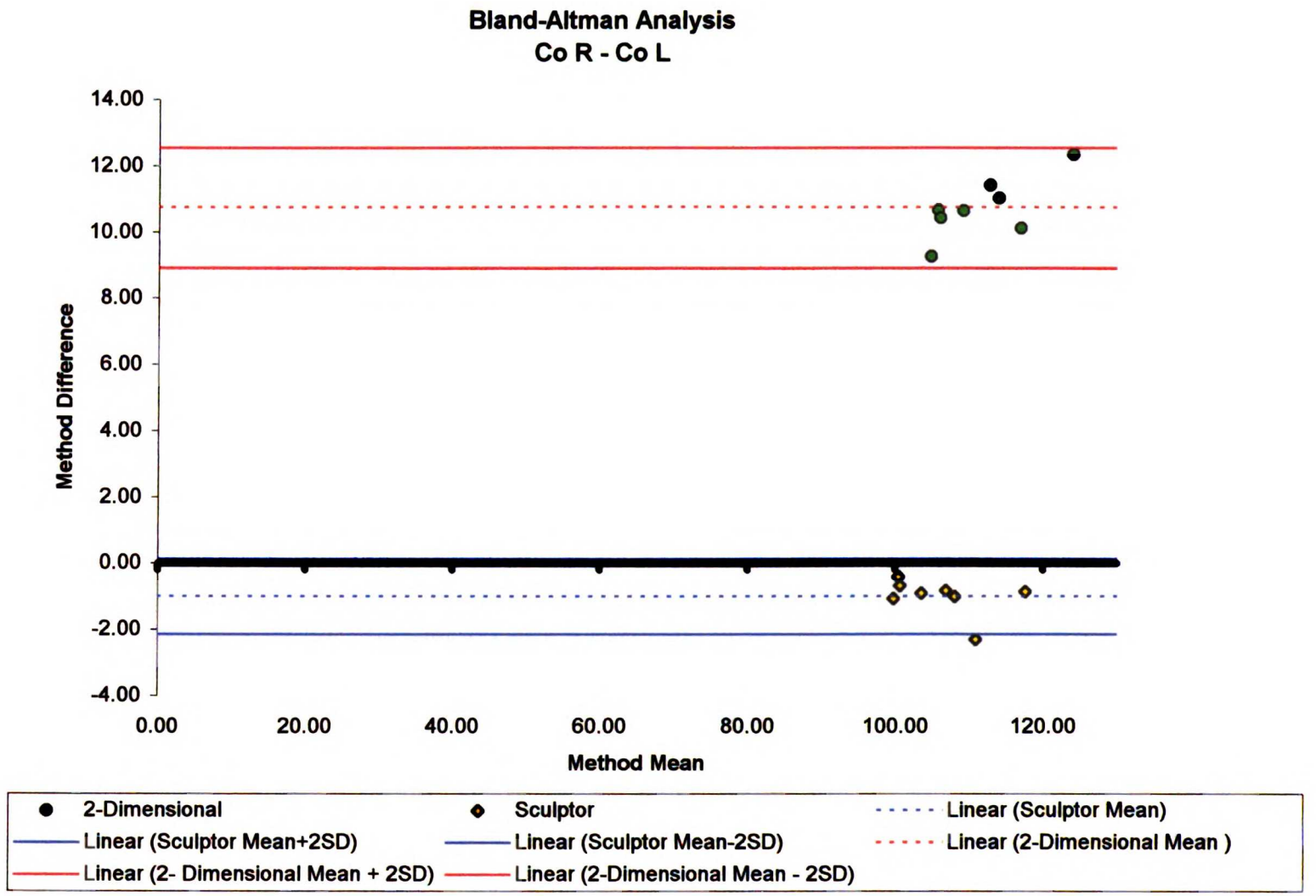
Bland-Altman Analysis
Co R - Co L
14.00
12.00
10.00
8.00
6.00
4.00
2.00
0.00
-2.00
-4.00
Method Difference
0.00
20.00
40.00
60.00
80.00
100.00
120.00
Method Mean
2-Dimensional
Sculptor
Linear (Sculptor Mean)
Linear (Sculptor Mean+2SD)
Linear (Sculptor Mean-2SD)
Linear (2-Dimensional Mean)
Linear (2- Dimensional Mean + 2SD)
Linear (2-Dimensional Mean - 2SD)

Figure 72.

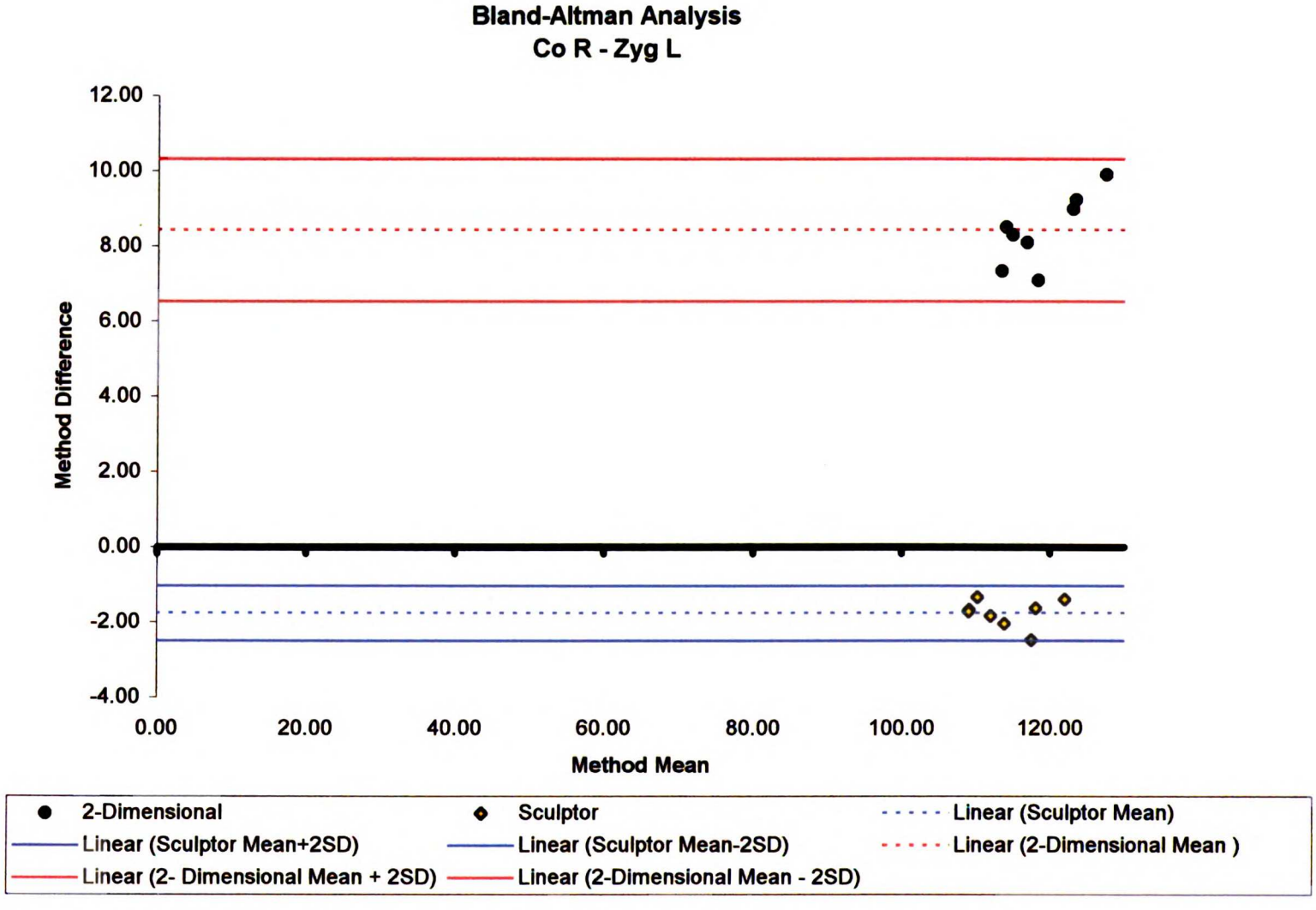
Bland-Altman Analysis
Co R - Zyg L
12.00
10.00
8.00
6.00
4.00
2.00
0.00
-2.00
-4.00
Method Difference
0.00
20.00
40.00
60.00
80.00
100.00
120.00
Method Mean
2-Dimensional
Sculptor
Linear (Sculptor Mean)
Linear (Sculptor Mean+2SD)
Linear (Sculptor Mean-2SD)
Linear (2-Dimensional Mean)
Linear (2- Dimensional Mean + 2SD)
Linear (2-Dimensional Mean - 2SD)

Figure 73.

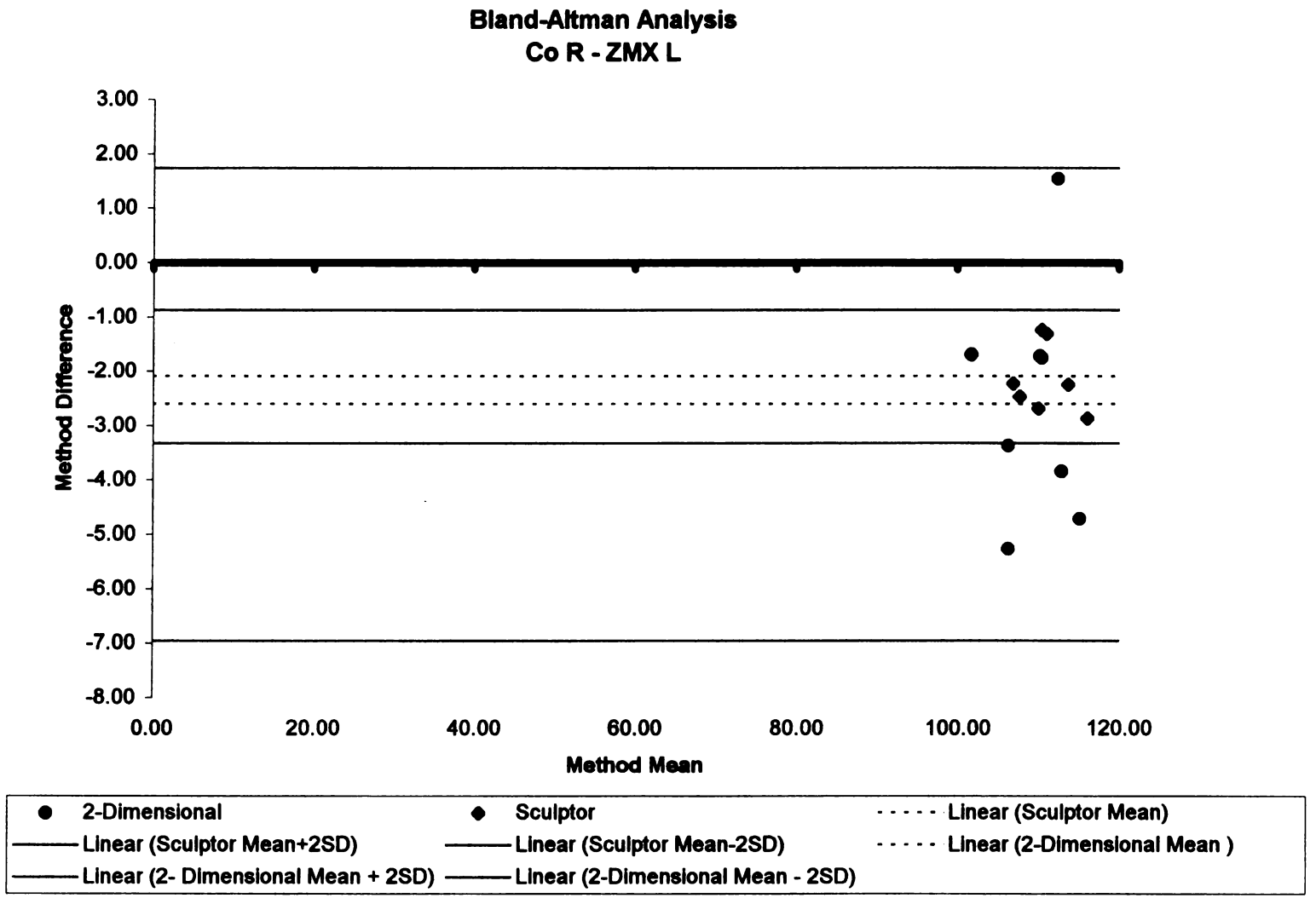
Bland-Altman Analysis
Co R - ZMX L
Method Difference
3.00
2.00
1.00
0.00
-1.00
-2.00
-3.00
-4.00
-5.00
-6.00
-7.00
-8.00
0.00
20.00
40.00
60.00
80.00
100.00
120.00
Method Mean
2-Dimensional
Sculptor
Linear (Sculptor Mean)
Linear (Sculptor Mean+2SD)
Linear (Sculptor Mean-2SD)
Linear (2-Dimensional Mean)
Linear (2- Dimensional Mean + 2SD)
Linear (2-Dimensional Mean - 2SD)

Figure 74.

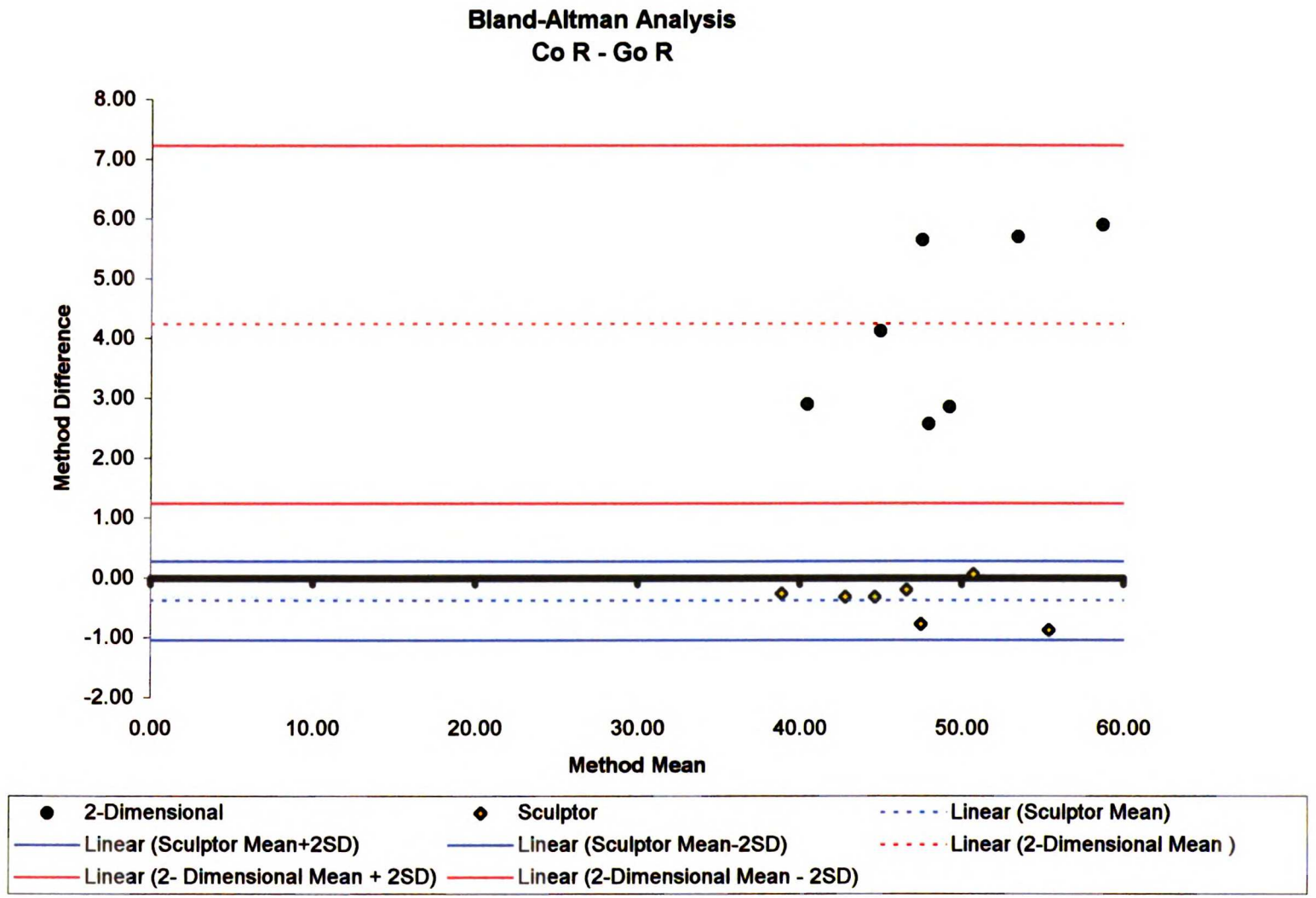
Bland-Altman Analysis
Co R - Go R
Method Difference
8.00
7.00
6.00
5.00
4.00
3.00
2.00
1.00
0.00
-1.00
-2.00
0.00
10.00
20.00
30.00
40.00
50.00
60.00
Method Mean
2-Dimensional
Sculptor
Linear (Sculptor Mean)
Linear (Sculptor Mean+2SD)
Linear (Sculptor Mean-2SD)
Linear (2-Dimensional Mean)
Linear (2- Dimensional Mean + 2SD)
Linear (2-Dimensional Mean - 2SD)

Figure 74.

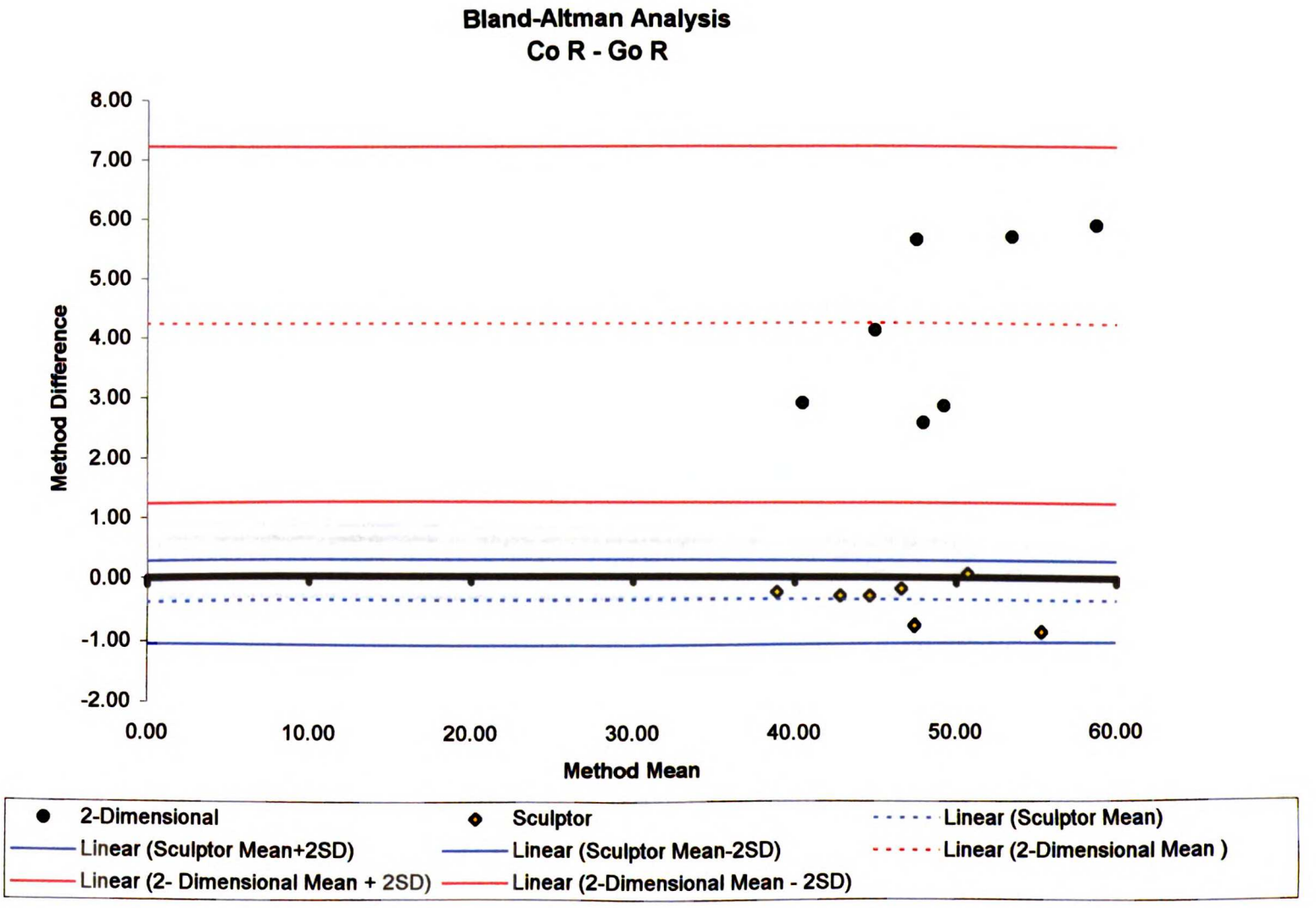
Bland-Altman Analysis
Co R - Go R
8.00
7.00
6.00
5.00
4.00
3.00
2.00
1.00
0.00
-1.00
-2.00
Method Difference
0.00
10.00
20.00
30.00
40.00
50.00
60.00
Method Mean
2-Dimensional
Sculptor
Linear (Sculptor Mean)
Linear (Sculptor Mean+2SD)
Linear (Sculptor Mean-2SD)
Linear (2-Dimensional Mean)
Linear (2- Dimensional Mean + 2SD)
Linear (2-Dimensional Mean - 2SD)

Figure 75.

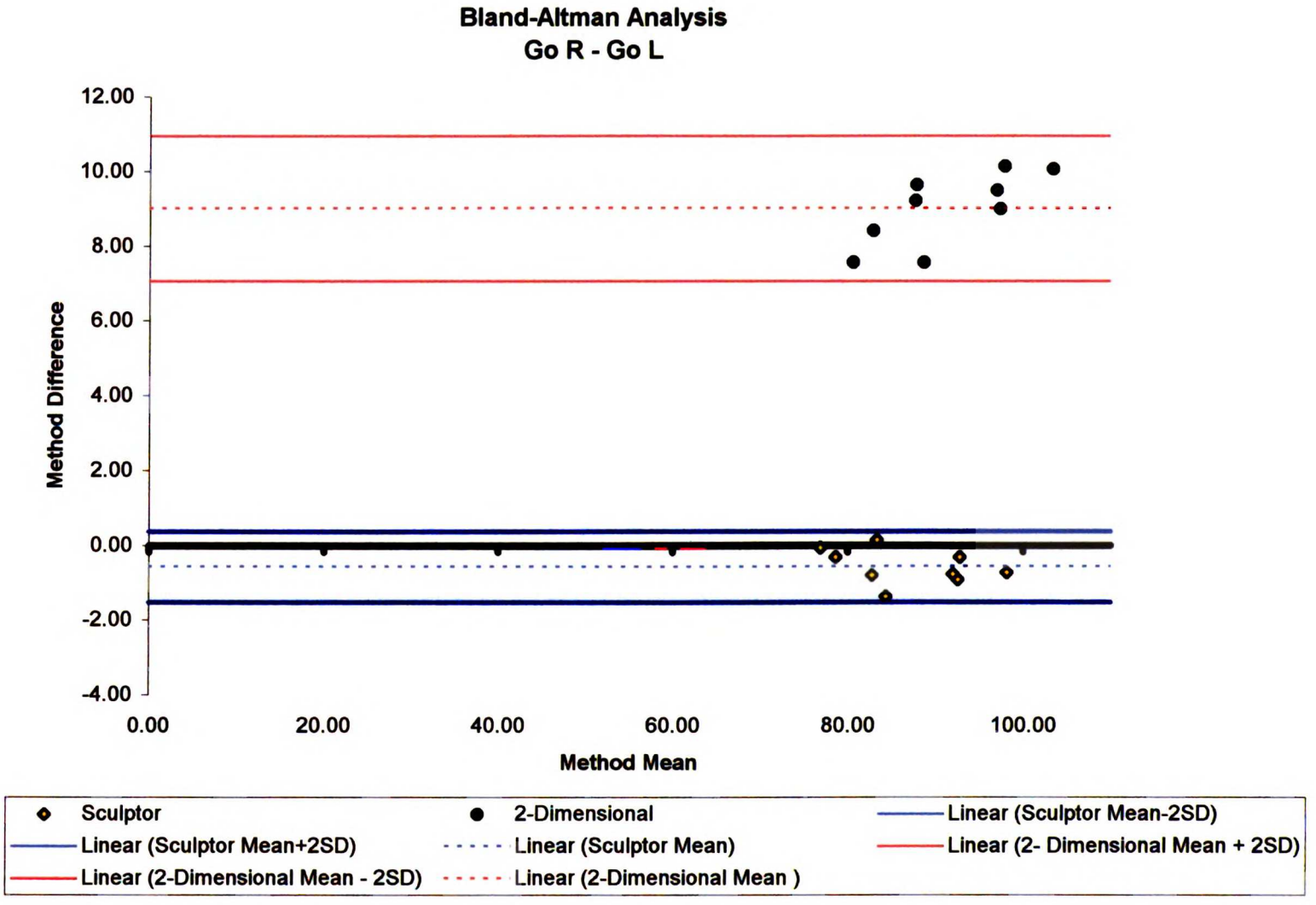
Bland-Altman Analysis
Go R - Go L
12.00
10.00
8.00
6.00
4.00
2.00
0.00
-2.00
-4.00
Method Difference
0.00
20.00
40.00
60.00
80.00
100.00
Method Mean
Sculptor
2-Dimensional
Linear (Sculptor Mean-2SD)
Linear (Sculptor Mean+2SD)
Linear (Sculptor Mean)
Linear (2- Dimensional Mean + 2SD)
Linear (2-Dimensional Mean - 2SD)
Linear (2-Dimensional Mean)

Figure 76.

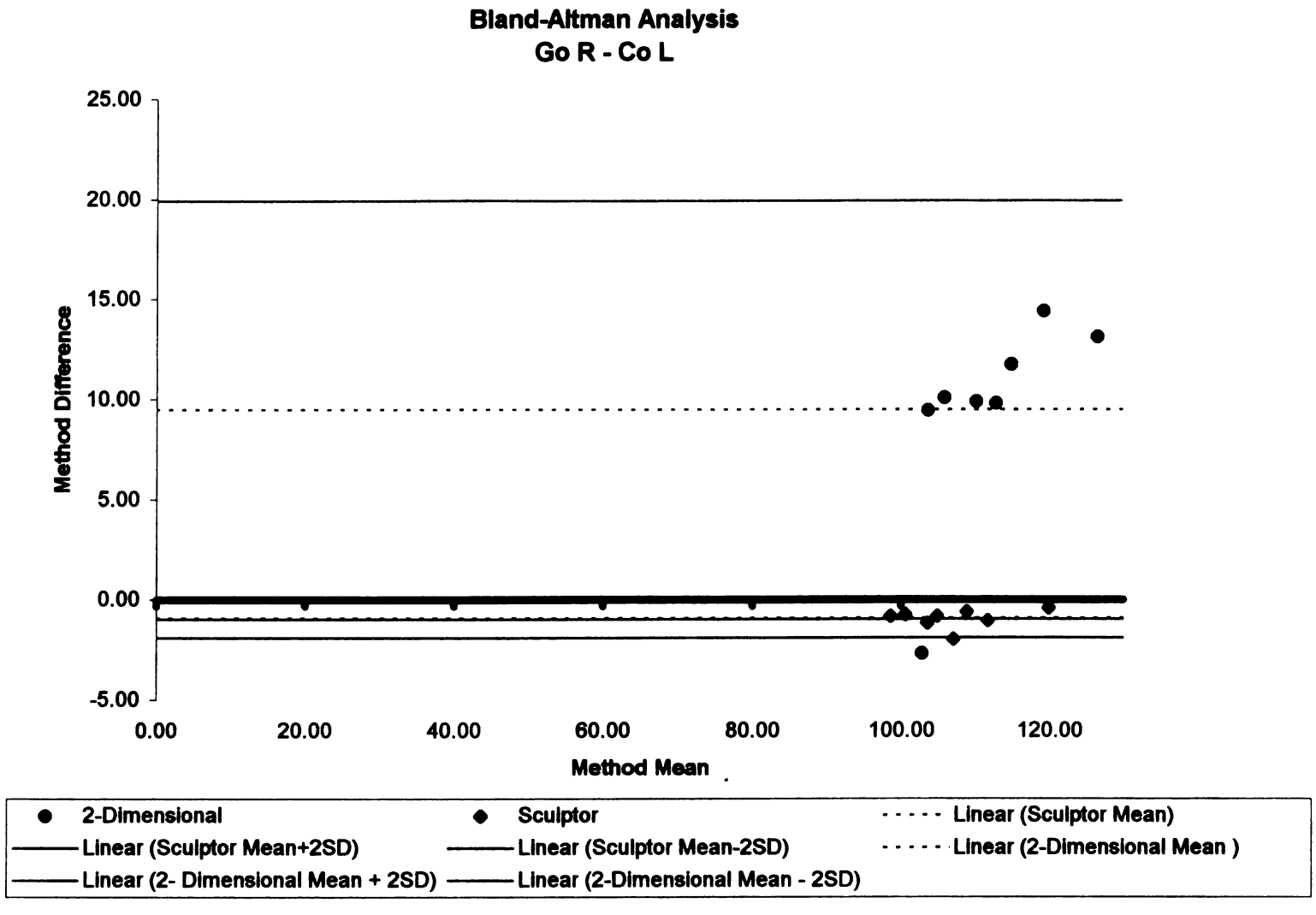
Bland-Altman Analysis
Go R - Co L
25.00
20.00
15.00
10.00
5.00
0.00
-5.00
Method Difference
0.00
20.00
40.00
60.00
80.00
100.00
120.00
Method Mean
2-Dimensional
Sculptor
Linear (Sculptor Mean)
Linear (Sculptor Mean+2SD)
Linear (Sculptor Mean-2SD)
Linear (2-Dimensional Mean)
Linear (2- Dimensional Mean + 2SD)
Linear (2-Dimensional Mean - 2SD)

Figure 77.

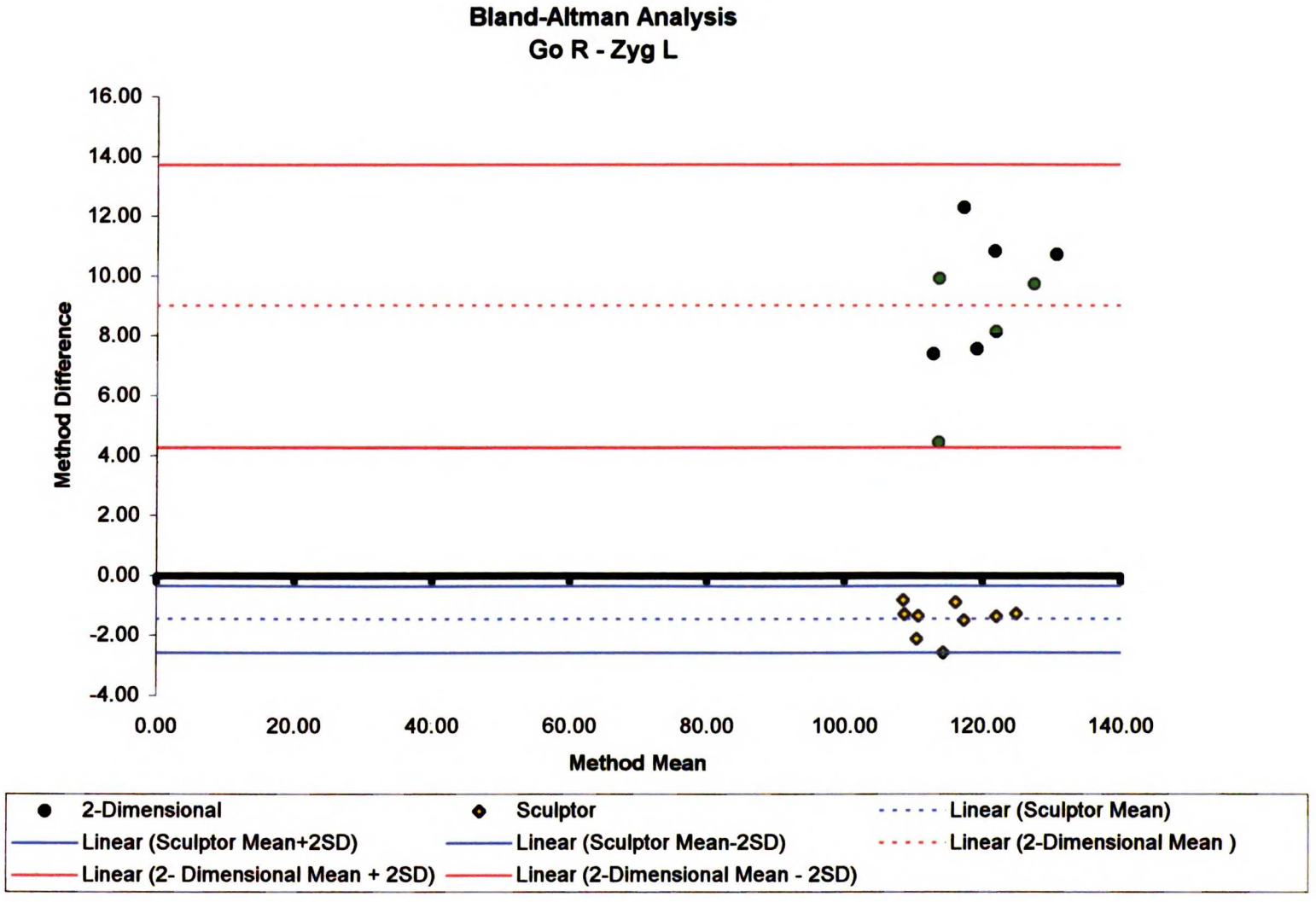
Bland-Altman Analysis
Go R - Zyg L
Method Difference
16.00
14.00
12.00
10.00
8.00
6.00
4.00
2.00
0.00
-2.00
-4.00
0.00
20.00
40.00
60.00
80.00
100.00
120.00
140.00
Method Mean
2-Dimensional
Sculptor
Linear (Sculptor Mean)
Linear (Sculptor Mean+2SD)
Linear (Sculptor Mean-2SD)
Linear (2-Dimensional Mean)
Linear (2- Dimensional Mean + 2SD)
Linear (2-Dimensional Mean - 2SD)

Figure 78.

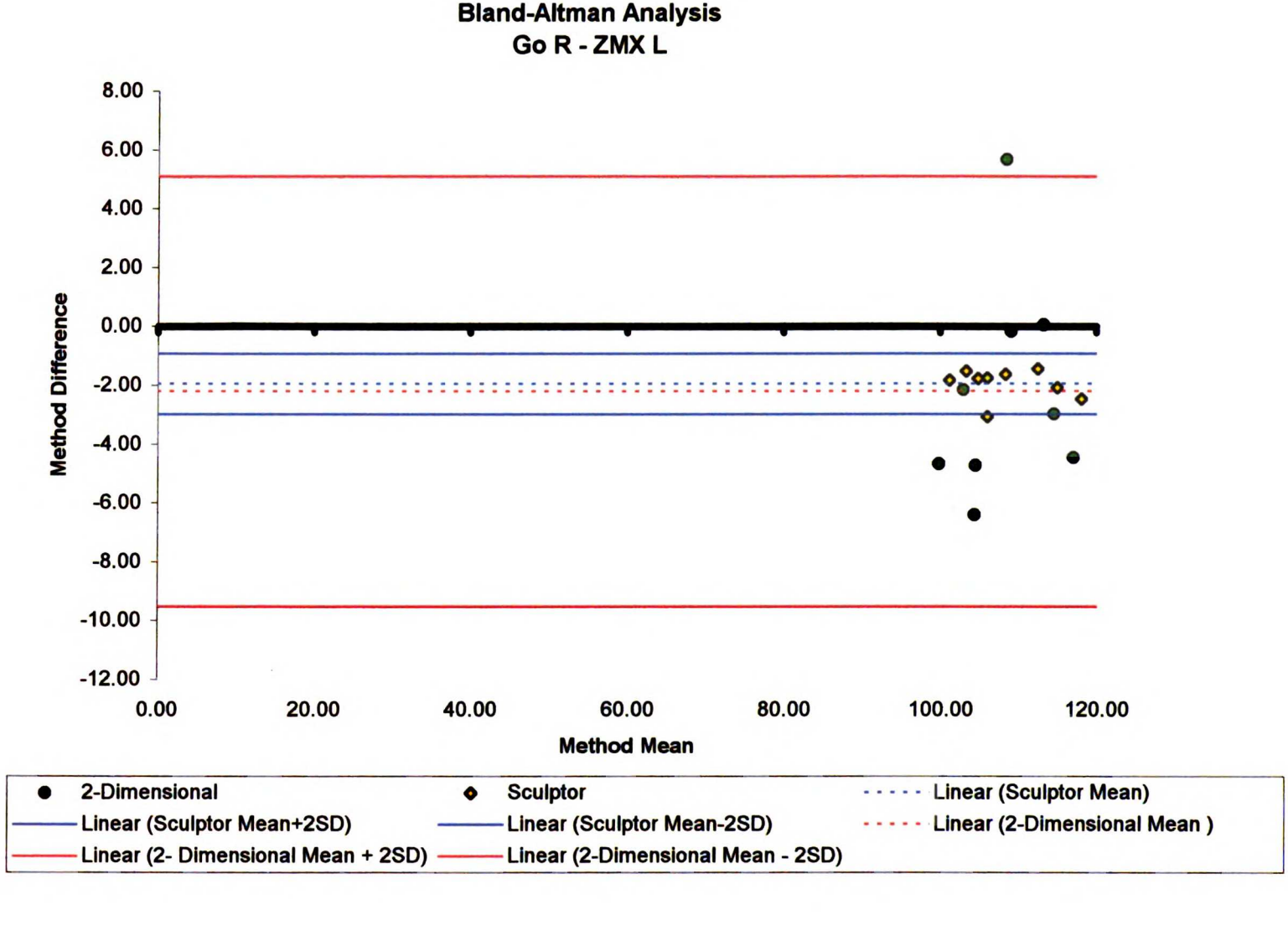
Bland-Altman Analysis
Go R - ZMX L
8.00
6.00
4.00
2.00
0.00
-2.00
-4.00
-6.00
-8.00
-10.00
-12.00
Method Difference
0.00
20.00
40.00
60.00
80.00
100.00
120.00
Method Mean
2-Dimensional
Sculptor
Linear (Sculptor Mean)
Linear (Sculptor Mean+2SD)
Linear (Sculptor Mean-2SD)
Linear (2-Dimensional Mean)
Linear (2- Dimensional Mean + 2SD)
Linear (2-Dimensional Mean - 2SD)

Figure 79.

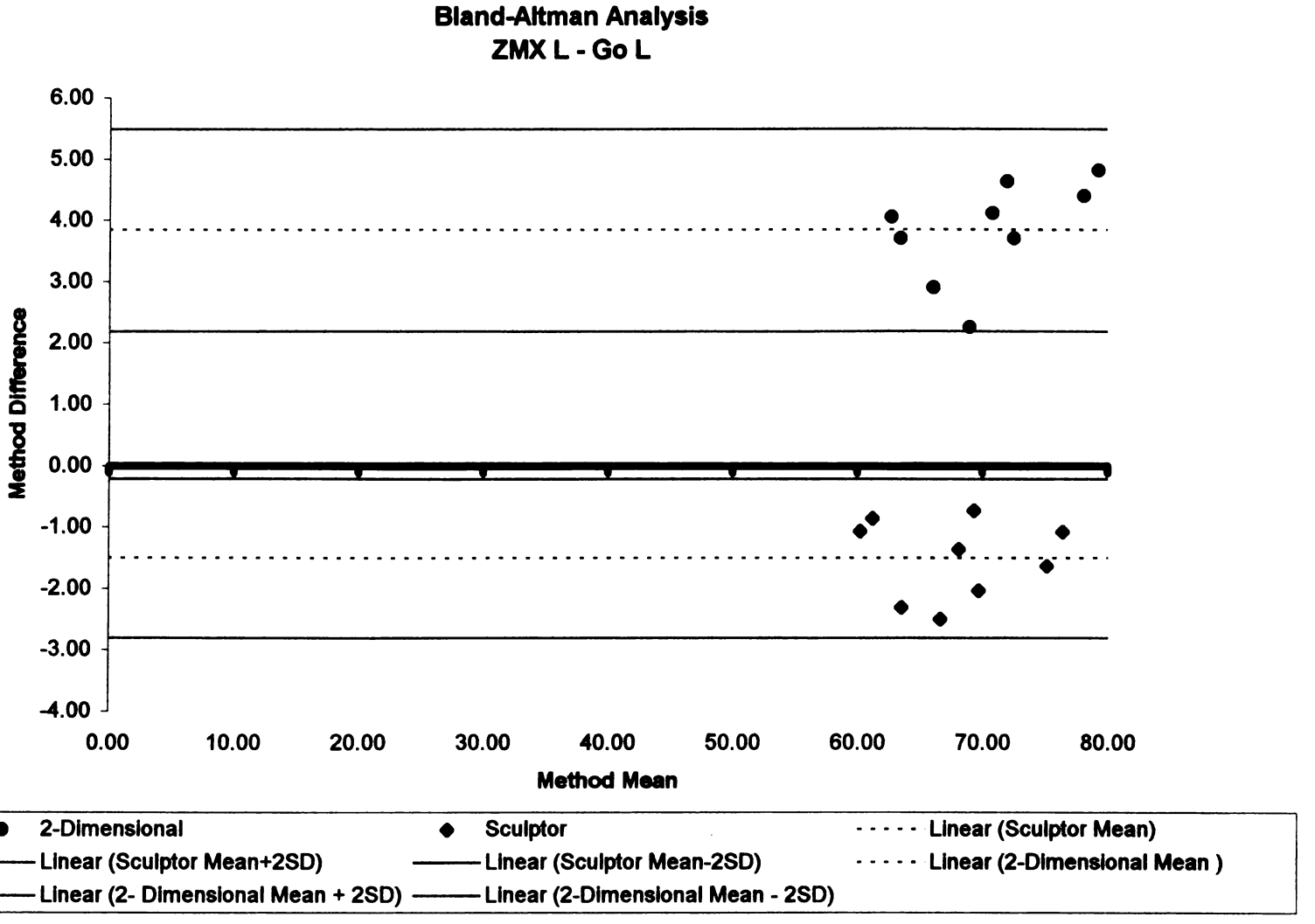
Bland-Altman Analysis
ZMX L - Go L
6.00
5.00
4.00
3.00
2.00
1.00
0.00
-1.00
-2.00
-3.00
-4.00
Method Difference
0.00
10.00
20.00
30.00
40.00
50.00
60.00
70.00
80.00
Method Mean
2-Dimensional
Sculptor
Linear (Sculptor Mean)
Linear (Sculptor Mean+2SD)
Linear (Sculptor Mean-2SD)
Linear (2-Dimensional Mean)
Linear (2- Dimensional Mean + 2SD)
Linear (2-Dimensional Mean - 2SD)

Figure 80.

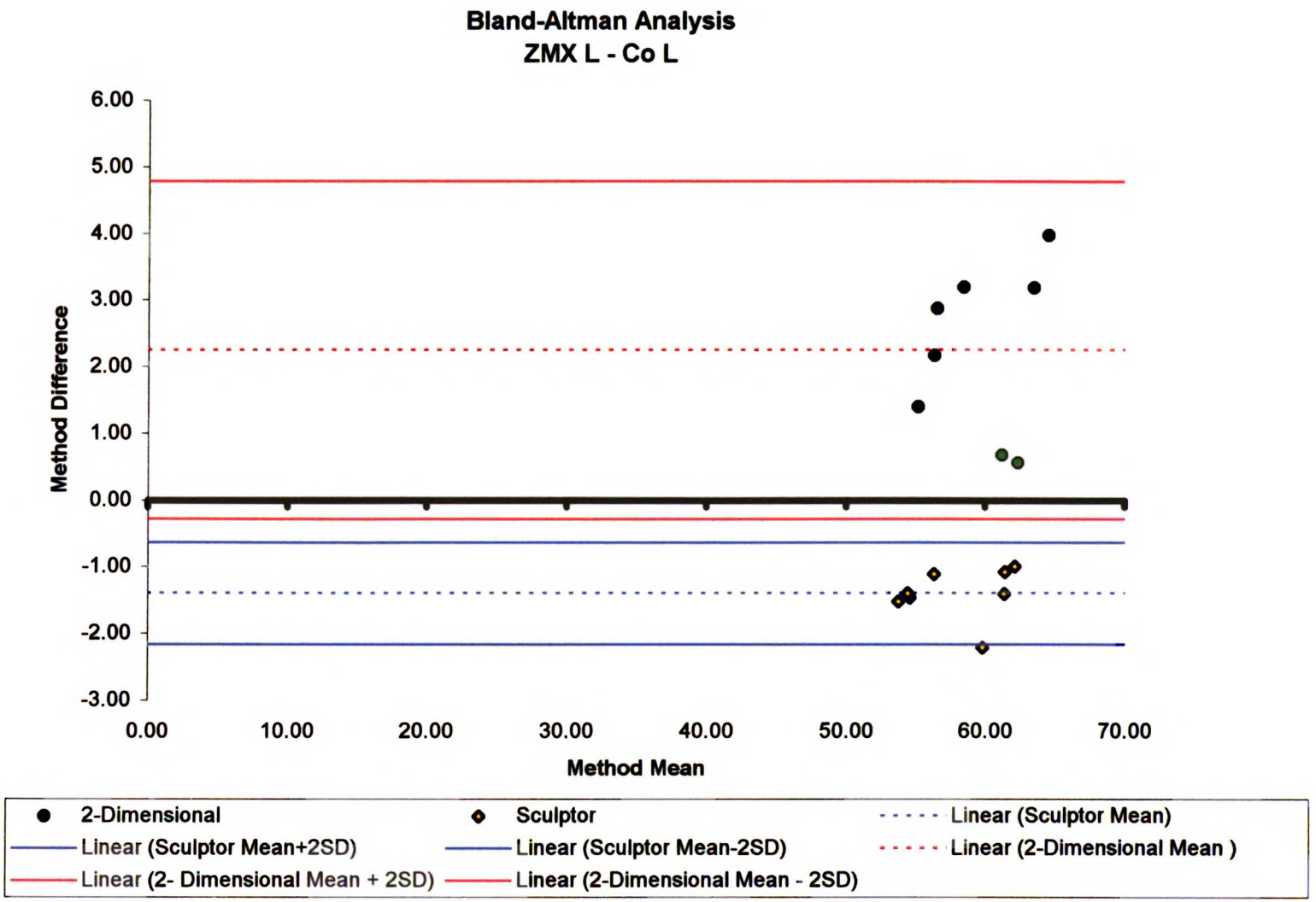
Bland-Altman Analysis
ZMX L - Co L
Method Difference
6.00
5.00
4.00
3.00
2.00
1.00
0.00
-1.00
-2.00
-3.00
0.00
10.00
20.00
30.00
40.00
50.00
60.00
70.00
Method Mean
2-Dimensional
Sculptor
Linear (Sculptor Mean)
Linear (Sculptor Mean+2SD)
Linear (Sculptor Mean-2SD)
Linear (2-Dimensional Mean)
Linear (2- Dimensional Mean + 2SD)
Linear (2-Dimensional Mean - 2SD)

Figure 81.

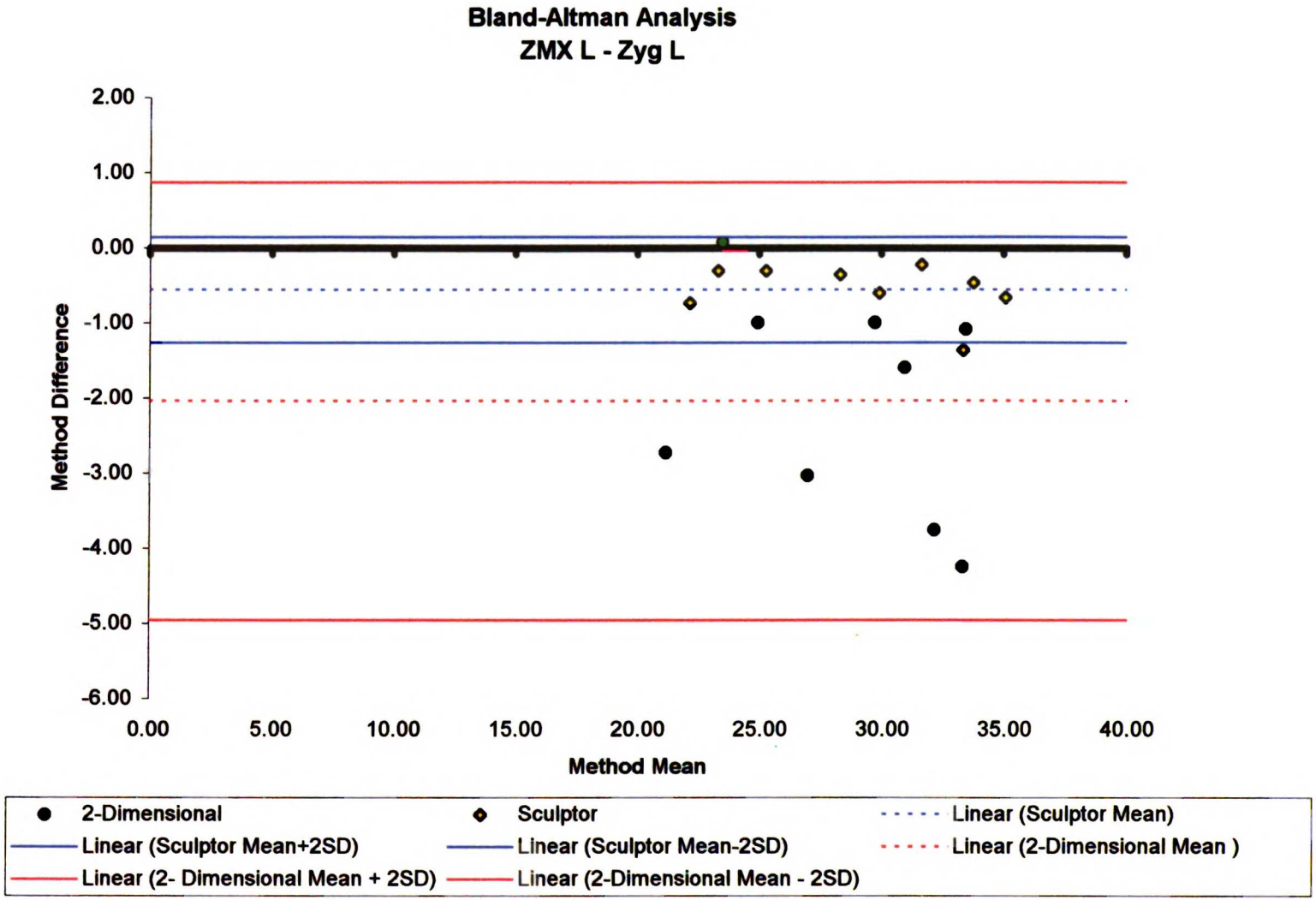
Bland-Altman Analysis
ZMX L - Zyg L
Method Difference
2.00
1.00
0.00
-1.00
-2.00
-3.00
-4.00
-5.00
-6.00
0.00
5.00
10.00
15.00
20.00
25.00
30.00
35.00
40.00
Method Mean
2-Dimensional
Sculptor
Linear (Sculptor Mean)
Linear (Sculptor Mean+2SD)
Linear (Sculptor Mean-2SD)
Linear (2-Dimensional Mean)
Linear (2- Dimensional Mean + 2SD)
Linear (2-Dimensional Mean - 2SD)

Figure 82.

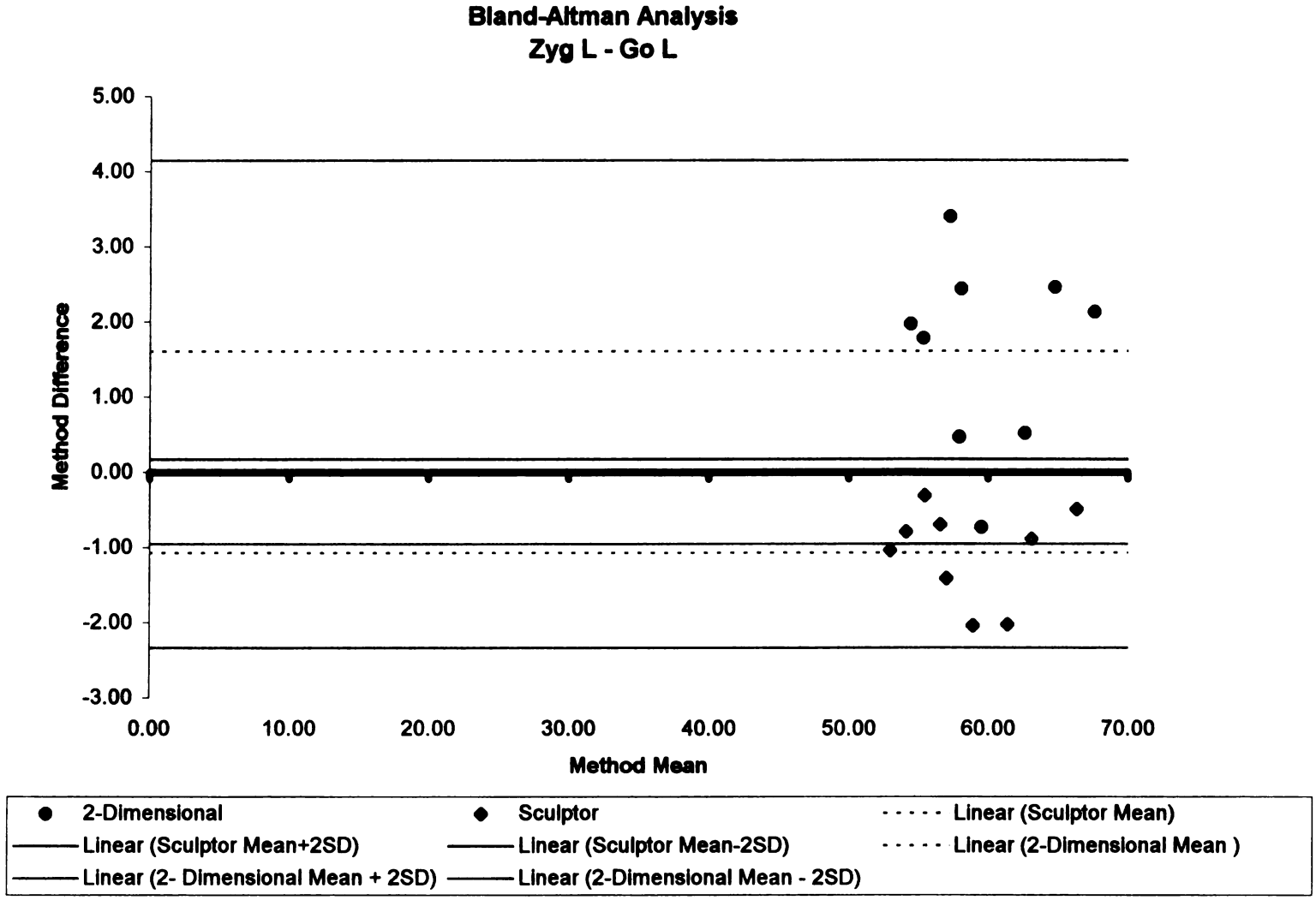
Bland-Altman Analysis
Zyg L - Go L
Method Difference
5.00
4.00
3.00
2.00
1.00
0.00
-1.00
-2.00
-3.00
0.00
10.00
20.00
30.00
40.00
50.00
60.00
70.00
Method Mean
2-Dimensional
Sculptor
Linear (Sculptor Mean)
Linear (Sculptor Mean+2SD)
Linear (Sculptor Mean-2SD)
Linear (2-Dimensional Mean)
Linear (2- Dimensional Mean + 2SD)
Linear (2-Dimensional Mean - 2SD)

Figure 83.

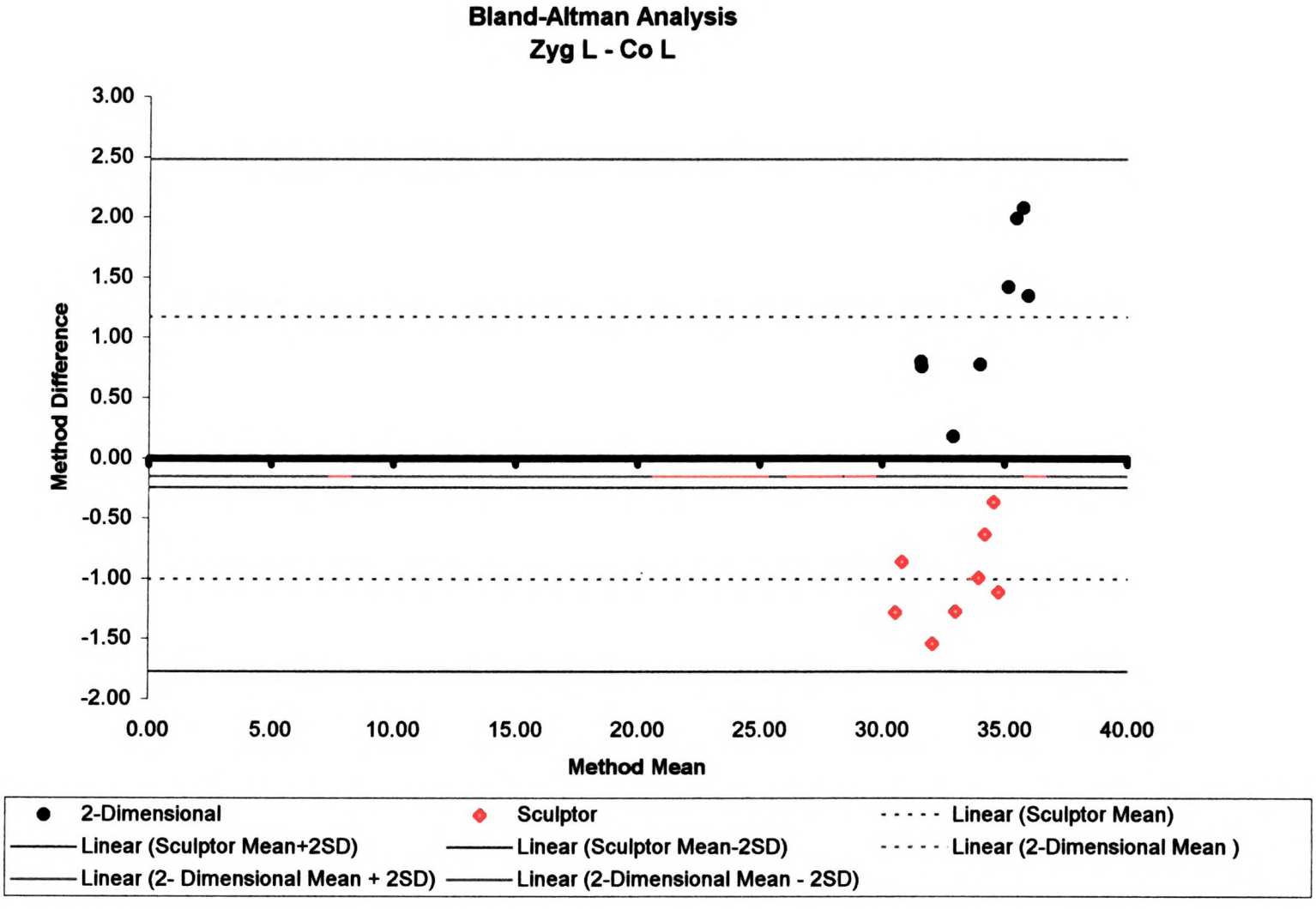
Bland-Altman Analysis
Zyg L - Co L
Method Difference
3.00
2.50
2.00
1.50
1.00
0.50
0.00
-0.50
-1.00
-1.50
-2.00
0.00
5.00
10.00
15.00
20.00
25.00
30.00
35.00
40.00
Method Mean
2-Dimensional
Sculptor
Linear (Sculptor Mean)
Linear (Sculptor Mean+2SD)
Linear (Sculptor Mean-2SD)
Linear (2-Dimensional Mean)
Linear (2- Dimensional Mean + 2SD)
Linear (2-Dimensional Mean - 2SD)

Figure 84.

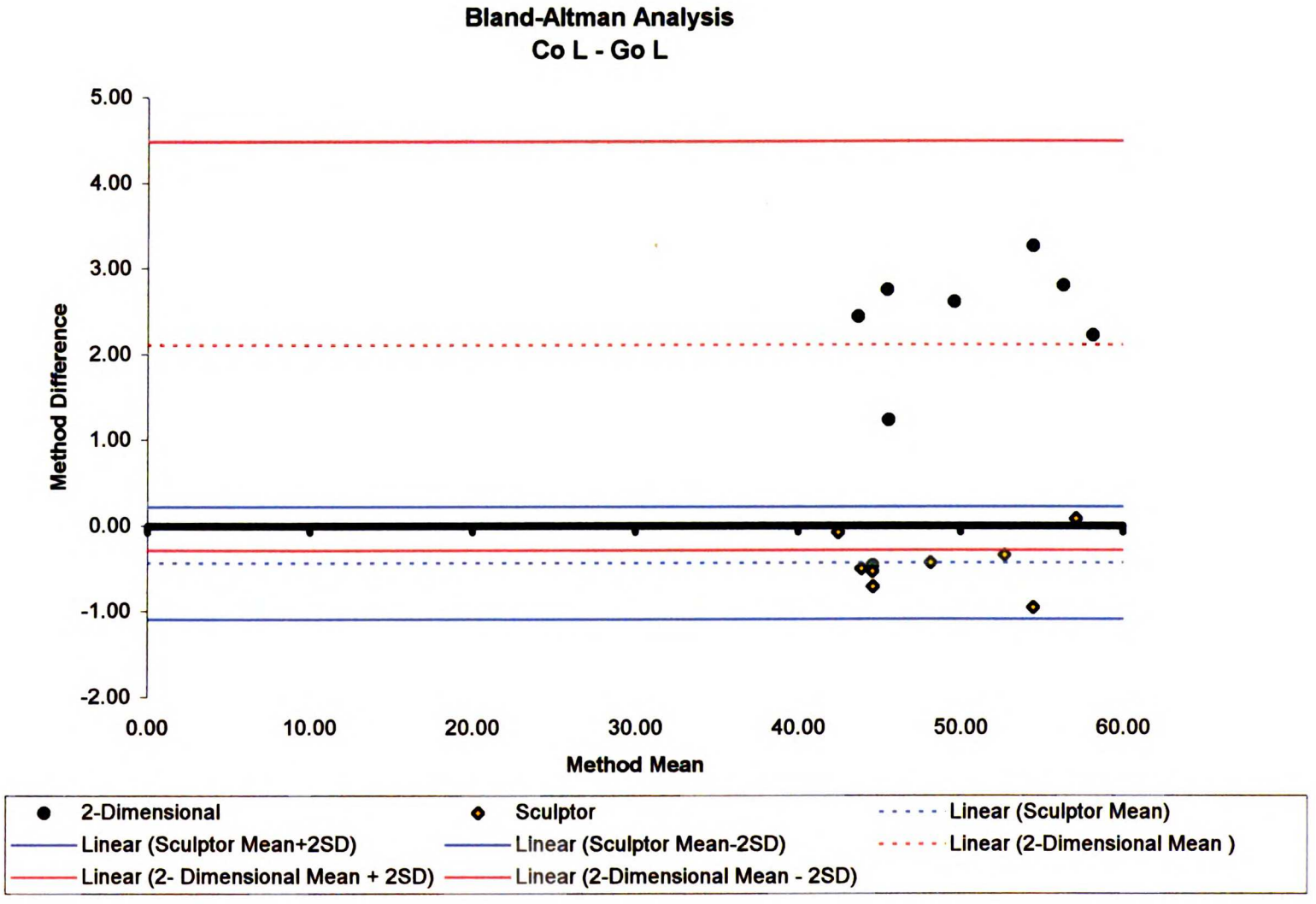
Bland-Altman Analysis
Co L - Go L
5.00
4.00
3.00
2.00
1.00
0.00
-1.00
-2.00
Method Difference
0.00
10.00
20.00
30.00
40.00
50.00
60.00
Method Mean
2-Dimensional
Sculptor
Linear (Sculptor Mean)
Linear (Sculptor Mean+2SD)
Linear (Sculptor Mean-2SD)
Linear (2-Dimensional Mean)
Linear (2- Dimensional Mean + 2SD)
Linear (2-Dimensional Mean - 2SD)

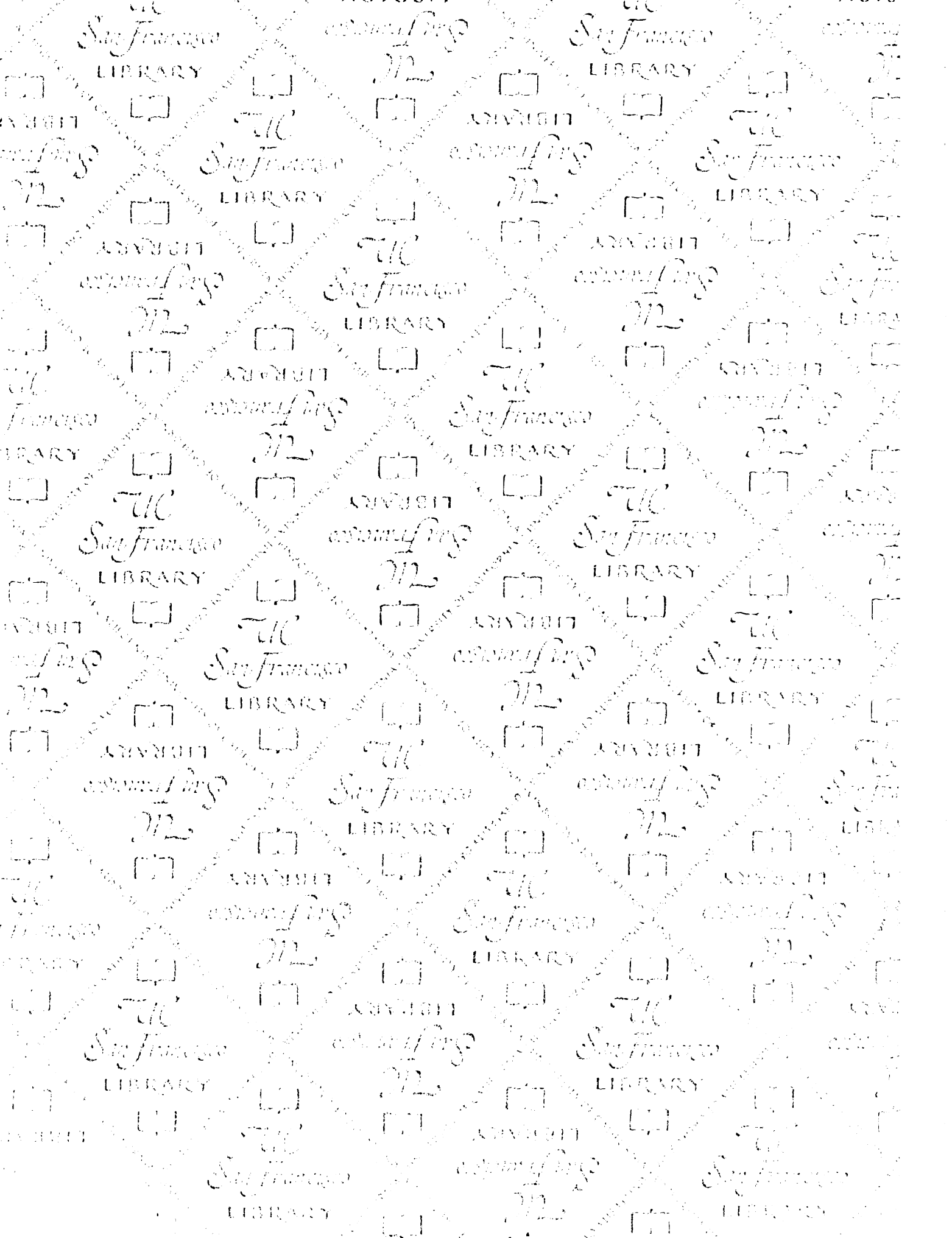
The San Francisco
LIBRARY

For reference

Not to be taken from the room.

6889342

3 1378 00688 9342

UC San Francisco LIBRARY